

UCSF

UC San Francisco Electronic Theses and Dissertations

Title

Regulation of HIV Vif by host factors

Permalink

<https://escholarship.org/uc/item/5nt1677m>

Author

Stanley, David James

Publication Date

2013

Peer reviewed|Thesis/dissertation

Regulation of HIV Vif by host factors

by

David J. Stanley

DISSERTATION

Submitted in partial satisfaction of the requirements for the degree of

DOCTOR OF PHILOSOPHY

in

Biophysics



in the

Copyright © 2013

By

David J. Stanley

ACKNOWLEDGEMENTS

The culture of UCSF is such that useful discussion is to be had at every turn, in and outside of the lab. While those acknowledged here directly contributed toward and supported my progress, the intellectual benefit I gained from the community at large could not be overestimated.

First and foremost, the continued and persistent mentoring, encouragement and enthusiasm of Dr. John D. Gross has helped to make this work a reality. I have considered it an uncommon privilege to have had his support and confidence while initiating a new project quite unrelated from other work taking place in the lab at the time. I do not know of another PI at UCSF who is willing to go as far out of his way as John does regularly for his students, even if that requires coming to lab late at night on a Sunday to assist a young graduate student with unfamiliar equipment. His commitment to mentorship is a model that I hope to carry forward.

My thesis committee members deserve credit for every now and then helping me to see the big picture and learn to always keep that important perspective. Drs. David O. Morgan, Holly Ingraham, and James A. Wells, have contributed much over the years.

I have had other mentors before arriving at UCSF, and without their guidance and encouragement I would surely be a different person today. Kevin Ahern and Indira Rajagopal are undoubtedly featured prominently in many other formal acknowledgements for reasons obvious to anyone familiar with the OSU Biochemistry and Biophysics program; their utmost dedication to teaching and mentorship is unparalleled. My undergraduate advisors Drs. Frank L. Moore, Linda Ciuffetti, and P. Andrew Karplus introduced me to a great variety of ways of doing biological research and taught me to follow my interests even if they led away from their immediate subject area.

I was lucky, as a new graduate student, to find myself in a small lab in which everyone knew everything about everyone else's project. The lab has grown substantially over the years, but the individual personalities made my experience what it was, and they must be thanked: Brittnee Jones for being the "guinea pig" graduate student in the Gross lab and mentoring John's younger students from a different angle, Stephen Floor for his scientific real talk and making his natural insight available in lab every day, Robin Aglietti for many late night conversations, Linda Yen for her unwavering enthusiasm, and more recently Adam Steeves for his thoughts and willingness to debate. Arabinda Nayak, who had the unusual distinction of being my rotation advisor more than once in both the Gross lab and his native Andino lab, has been a wellspring of discussion leading to fruitful collaboration throughout my time at UCSF. Our work on the crystal structure and biochemistry of CrPV1A is not featured in this dissertation,

but has been an enjoyable project over the last many years through which I have learned much.

Lastly, my family and Lis deserve great credit for being a counterbalance to my life in science while still supporting it wholeheartedly.

ABSTRACT

Hijack of the ubiquitin proteasome system is a recurring theme in host-pathogen interactions. HIV-1 encodes at least three ‘accessory factor’ proteins, Vif, Vpr, and Vpu, each known to interact with and retarget a human ubiquitin ligase with deleterious consequences for the host. The best characterized of the accessory factors is Vif, which is required for viral infectivity in T-lymphocytes. In the absence of Vif, the APOBEC3 family of restriction factors is expressed in these cells and induces lethal hypermutation of the viral genome. Vif serves as a viral countermeasure to APOBEC3 proteins by recruiting them to CUL5, a member of the CRL ubiquitin ligases, for K48-linked polyubiquitination thereby sentencing them to proteasomal degradation. Affinity purification-mass spectrometry approaches implicate a large cast of cellular proteins as Vif interactors; the work in this dissertation focuses on understanding the functional significance of a small number of them for Vif. In summary, we find the NEDD8 E2 enzyme UBE2F is critical for activation of the Vif-hijacked ubiquitin ligase, and is recruited to CUL5 by the RING-protein RBX2. The NEDD8 pathway is druggable at the E1 step, and the UBE2F pathway represents a novel drug target for relatively specific inhibition of Vif. Ligands influence the conformational state of Vif, a natively disordered protein. We find that Vif is able to simultaneously bind nucleic acids and components of the ubiquitylation machinery, resulting in a conformation with physical properties not observed in Vif complexes lacking either nucleic acid or ubiquitylation components.

Table of Contents

<i>Title page</i>	<i>i</i>
<i>Acknowledgements</i>	<i>iii</i>
<i>Abstract</i>	<i>vi</i>
<i>Table of Contents</i>	<i>vii</i>
<i>List of Figures</i>	<i>viii</i>
Chapter 1: Introduction	2
References	8
Chapter 2: Inhibition of a NEDD8 cascade restores restriction of HIV by APOBEC3G	9
Abstract	13
Author Summary	14
Introduction	15
Results	18
Discussion	26
Materials & Methods	31
References	41
Figure Legends	46
Supplemental Figure Legends	52
Figures	57
Supplemental Figures	64
Chapter 3: A role for lysine acetylation in regulation of NEDD8ylation?	69
Abstract	70
Introduction	71
Results and Discussion	74
Materials & Methods	78
Figure Legends	81
Supplemental Figure Legends	82
Figures	84
Supplemental Figures	88
References	92
Chapter 4: Conformational dependence of Vif on the complement of bound ligands	95
Abstract	96
Introduction	97
Results and Discussion	101
Materials & Methods	107
Figure Legends	110

Supplemental Figure Legends	112
Figures	113
Supplemental Figures	119
References	120

List of Figures

Chapter 2:

Figure 1	46
Figure 2	47
Figure 3	48
Figure 4	49
Figure 5	50
Figure 6	51
Figure 7	52
Supplemental Figure 1	53
Supplemental Figure 2	54
Supplemental Figure 3	55
Supplemental Figure 4	56
Supplemental Figure 5	57

Chapter 3:

Figure 1	84
Figure 2	85
Figure 3	86
Figure 4	87
Supplemental Figure 1	88
Supplemental Figure 2	89
Supplemental Figure 3	90
Supplemental Figure 4	91

Chapter 4:

Figure 1	113
Figure 2	114
Figure 3	115
Figure 4	116
Figure 4	117
Supplemental Figure 1	118

CHAPTER 1

Introduction to **“Regulation of HIV Vif by host factors”**

David J. Stanley

INTRODUCTION

Evolutionary conflict between pathogens and the hosts they infect has given rise to adaptations on both sides of the host-pathogen interface that are specifically evolved to combat the other. The Red Queen Hypothesis states that in order to remain competitive in a dynamic environment, an organism must continually adapt to shifting pressures. Examination of the evolutionary record across humans and other primates reveals the accelerated evolution of innate immunity factors in the form of an increased level of non-synonymous changes to the genetic code, believed to be the product of selective pressure from viral countermeasures over the time-span of millions of years (7). In some cases, these factors and their viral counterparts physically interact, and the evolutionary rate is particularly great at the molecular interface between them (6, 21, 22, 33, 39).

Competitive evolution between the HIV protein Vif and the human innate immunity factor APOBEC3G (A3G) has been especially well studied (4, 11, 32). While A3G is a cytoplasmic cytidine deaminase that is able to cause a lethal mutational load in the viral genome, Vif counteracts the restrictive effect of A3G using by binding and recruiting it to an E3 ubiquitin ligase for K48-linked polyubiquitylation leading to proteasomal degradation (12, 18, 23, 25, 36, 40). Specifically, the ligase belongs to the Culling-RING Ligase (CRL) family of which the well-characterized SCF complex is the founding member (2, 28). CRLs

consist of an elongated Cullin (CUL) scaffold, and an E2-recruiting RING-box protein (RBX) subunit at the C-terminal end, and a substrate adaptor subunit (SR) at the N-terminal end (42). Vif is but a single representative of the HIV accessory proteins, of which there are two others, Vpr and Vpu. All three are known to hijack human CRLs; however, whereas Vif binds to CUL5, Vpr and Vpu utilize CUL4A and CUL1 respectively (24).

A global analysis of physical interactions between HIV and human proteins using an affinity-purification approach coupled with mass spectrometry (AP-MS) recapitulated known interactors, and also suggested several novel associations (15). Among the implicated interactors of Vif were the transcriptional regulator CBF β , and RBX2. We found that CBF β is an obligate binding partner of Vif for its role as a countermeasure to A3G, and additionally found that sequestration of CBF β by Vif away from its normal binding partners, the RUNX family of transcription factors, modulated the transcriptional program of the cell (16, 17). At the time of the AP-MS studies, the role of RBX2 in CRL biology was not well understood, and we therefore conducted experiments to determine the implications of a CUL5-RBX2 complex rather than the expected CUL5-RBX1 for the function and regulation of Vif (40).

RBX2 dictates regulation of the Vif E3 ligase by the NEDD8 E2 UBE2F

RING-domains are a common and modular fold that is typically found in ubiquitin E3 ligases, where they interact with and stimulate the conjugating

activity of E2 enzymes (9). In the SCF complex, RBX1 interacts with both ubiquitin-conjugating enzymes UbcH5b and Cdc34 and the NEDD8-conjugating enzyme UBE2M. NEDD8 is a ubiquitin-like protein, the conjugation of which to the CUL scaffold is critical for CRL function in metazoans (8). Similarly to that of ubiquitin, an E1-E2-E3 cascade uses ATP to drive the conjugation of NEDD8 to substrate. NEDD8ylation induces a large conformational change in the CUL CTD, both increasing the ubiquitylation rate and processivity of CRLs, and playing a role in the efficient sampling of the available SR pool (10, 29, 31), thereby enhancing the timely turnover of substrates - a critical step in a broad array of cellular pathways including cell-cycle control, transcription, DNA repair and signaling (28). By analogy, HIV Vif requires CUL5 NEDD8ylation to degrade APOBEC3G (40).

Initial experiments were puzzling, in that we were unable to NEDD8ylate CUL5-RBX2 complexes *in vitro* using the E2 UBE2M; however, by cloning and expressing the full panel of known human E2 enzymes, we were able to find another E2, now known as UBE2F, that was able to function as a NEDD8 E2 and fully NEDD8ylate CUL5-RBX2. Soon after this, a study was published detailing functional links between RBX1-UBE2M and RBX2-UBE2F pairs, confirming our unpublished result (13). We went on to show a requirement of both RBX2 and UBE2F for efficient Vif-mediated escape of A3G restriction, and detailed molecular specificity determinants thereof. Additionally, we validated the inhibition of NEDD8 cascades as a proof of concept for the block of virally-

hijacked CRLs, extending the potential use of the NEDD8 E1 inhibitor MLN4924 (37). These results are published, and fully described in Chapter 2 herein (38).

Additional regulation mechanisms of CRL5

Having established the RBX2-UBE2F NEDD8ylation pathway is a viable target for the semi-specific block of Vif-mediated A3G degradation, we sought additional cellular factors that might play a role in this process. The Defective in Cullin Nedd8ylation (Dcn) protein in the yeast *S. cerevisiae* is thought of as a NEDD8ylation E3, promoting the conjugation step by binding both CUL and N-terminally acetylated E2 tail, and is required for efficient substrate turnover (19, 20, 34, 35). In humans, the DCN-like (DCNL) family has five family members that share a conserved core PONY-domain with the yeast Dcn protein, and is tentatively thought to impart a layer of specificity to CRL NEDD8ylation (26, 27).

An shRNA-knockdown screen for dependence of Vif-conferred infectivity in cells expressing A3G on the expression of individual DCNL proteins was inconclusive, and suggested that if DCNL-mediated enhancement of CUL5 NEDD8ylation is indeed important there is likely some redundancy in the pathways (D. Crosby, personal communication). Aside from a major dependence of CUL3 localized to the plasma membrane on DCNL3 for NEDD8ylation (26), no other phenotypes have been reported for knockdown of individual DCNL proteins despite significant effort to discern specificity in DCNL-CUL-N8E2 interactions (27).

Therefore, we asked whether interactions between NEDD8 E2s and DCNL proteins might be regulated not through specificity of molecular recognition, but through post-translational modifications that might control the physical interactions or activity of the pathway. Proteome-wide studies detected acetyl-lysine modifications in the N-terminal tail of both NEDD8 E2s (3), a region of the proteins that interacts both with DCNL and E1 enzyme in distinct conformations (14, 34). Using a surface plasmon resonance-based assay with semi-synthetic UBE2F bearing acetyl-lysine modifications, we tested whether lysine acetylation controls the interaction between UBE2F and the DCNL family. No strong dependence of UBE2F-DCNL K_d equilibrium binding constants on lysine acetylation was detected, but remains possible that the E1 step is regulated by this modification. These experiments are presented in Chapter 3.

Characterization of the nucleic acid binding activity of Vif in complex with CBF β and Elongins B and C

When not bound to ligand, Vif displays significant amounts of conformational disorder and is known to bind RNA; these properties are known to be characteristic of RNA chaperones (1, 5, 30). Given the precedence in our lab of a stabilizing influence on Vif exerted by the interaction with binding partners CBF β and Elongins B and C, we asked whether the Vif-CBF β -EloB-EloC (VCBC) complex could bind nucleic acids similarly to monomeric Vif, and if this association might provide further stabilization that could prove useful for

structural studies of Vif. Little structural information on Vif is available despite very significant effort; the protein appears to be conformationally dynamic, and the stabilization of a specific conformation may enable experiments that will unlock a detailed biophysical understanding of Vif.

We found that VCBC bound both RNA and DNA in a highly salt-dependant manner, and protected a ~12 nt fragment of poly(U) from degradation by RNase A. Relative to experiments using monomeric Vif (41), a different base specificity is found in our K_d measurements of VCBC with a panel of oligonucleotides representing all 8 standard homopolymeric RNAs and DNAs, but it remains unclear what drives the observed preference, or if it has biological relevance. A preliminary physical characterization of the oligonucleotide-bound VCBC complex by gel filtration and small angle X-ray scattering (SAXS) suggests a conformational compaction relative to VCBC alone. This series of experiments is described in Chapter 4.

REFERENCES

1. **Batiste, J., S. Guerrero, S. Bernacchi, D. Sleiman, C. Gabus, J. L. Darlix, R. Marquet, C. Tisne, and J. C. Paillart.** 2012. The role of Vif oligomerization and RNA chaperone activity in HIV-1 replication. *Virus Res* **169**:361-76.
2. **Cardozo, T., and M. Pagano.** 2004. The SCF ubiquitin ligase: insights into a molecular machine. *Nat Rev Mol Cell Biol* **5**:739-51.
3. **Choudhary, C., C. Kumar, F. Gnad, M. L. Nielsen, M. Rehman, T. C. Walther, J. V. Olsen, and M. Mann.** 2009. Lysine acetylation targets protein complexes and co-regulates major cellular functions. *Science* **325**:834-40.
4. **Compton, A. A., V. M. Hirsch, and M. Emerman.** 2012. The host restriction factor APOBEC3G and retroviral Vif protein coevolve due to ongoing genetic conflict. *Cell Host Microbe* **11**:91-8.
5. **Cristofari, G., and J. L. Darlix.** 2002. The ubiquitous nature of RNA chaperone proteins. *Prog Nucleic Acid Res Mol Biol* **72**:223-68.
6. **Dar, A. C., and F. Sicheri.** 2002. X-ray crystal structure and functional analysis of vaccinia virus K3L reveals molecular determinants for PKR subversion and substrate recognition. *Mol Cell* **10**:295-305.
7. **Daugherty, M. D., and H. S. Malik.** 2012. Rules of engagement: molecular insights from host-virus arms races. *Annu Rev Genet* **46**:677-700.
8. **Deshaies, R. J., E. D. Emberley, and A. Saha.** 2010. Control of cullin-ring ubiquitin ligase activity by nedd8. *Subcell Biochem* **54**:41-56.
9. **Deshaies, R. J., and C. A. Joazeiro.** 2009. RING domain E3 ubiquitin ligases. *Annu Rev Biochem* **78**:399-434.
10. **Duda, D. M., L. A. Borg, D. C. Scott, H. W. Hunt, M. Hammel, and B. A. Schulman.** 2008. Structural insights into NEDD8 activation of cullin-RING ligases: conformational control of conjugation. *Cell* **134**:995-1006.
11. **Duggal, N. K., H. S. Malik, and M. Emerman.** 2011. The breadth of antiviral activity of APOBEC3DE in chimpanzees has been driven by positive selection. *J Virol* **85**:11361-71.
12. **Harris, R. S., K. N. Bishop, A. M. Sheehy, H. M. Craig, S. K. Petersen-Mahrt, I. N. Watt, M. S. Neuberger, and M. H. Malim.** 2003. DNA deamination mediates innate immunity to retroviral infection. *Cell* **113**:803-9.
13. **Huang, D. T., O. Ayrault, H. W. Hunt, A. M. Taherbhoy, D. M. Duda, D. C. Scott, L. A. Borg, G. Neale, P. J. Murray, M. F. Roussel, and B. A. Schulman.** 2009. E2-RING expansion of the NEDD8 cascade confers specificity to cullin modification. *Mol Cell* **33**:483-95.
14. **Huang, D. T., D. W. Miller, R. Mathew, R. Cassell, J. M. Holton, M. F. Roussel, and B. A. Schulman.** 2004. A unique E1-E2 interaction required for optimal conjugation of the ubiquitin-like protein NEDD8. *Nat Struct Mol Biol* **11**:927-35.
15. **Jäger, S., P. Cimermancic, N. Gulbahce, J. R. Johnson, K. E. McGovern, S. C. Clarke, M. Shales, G. Mercenne, L. Pache, K. Li, H. Hernandez, G. M. Jang,**

- S. L. Roth, E. Akiva, J. Marlett, M. Stephens, I. D'Orso, J. Fernandes, M. Fahey, C. Mahon, A. J. O'Donoghue, A. Todorovic, J. H. Morris, D. A. Maltby, T. Alber, G. Cagney, F. D. Bushman, J. A. Young, S. K. Chanda, W. I. Sundquist, T. Kortemme, R. D. Hernandez, C. S. Craik, A. Burlingame, A. Sali, A. D. Frankel, and N. J. Krogan.** 2012. Global landscape of HIV-human protein complexes. *Nature* **481**:365-370.
16. **Jäger, S., D. Y. Kim, J. F. Hultquist, K. Shindo, R. S. LaRue, E. Kwon, M. Li, B. D. Anderson, L. Yen, D. Stanley, C. Mahon, J. Kane, K. Franks-Skiba, P. Cimermancic, A. Burlingame, A. Sali, C. S. Craik, R. S. Harris, J. D. Gross, and N. J. Krogan.** 2012. Vif hijacks CBF-beta to degrade APOBEC3G and promote HIV-1 infection. *Nature* **481**:371-5.
17. **Kim, D. Y., E. Kwon, P. D. Hartley, D. C. Crosby, S. Mann, N. J. Krogan, and J. D. Gross.** 2013. CBFbeta Stabilizes HIV Vif to Counteract APOBEC3 at the Expense of RUNX1 Target Gene Expression. *Mol Cell* **49**:632-44.
18. **Kobayashi, M., A. Takaori-Kondo, Y. Miyauchi, K. Iwai, and T. Uchiyama.** 2005. Ubiquitination of APOBEC3G by an HIV-1 Vif-Cullin5-Elongin B-Elongin C complex is essential for Vif function. *J Biol Chem* **280**:18573-8.
19. **Kurz, T., Y. C. Chou, A. R. Willems, N. Meyer-Schaller, M. L. Hecht, M. Tyers, M. Peter, and F. Sicheri.** 2008. Dcn1 functions as a scaffold-type E3 ligase for cullin neddylation. *Mol Cell* **29**:23-35.
20. **Kurz, T., N. Ozlu, F. Rudolf, S. M. O'Rourke, B. Luke, K. Hofmann, A. A. Hyman, B. Bowerman, and M. Peter.** 2005. The conserved protein DCN-1/Dcn1p is required for cullin neddylation in *C. elegans* and *S. cerevisiae*. *Nature* **435**:1257-61.
21. **Laguet, N., N. Rahm, B. Sobhian, C. Chable-Bessia, J. Munch, J. Snoeck, D. Sauter, W. M. Switzer, W. Heneine, F. Kirchhoff, F. Delsuc, A. Telenti, and M. Benkirane.** 2012. Evolutionary and functional analyses of the interaction between the myeloid restriction factor SAMHD1 and the lentiviral Vpx protein. *Cell Host Microbe* **11**:205-17.
22. **Lim, E. S., O. I. Fregoso, C. O. McCoy, F. A. Matsen, H. S. Malik, and M. Emerman.** 2012. The ability of primate lentiviruses to degrade the monocyte restriction factor SAMHD1 preceded the birth of the viral accessory protein Vpx. *Cell Host Microbe* **11**:194-204.
23. **Malim, M. H.** 2009. APOBEC proteins and intrinsic resistance to HIV-1 infection. *Philos Trans R Soc Lond B Biol Sci* **364**:675-87.
24. **Malim, M. H., and M. Emerman.** 2008. HIV-1 accessory proteins--ensuring viral survival in a hostile environment. *Cell Host Microbe* **3**:388-98.
25. **Mehle, A., B. Strack, P. Ancuta, C. Zhang, M. McPike, and D. Gabuzda.** 2004. Vif overcomes the innate antiviral activity of APOBEC3G by promoting its degradation in the ubiquitin-proteasome pathway. *J Biol Chem* **279**:7792-8.
26. **Meyer-Schaller, N., Y. C. Chou, I. Sumara, D. D. Martin, T. Kurz, N. Katheder, K. Hofmann, L. G. Berthiaume, F. Sicheri, and M. Peter.** 2009. The human Dcn1-like protein DCNL3 promotes Cul3 neddylation at membranes. *Proc Natl Acad Sci U S A* **106**:12365-70.

27. **Monda, J. K., D. C. Scott, D. J. Miller, J. Lydeard, D. King, J. W. Harper, E. J. Bennett, and B. A. Schulman.** 2013. Structural conservation of distinctive N-terminal acetylation-dependent interactions across a family of mammalian NEDD8 ligation enzymes. *Structure* **21**:42-53.
28. **Petroski, M. D., and R. J. Deshaies.** 2005. Function and regulation of cullin-RING ubiquitin ligases. *Nat Rev Mol Cell Biol* **6**:9-20.
29. **Pierce, N. W., J. E. Lee, X. Liu, M. J. Sweredoski, R. L. Graham, E. A. Larimore, M. Rome, N. Zheng, B. E. Clurman, S. Hess, S. O. Shan, and R. J. Deshaies.** 2013. Cnd1 Promotes Assembly of New SCF Complexes through Dynamic Exchange of F Box Proteins. *Cell*.
30. **Reingewertz, T. H., H. Benyamini, M. Lebediker, D. E. Shalev, and A. Friedler.** 2009. The C-terminal domain of the HIV-1 Vif protein is natively unfolded in its unbound state. *Protein Eng Des Sel* **22**:281-7.
31. **Saha, A., and R. J. Deshaies.** 2008. Multimodal activation of the ubiquitin ligase SCF by Nedd8 conjugation. *Mol Cell* **32**:21-31.
32. **Sawyer, S. L., M. Emerman, and H. S. Malik.** 2004. Ancient adaptive evolution of the primate antiviral DNA-editing enzyme APOBEC3G. *PLoS Biol* **2**:E275.
33. **Sawyer, S. L., L. I. Wu, M. Emerman, and H. S. Malik.** 2005. Positive selection of primate TRIM5alpha identifies a critical species-specific retroviral restriction domain. *Proc Natl Acad Sci U S A* **102**:2832-7.
34. **Scott, D. C., J. K. Monda, E. J. Bennett, J. W. Harper, and B. A. Schulman.** 2011. N-terminal acetylation acts as an avidity enhancer within an interconnected multiprotein complex. *Science* **334**:674-8.
35. **Scott, D. C., J. K. Monda, C. R. Grace, D. M. Duda, R. W. Kriwacki, T. Kurz, and B. A. Schulman.** 2010. A dual E3 mechanism for Rub1 ligation to Cdc53. *Mol Cell* **39**:784-96.
36. **Sheehy, A. M., N. C. Gaddis, J. D. Choi, and M. H. Malim.** 2002. Isolation of a human gene that inhibits HIV-1 infection and is suppressed by the viral Vif protein. *Nature* **418**:646-50.
37. **Soucy, T. A., P. G. Smith, M. A. Milhollen, A. J. Berger, J. M. Gavin, S. Adhikari, J. E. Brownell, K. E. Burke, D. P. Cardin, S. Critchley, C. A. Cullis, A. Doucette, J. J. Garnsey, J. L. Gaulin, R. E. Gershman, A. R. Lublinsky, A. McDonald, H. Mizutani, U. Narayanan, E. J. Olhava, S. Peluso, M. Rezaei, M. D. Sintchak, T. Talreja, M. P. Thomas, T. Traore, S. Vyskocil, G. S. Weatherhead, J. Yu, J. Zhang, L. R. Dick, C. F. Claiborne, M. Rolfe, J. B. Bolen, and S. P. Langston.** 2009. An inhibitor of NEDD8-activating enzyme as a new approach to treat cancer. *Nature* **458**:732-6.
38. **Stanley, D. J., K. Bartholomeeusen, D. C. Crosby, D. Y. Kim, E. Kwon, L. Yen, N. C. Cartozo, M. Li, S. Jager, J. Mason-Herr, F. Hayashi, S. Yokoyama, N. J. Krogan, R. S. Harris, B. M. Peterlin, and J. D. Gross.** 2012. Inhibition of a NEDD8 Cascade Restores Restriction of HIV by APOBEC3G. *PLoS Pathog* **8**:e1003085.
39. **Stremlau, M., C. M. Owens, M. J. Perron, M. Kiessling, P. Autissier, and J. Sodroski.** 2004. The cytoplasmic body component TRIM5alpha restricts HIV-1 infection in Old World monkeys. *Nature* **427**:848-53.

40. **Yu, X., Y. Yu, B. Liu, K. Luo, W. Kong, P. Mao, and X. F. Yu.** 2003. Induction of APOBEC3G ubiquitination and degradation by an HIV-1 Vif-Cul5-SCF complex. *Science* **302**:1056-60.
41. **Zhang, H., R. J. Pomerantz, G. Dornadula, and Y. Sun.** 2000. Human immunodeficiency virus type 1 Vif protein is an integral component of an mRNP complex of viral RNA and could be involved in the viral RNA folding and packaging process. *J Virol* **74**:8252-61.
42. **Zheng, N., B. A. Schulman, L. Song, J. J. Miller, P. D. Jeffrey, P. Wang, C. Chu, D. M. Koepp, S. J. Elledge, M. Pagano, R. C. Conaway, J. W. Conaway, J. W. Harper, and N. P. Pavletich.** 2002. Structure of the Cul1-Rbx1-Skp1-F boxSkp2 SCF ubiquitin ligase complex. *Nature* **416**:703-9.

CHAPTER 2

Inhibition of a NEDD8 cascade restores restriction of HIV by APOBEC3G

David J. Stanley^{1,9,11}, Koen Bartholomeeusen^{2,11}, David C. Crosby³, Dong Young Kim¹, Eunju Kwon¹, Linda Yen¹, Nathalie Caretta Cartozo¹, Ming Li⁴, Stefanie Jäger⁵, Jeremy Mason-Herr¹, Fumiaki Hayashi⁶, Shigeyuki Yokoyama^{6,7}, Nevan J. Krogan^{5,8,10}, Reuben S. Harris⁴, Boris Matija Peterlin² and John D. Gross^{1,8*}

¹Dept. of Pharmaceutical Chemistry, UCSF, 600 16th Street, San Francisco, CA 94158, USA

²Dept. of Medicine, UCSF, 533 Parnassus Avenue, San Francisco, CA 94143-0703

³Dept. of Biochemistry and Biophysics, UCSF, 600 16th Street, San Francisco, CA 94158, USA

⁴Department of Biochemistry, Molecular Biology and Biophysics, Institute for Molecular Virology, Center for Genome Engineering, University of Minnesota, Minneapolis, Minnesota 55455

⁵Dept. of Molecular & Cellular Pharmacology, UCSF, 600 16th Street, San Francisco, CA 94158, USA

⁶RIKEN Systems and Structural Biology Center, 1-7-22 Suehiro-cho, Tsurumi, Yokohama 230-0045, Japan

⁷Department of Biophysics and Biochemistry, Graduate School of Science, The University of Tokyo, 7-3-1 Hongo, Bunkyo-ku, Tokyo 113-0033, Japan

⁸California Institute for Quantitative Biosciences, QB3, UCSF, 600 16th Street, San Francisco, CA 94158, USA

⁹Graduate Program in Biophysics, UCSF, 600 16th Street, San Francisco, CA 94158, USA

¹⁰J. David Gladstone Institutes, San Francisco, CA 94158, USA

¹¹These authors contributed equally

*Correspondence: jdgross@cgl.ucsf.edu (J.D.G.)

*This work was previously published in *PLoS Pathog*, **8(12)**: e1003085, 2012, and is reprinted here with permission.

ABSTRACT

Cellular restriction factors help to defend humans against human immunodeficiency virus (HIV). HIV accessory proteins hijack at least three different Cullin-RING ubiquitin ligases, which must be activated by the small ubiquitin-like protein NEDD8, in order to counteract host cellular restriction factors. We found that conjugation of NEDD8 to Cullin-5 by the NEDD8-conjugating enzyme UBE2F is required for HIV Vif-mediated degradation of the host restriction factor APOBEC3G (A3G). Pharmacological inhibition of the NEDD8 E1 by MLN4924 or knockdown of either UBE2F or its RING-protein binding partner RBX2 bypasses the effect of Vif, restoring the restriction of HIV by A3G. NMR mapping and mutational analyses define specificity determinants of the UBE2F NEDD8 cascade. These studies demonstrate that disrupting host NEDD8 cascades presents a novel antiretroviral therapeutic approach enhancing the ability of the immune system to combat HIV.

AUTHOR SUMMARY

The APOBEC3 family of editing enzymes catalyzes lethal hypermutation of retroviral genomes to block spread of virus in host. HIV Vif targets APOBEC3 family members for destruction by a cellular ubiquitin ligase containing CUL5. A major goal in the design of the next generation of antiretroviral therapies is to find an inhibitor of Vif so that the activity of the APOBEC3 family of antiretroviral enzymes can be restored. We define a three-enzyme cascade that is required to activate Vif by addition of the ubiquitin-like NEDD8 protein to CUL5. MLN4924, an anti-cancer compound currently in phase 1 clinical trials, inhibits the NEDD8 cascade, blocks the action of Vif, and thus has potent anti-HIV activity.

Furthermore, our studies define downstream drug targets in the NEDD8 cascade more selective for inhibition of HIV Vif. We demonstrate pharmacological inhibition of HIV replication through a mechanism that restores the innate immunity provided by APOBEC3 enzymes by targeting a host pathway, providing additional candidates that could be further exploited for therapeutic development. Inhibition of this NEDD8 cascade alone, or in combination with existing antiretroviral drugs could prove to be a useful treatment for HIV.

INTRODUCTION

HIV relies on extensive interactions with the host in order to co-opt cellular transcription, mRNA export, translation and ESCRT pathways [1,2,3,4]. In addition, HIV must subvert the immune system to achieve a chronic infection [5]. The global landscape of human-HIV protein interactions was recently reported, identifying a network of host pathways that could be potentially exploited to block viral replication [6]. However, physical maps do not provide evidence for function, and the task of validating the interdependences of HIV on host pathways remains an outstanding challenge required before alternative therapeutic strategies can be considered.

The accessory proteins of HIV are considered to be prime targets because they often hijack the ubiquitin-proteasome pathway to downregulate restriction factors that would otherwise block the spread of virus in host [5]. For example, the APOBEC3 (A3) family of cytidine deaminases restricts retroviral replication to protect the infected host. When HIV lacks the viral infectivity factor (Vif), A3G and A3F enzymes are packaged into virions and perform lethal editing of viral cDNA, which occurs at the reverse transcription step [7,8,9,10]. HIV Vif counteracts A3 enzymes by recruiting them to a Cullin-RING Ubiquitin Ligase (CRL) consisting of CUL5, a RING-box subunit (RBX), the canonical adaptor proteins Elongins B and C, and the recently described Vif-specific subunit core binding factor beta (CBF β), which is normally involved in the control of transcription of RUNX genes [11,12,13,14]. These subunits form the CRL5^{Vif-CBF β}

holoenzyme, which acts in the last step of a three enzyme E1-E2-E3 cascade responsible for forming K48-linked polyubiquitin chains on APOBEC3 family members, targeting them for degradation by the 26S proteasome [11,12,15,16,17].

Covalent modification of a conserved lysine in the C-terminal domain of the Cullin subunit with the ubiquitin-like protein NEDD8 is essential for CRL function in metazoans [18]. This requires the action of a three-enzyme E1-E2-E3 cascade much like that of ubiquitin. NEDD8ylation activates a CRL, thus promoting the degradation of its substrates - a critical step in a broad array of cellular pathways including cell-cycle control, transcription, DNA repair and signaling [19]. As such, HIV Vif requires CUL5 NEDD8ylation to degrade APOBEC3G [11]. Given the broad dependencies of cellular protein homeostasis on CRL function, a potent mechanism-based inhibitor of the NEDD8 E1, MLN4924, was developed and found to be effective in suppressing tumor growth in xenograft models of cancer and is currently in phase 1 clinical trials [19,20,21].

In metazoans, there are parallel NEDD8 cascades wherein a single NEDD8 E1 charges the E2s, UBE2M and UBE2F, to promote NEDD8 conjugation of CRLs containing RBX1 or RBX2 respectively [22]. The RBX subunit is a critical determinant of cascade selection by making specific interactions with the NEDD8 E2 [22]. An important but unresolved question is the identity of the

NEDD8 pathway responsible for activating the Vif-associated CRL responsible for A3G degradation. Early studies on the Vif-CUL5 complex implicated RBX1 as the RING subunit, since Vif co-immunoprecipitated with RBX1 in HIV-infected T-cells and overexpression of RBX1 or a mutant of CUL5 impaired in RBX1 binding had a dominant negative effect on Vif function [11]. However, subsequent studies of endogenous Cullin complexes suggested that CUL1-4 associate with RBX1, whereas CUL5 is normally in complex with RBX2 [22,23]. In agreement, we recently found using tandem AP-MS that RBX2 is an integral part of the CUL5-Vif complex [6]. Here we define the NEDD8 cascade required for activation of HIV Vif and validate the concept that pharmacological inhibition of NEDD8 pathways can restore the restriction potential of the innate immune system. The pan-CRL inhibitor MLN4924 restores the restriction potential of A3G. The recently discovered NEDD8 conjugating enzyme UBE2F is the sole NEDD8 E2 necessary for Vif to counteract A3G, and the RING box protein RBX2 is required for Vif to promote spread of HIV in CD4+ T-cells. Structural and kinetic analysis of NEDD8 conjugation reveals how residues linking RBX2 to UBE2F impart specificity to the UBE2F NEDD8 cascade. These results advance our understanding of the activation of CRL5^{Vif-CBF β} by NEDD8 and suggest avenues by which Vif inhibition may be achieved.

RESULTS

Pharmacological inhibition of the NEDD8 E1 with MLN4924 restores the restriction potential of A3G

Given the requirement of CUL5 NEDD8ylation for Vif activity, we reasoned that pharmacological inhibition of the NEDD8 modification would block Vif-mediated A3G degradation and cripple HIV infectivity. As proof-of-principle for the use of NEDD8 cascade inhibitors for antiretroviral therapy, we employed the recently described NEDD8 E1 inhibitor, MLN4924 [20]. A fully infectious molecular clone of HIV, HIV_{NL4-3}, was co-transfected into HEK293 cells along with a mammalian expression construct containing A3G or empty vector. These cells were then treated with increasing concentrations of MLN4924, and the infectivity of resultant virus determined. Although increasing concentrations of MLN4924 did not significantly impact HIV infectivity in the absence of A3G (**Fig. 1A, white bars**), nanomolar concentrations of MLN4924 strongly reduced infectivity in the presence of A3G (**Fig. 1A, black bars**), indicating that MLN4924 impaired the ability of Vif to counteract APOBEC3G. Parallel immunoblots indicated that the compound impaired degradation of A3G and restored the ability of A3G to be packaged (**Fig. 1B**). Consequently and characteristic of A3G function, sequencing of viral genomic DNA from virus produced in the presence of MLN4924 revealed a significant increase in G to A mutations compared to virus produced in DMSO treated cells (**Figs. 1C, S1A**). It is important to note the dinucleotide context of the observed mutations, as A3G-dependent G-to-A

mutations are thought to occur preferentially in a 5'GG context resulting in 5'AG, whereas mutations in the 5' GA context occur by other mechanisms [9,24,25,26,27]. Consistent with this, the mutational context was 89% 5'GG (39) and 11% 5'GA (5) in the MLN4924-treated group, whereas it was 100% 5'GA (7) in the MLN4924-naïve group. Together, these data lend direct evidence as to how MLN4924 restored the restriction potential of A3G.

Vif requires the NEDD8 E2 UBE2F to counteract A3G

Although inhibition of the NEDD8 E1 by MLN4924 potently restores the restriction potential of A3G, this compound inhibits NEDD8 conjugation of all Cullins and is toxic to CD4+ T-lymphocytes with a CT50 of 100 nM (**Fig S1B**). We next sought to identify the NEDD8 cascade responsible for activating CRL5^{Vif-CBF β} , reasoning that definition of downstream targets might allow for more selective inhibition. Initially, RBX1 was found to co-IP with Vif [11], but in a recent AP-MS study to identify new Vif-interacting partners we observed RBX2 in complex with Vif [12]. Since the identity of the RBX subunit determines NEDD8 E2 selectivity, we asked which NEDD8 E2 is responsible for Vif function and thus HIV infectivity in the presence of A3G [22]. Accordingly, we knocked down different NEDD8 E2s followed by co-transfection of HIV_{NL4-3} and A3G-V5 into HEK293T cells and performed single-cycle infectivity assays. Knockdown of UBE2F but not UBE2M or non-silencing control reduced infectivity by 10-fold with a concomitant increase in cellular A3G levels (**Fig. 2A,B**).

To systematically address the requirement of UBE2F for viral infectivity, experiments were performed with a Vif-deficient provirus (HIV_{NL4-3}ΔVif) with transfected A3G and increasing concentrations of Vif-FLAG, following transduction with shUBE2F, shUBE2M or the non-silencing control shRNA (**Fig. 2C**). In the absence of Vif, virus infectivity was significantly impaired in all three knockdowns. With increasing amounts of Vif, knockdown of UBE2F blocked the ability of Vif to counteract A3G whereas non-silencing control and UBE2M knockdown had no effect on Vif function. Parallel immunoblot analyses revealed that knockdown of UBE2F impaired the ability of Vif to block viral packaging of A3G, consistent with the infectivity data (**Fig. 2D**). Additionally, the fraction of CUL5 containing the NEDD8 modification was reduced by knockdown of UBE2F, whereas knockdown of UBE2M had no effect on CUL5 NEDD8ylation in HEK293T cells (**Fig. S2**). The role of UBE2F was confirmed using an RNAi-knockdown and complementation strategy where expression of RNAi-immune UBE2F was able to partially restore the defect in viral infectivity observed when UBE2F was knocked down, decreasing the amount of APOBEC3G in cell lysates and packaged into virions (**Fig. 2E,F**). We conclude that NEDD8ylation of CUL5 by UBE2F is essential for viral infectivity.

UBE2F stimulates polyubiquitin chain formation on APOBEC3G

Previous studies indicate that formation of K48-linked ubiquitin chains on APOBEC3G is required for degradation and exclusion from virions and that

recombinant purified CRL5^{Vif-CBF β} was able to catalyze synthesis of K48 linked chains on A3G [12,17,28]. Accordingly, we evaluated the effect of NEDD8 conjugation on activity of recombinant purified CRL5^{Vif-CBF β} as illustrated in **Fig. 3A**. We found that NEDD8ylation of CUL5 by UBE2F has a switch-like effect on formation of polyubiquitin chains on A3G but not the Vif-resistant deaminase A3A (**Fig. 3B**). An additional specificity control indicates this NEDD8-conjugated E3 ligase was also inactive in polyubiquitin chain formation on the Vif-resistant mutant of A3G (D128K, D130K) (**Fig. S3A,B**)[29]. In contrast, UBE2M only weakly affected activity of CRL5^{Vif-CBF β} , which correlated with a low level of CUL5 NEDD8ylation (**Fig. 3B,C**). These observations are explained by ¹⁵N-HSQC NMR spectra showing UBE2F binds RBX2 but UBE2M does not (**Fig. 3D**). Consistent with the effect on viral infectivity, inhibition of the NEDD8 E1 by MLN4924 blocks charging of UBE2F with NEDD8, explaining why MLN4924 is able to restore the restriction potential of A3G (**Fig. S1C**). These results indicate UBE2F promotes activation of the polyubiquitin synthesis activity of CRL5^{Vif-CBF β} *in vitro*.

RBX2 is required for replication of HIV in non-permissive CD4+ T-cells

We next evaluated the role of RBX2 in viral infectivity, since UBE2F is required for Vif function and previous studies indicate UBE2F forms a functional E2/RING pair with RBX2 [22]. Accordingly, we used shRNA to knockdown RBX1 or RBX2 and assayed for replication of HIV in non-permissive H9 or permissive SupT1 CD4+ T-cell lines that express high or very low levels of APOBEC3 restriction

factors, respectively [30]. Although stable knockdown of RBX2 had no effect on HIV spread through permissive SupT1 cells, knockdown of RBX2 resulted in a sustained suppression of HIV spread through non-permissive H9 cells (**Fig. 4A,B**). Indeed, the degree of RBX2 knockdown correlated with increased suppression of HIV spread through non-permissive H9 cells (**Fig. S4**).

Transduction with non-silencing control shRNA did not hinder the replication of virus in either cell line (**Fig. 4A,B**). Culture supernatant HIV p24 antigen concentrations were commensurate with the fraction of cells positive for HIV antigen expression as determined by immunofluorescence assay (data not shown). Knockdown of RBX1 resulted in cell death in both H9 and SupT1 cells and precluded comparisons of viral replication. The observed toxicity of RBX1 knockdown is consistent with the established role of RBX1 as RING subunit of CRL1-4 [22]. In contrast, when RBX2 mRNA was reduced by more than 80%, greater than 90% of H9 cells were viable at 6 weeks post-transduction, as evidenced by trypan blue exclusion, and cells retained resistance to the stably integrated puromycin selective marker (data not shown). These findings are consistent with recent interaction and functional studies indicating RBX2 is the RING subunit of CRL5 [6,22,23]. We conclude that the NEDD8 cascade containing UBE2F and RBX2 is critical for activation of CRL5^{Vif-CBF β} and the ability of HIV Vif to counteract A3 restriction factors.

Specificity determinants of the UBE2F/RBX2 NEDD8 cascade

Previous domain-swapping experiments indicated the RING domain of the RBX subunit was a major specificity determinant for CRL conjugation by NEDD8 conjugating enzymes [22]. The structural basis for specificity is not well understood, especially since RBX1 and RBX2 are 50% identical in amino acid sequence. To understand in more detail how the RBX2 subunit of CUL5 discriminates between NEDD8 cascades, we used NMR chemical shift changes to map the binding interface and reveal divergent surface residues that could provide a basis for specificity. The binding surface mapped by NMR agrees well with other RING-E2 pairs, and guided our substitution analyses (**Fig. S3C, top**). We found two divergent surface regions centered on R63 and Q95 of RBX2 that line the interface with UBE2F, which is otherwise conserved with RBX1 (**Figs. S3C,D**). If these surfaces are important for conferring NEDD8 E2 specificity, then swapping residues from these regions between RBX1 and RBX2 should restore function of UBE2M with RBX2. An RBX2 mutant, RBX2(Swap4), was designed that swapped in four RBX1 residues to their equivalent positions in RBX2 (**Figs. 5A and S3E**). We compared conjugation of NEDD8 to CUL5/RBX2 or CUL5/ RBX2(Swap4) and CUL5/RBX1 to evaluate the role of divergent RBX residues in conferring NEDD8 E2 specificity. Although CUL5/RBX1 complexes are not detected under physiological conditions, this heterodimer can be prepared by overexpression as described previously and serves as a positive control for NEDD8 conjugation by UBE2M [22,23,31,32].

Conjugation of NEDD8 to CUL5/RBX1, CUL5/RBX2 or CUL5/RBX2(Swap4) was followed over time and revealed that UBE2M is able to conjugate CUL5/RBX1 but not CUL5/RBX2. Remarkably, CUL5/RBX2(Swap4) partially restored the ability of UBE2M to NEDD8ylate CUL5 (**Figs. 5B,C and S3F**). The ability of UBE2F to conjugate CUL5/RBX1 or CUL5/RBX2 was identical, and the Swap4 variant of RBX2 had only a small effect on the ability of UBE2F to conjugate CUL5 (**Fig. S3G-I**). These data indicate divergent residues of RBX2 block interactions with UBE2M and allow function with UBE2F.

Similar analyses of divergent surface features of UBE2F identified an active site proximal loop extension spanned by residues Ser124 to Gly129 (**Fig. S5A-C**). Deletion of this loop insertion in UBE2F (Δ Loop) reduced the rates of CUL5/RBX2 NEDD8ylation by more than 100-fold but did not affect binding to the RBX2 core domain as detected by NMR. In contrast, mutation of Asn92 of UBE2F to alanine blocked binding as observed by NMR and reduced activity by nearly 3 orders of magnitude, consistent with its predicted position on the UBE2F/RBX2 interface (**Figs. 5D-F, S5D,E**). HSQC NMR spectra indicate the mutants are folded (data not shown). A homology model of the CUL5/RBX2/UBE2F complex based on a recent crystal structure of the C-terminal domain of CUL1 in complex with RBX1 suggests the divergent loop of UBE2F may function to stabilize a catalytically active form of CUL5/RBX2/UBE2F that is poised for NEDD8 transfer (**Fig. 5G**) [33].

To evaluate the requirement for the unique loop insertion of UBE2F for HIV infectivity, UBE2F was knocked down in HEK293T cells followed by transient transfection of HIV_{NL4-3}ΔVif in the presence of A3G and Vif and increasing amounts of RNAi-immune plasmid encoding wild-type or UBE2F (ΔLoop). A catalytically dead UBE2F (C116A) that cannot be charged with NEDD8 was incorporated as a negative control. While UBE2F (C116A) was unable to rescue infectivity or A3G degradation by Vif, expression of wild-type UBE2F partially restored the defect in viral infectivity, when endogenous UBE2F was knocked down (**Fig 6A,B**). Restoration of infectivity by wild-type UBE2F was dose-dependent and correlated with a decrease in cellular and virion packaged A3G as detected by immunoblot (**Fig 6A,B**). In contrast and in line with our biochemical data, titration of UBE2F (ΔLoop) indicated that deletion of these UBE2F specific residues impaired its ability to complement UBE2F knockdown and restore infectivity, which was reflected in the absence of A3G degradation (**Fig 6A,B**). These results indicate the unique loop insertion of UBE2F is important for viral infectivity, consistent with the strong requirement of the loop for UBE2F activity *in vitro*. We conclude that the RBX2/UBE2F components of the metazoan specific NEDD8 cascade have evolved loop residues that act as specificity determinants during binding or promote the catalytic step, suggesting structural features that could be exploited for targeted pharmacological inhibition.

DISCUSSION

CRLs are estimated to affect turnover of 10% of cellular proteins, and hijack of this enzyme superfamily is a common viral strategy to evade the host immune response [20,34]. Herein, we validate the concept that inhibition of NEDD8 cascades required to activate CRLs restores the innate immunity provided by restriction factors (**Fig. 7**). Pharmacological inhibition of the NEDD8 E1 by MLN4924 restored the ability of A3G to restrict HIV by disabling the Vif-hijacked E3 ligase, CRL5^{VIF-CBF β} . Nanomolar concentrations of MLN4924 effected a strong increase in the amount of A3G detected in both HIV-infected cells and virions produced from these cells, resulting in significantly less infectious virions compared to those produced in untreated cells. Exposure of HIV to MLN4924 caused a significant increase in G to A mutations in the viral genomic DNA of progeny viruses, compared to inhibitor-naïve viruses, indicating that the loss in infectivity is due to A3G activity.

As MLN4924 inhibits NEDD8ylation of all CRLs, we asked which NEDD8 E2 and RING-subunit were responsible for activating CRL5^{Vif-CBF β} to potentially allow for more selective inhibition of NEDD8 conjugation. Such a strategy, if successful, would allow inhibition of Vif while minimizing the perturbation of protein homeostasis observed in cells treated with MLN4924 [20]. The RING subunit of CRLs designates the NEDD8 cascade and recent studies established CUL5/RBX2 is the functional heterodimer in cells [12,22,23]. Consistent with these observations, we find the NEDD8 conjugating enzyme UBE2F is required

for HIV infectivity by acting as an essential activator of Vif-mediated degradation of A3G. Furthermore, we observed that RBX2 is critical for the replication of HIV in CD4+ T-cells expressing APOBEC3 restriction factors. These results are in line with previous work indicating that UBE2F and RBX2 are required for NEDD8ylation of CUL5 [22] and indicate the expanded NEDD8 cascade containing UBE2F is an important host pathway required for HIV infectivity.

Our *in vitro* studies suggest UBE2F is an essential cofactor for Vif likely because NEDD8 conjugation imparts a switch-like response on the polyubiquitin chain synthesis activity of the CRL5^{Vif-CBF β} ligase in a manner similar to that described for CRL1 (also known as the SCF) [35]. This effect requires specific interactions between UBE2F, RBX2, and CUL5 formed by residues at the periphery of the UBE2F-binding surface of RBX2, and a unique loop found in UBE2F that enhances NEDD8ylation activity for CUL5. The interactions identified by our combined NMR, mutational and kinetic analyses are consistent with a recent crystallographic study showing how NEDD8~E2 thioester may be positioned by the RBX subunit and the Cullin C-terminal domain (CTD) for efficient conjugation [33]. The unique active site proximal loop of UBE2F is important for viral infectivity and was found to contribute 2 log-units to the rate of NEDD8 conjugation but was dispensable for binding of RBX2. These observations are consistent the notion that the active site proximal loop of UBE2F could stabilize the transition state for catalysis, possibly by directly binding CUL5, but more detailed structural and kinetic studies will be required to prove this point.

The results presented here are at variance with the initial identification of RBX1 as the RING subunit of the Vif-CUL5 complex[11]. RBX1 was found to co-IP with Vif in HIV-infected T-cells, but the presence of RBX2 was not evaluated. Two experiments supported the function of RBX1 with Vif. Overexpression of a mutant CUL5(Δ RBX1) that blocked association with RBX1 was found to have a dominant negative effect on Vif function; however, this mutation disrupts a region of the CUL5 CTD that interacts with a strand conserved between RBX1 and RBX2 (**Fig. S3**) [36]; therefore, the effect of this mutant may derive from a loss of RBX2 as well as RBX1 binding. Additionally, it was shown that overexpression of RBX1 could inhibit Vif function, though RBX1 can interact with multiple ubiquitin and NEDD8 conjugating enzymes, so overexpression could titrate away E2 coenzymes required for endogenous CRL activity. We suggest the initial detection of RBX1 in Vif immunoprecipitates may result from copurified CUL2, which together with CUL5, was recently detected by affinity-purification mass-spectrometry studies of Vif expressed in Jurkat T-cells [6]. The observation that knockdown UBE2F or RBX2 impairs the ability of Vif to counteract APOBEC3G is in line with a body of work showing CUL5/RBX2 form a functional heterodimer in metazoans [22,23,37].

Prior studies indicate that NEDD8ylation of target CRL could be regulated, leading to the possibility that cofactors other than UBE2F and NEDD8 modulate Vif activity. In support of this idea, it was found that UBE2F activity was

restricted to CUL5/RBX2 *in vivo* though it can function with RBX1 and RBX2 when overexpressed in cells or at high levels *in vitro* [22]. Negative and positive regulation of CRL activity can be achieved at the level of RING/E2 association as reported in recent studies. For example, Glomulin is an RBX1-specific binding factor that blocks association with ubiquitin conjugating enzymes thereby inhibiting chain formation activity of CRLs [38]. The yeast Defective in Cullin Nedd8ylation (DCN1) gene is required for the UBE2M homologue (UBC12) to promote NEDD8ylation of CUL1 (CDC53) [39]. Structural and functional studies indicate DCN1 and RBX subunits of the CRL work together as dual E3s to promote NEDD8 conjugation [40,41]. An important challenge for future work is to understand RBX2 and UBE2F-specific cofactors that modulate CRL5 activity and affect virus/host conflict through the Vif-APOBEC3 axis.

The Vif-APOBEC3 axis has long been considered an attractive drug target [42]. In terms of selectivity, direct and rational targeting of the interaction between Vif and APOBEC3 restriction factors would be ideal; however, high resolution structures of these complexes are unavailable and the absence of robust reconstituted systems for *in vitro* high-throughput screening have hampered this approach. Accordingly, most efforts to inhibit Vif function to date have utilized cell-based high throughput screens [43,44]. Potentially promising lead compounds have been identified although selectivity and mechanisms of action are poorly understood [44,45,46]. MLN4924 represents an alternative approach to inhibiting Vif: it has a well-characterized mechanism of action; it is highly

selective for the NEDD8 E1 (over Sumo and Ubiquitin UBE1); it is validated in mouse models of cancer and currently in clinical trials [20,21]. It is tempting to speculate that MLN4924 might be useful for treating individuals infected with HIV and resistant to HAART but evaluation of efficacy and how this would be tolerated in the case of chronic infection remains a challenge for preclinical studies.

Alternatively, inhibition of UBE2F would block activation of CRL5 but not CRL1-4 and could therefore be a more selective route to Vif inhibition than MLN4924. Since Vif counteracts several A3 enzymes present in T-lymphocytes [5,30,47], selective targeting of UBE2F with small molecule inhibitors to reduce the activity of CRL5 could potentially unleash the restriction potential of A3 enzymes without perturbing the function of CRL1-4. The recent discovery of a specific allosteric small molecule inhibitor of a ubiquitin E2 (hCDC34a) suggests selective inhibition of NEDD8 conjugating enzymes is indeed possible [48]. Inhibition of host pathways required for HIV infectivity such as NEDD8 cascades, in isolation or in combination with current antiretroviral therapies, could be an important strategy to avoid resistance mutations and could be a viable antiretroviral therapy.

MATERIALS AND METHODS

Stable shRNA knockdown of host factors in HEK293T cells and single-cycle infectivity assay

pLKO.I lentiviral vector plasmids expressing shRNA targeting UBE2M/F and a puromycin selectable marker were purchased from Open Biosystems: UBE2M: TRCN0000007259 ; UBE2F: TRCN0000034110. A control pLKO.I lentivector plasmid expressing a scramble shRNA was obtained from Addgene [49]. Lentiviral vectors pseudotyped with vesicular stomatitis virus glycoprotein G (VSV-G) were produced and normalized for p24 capsid content as previously described [50]. At day 1, HEK293T cells were transduced with shRNA vectors in 12-well plates for 36 hours. At day 3, transduced cells were replated in 6-well plates and stably transduced cells selected in 4 µg/ml puromycin (Invitrogen) for 72 hours. At day 5, transduced and selected cells were transfected with relevant plasmids to produce HIV_{NL4-3}ΔVif or NL4-3-Luc reporter virus, in the presence or absence of exogenous APOBEC3G, and HIV Vif, using Fugene 6 transfection reagent (Roche). After 48 hours, virus was harvested and filtered using 0.45 µm filters (Millipore) to remove cell debris. TZMbl reporter (in case of HIV_{NL4-3}ΔVif or WT virus) or GHOST (in case of NL4-3-Luc reporter virus) cells were infected with virus normalized for p24 capsid content as determined by p24 ELISA (Pierce). After 48 hours cells were lysed and luciferase activity determined using a Luciferase Assay Kit (Promega). To determine viral infectivity in the presence of MLN4924 (ActiveBiochem), HEK293T cells were transfected for 24 hours with plasmid pNL4-

3 WT before compound was added. After 24 hours, virus was harvested and TZMbl cells infected with virus normalized for p24 capsid content as determined by p24 ELISA (Pierce) for 6 hours. After 24 hours cells were lysed, and luciferase activity determined using a Luciferase Assay Kit (Promega). For analysis of APOBEC3G incorporation in the viral particles, virus was concentrated by sucrose cushion ultracentrifugation as described previously [10]. Plasmids expressing APOBEC3G-V5 and Vif-FLAG were described previously [10]. HIV_{NL4-3}ΔVif was produced by deletion of the Vif start codon and introduction of tandem stop codons introduced downstream in the Vif gene of the HIV_{NL4-3} WT plasmid. All transfections were performed with the same total amount of DNA and were complemented with empty plasmid vector pcDNA3.1 when either Vif, A3G or both were withheld from the experiment.

Determination of G to A mutation rate in viral genomic DNA

Viral gDNA mutation rates were determined as described previously by Russell et al. [51]. In short, virus was produced in the presence of A3G in HEK293T cells in the presence of 500 nM MLN4924 or DMSO. The resulting virus was used to infect TZMbl cells and after 36 hours viral gDNA was prepared using QIAGEN Genomic DNA Purification kit (Qiagen). HIV specific sequences were Taq PCR amplified using primers F: GTCTGTTGTGTGACTCTGGTAAC and R: CCTGTCTGAAGGGATGGTTGTAG and TOPO-TA subcloned (Invitrogen). Sequences were determined and the amount of G to A mutations counted in each viral sequence.

Immunoblots

Immunoprecipitated complexes were separated by 15% SDS-PAGE and transferred to HyBond-ECL nitrocellulose membranes. Following blockage in a 5% milk TBS solution, membranes were probed with appropriate primary antibodies to FLAG-peptide (Sigma), V5 (R961-25, Invitrogen), Actin (Ab8227, Abcam), Myc (Ab9106, Abcam), tubulin (Ab4074, Abcam), UBE2F (15707, Abcam), UBE2M (Rockland Pharmaceuticals), RBX1 (Invitrogen), HIV p24 (Ab9071, Abcam). Appropriate secondary antibodies were applied and immunoblots were visualized by ECL.

Ubiquitination assays

Ubiquitination assays were performed at room temperature with the ubiquitin activating system containing: 2 mM ATP, human ubiquitin activating enzyme (UBE1) (200 nM), wild-type ubiquitin or variants (methylated or K48R) (75 μ M), 4 μ M E2 (UBE2R1) in addition to 0.625 μ M Vif E3 and 200 nM APOBEC3 proteins in buffer containing 30 mM Tris-Cl (pH 7.3), 100 mM NaCl, 5 mM MgCl₂, in a total reaction volume of 10 ml. CRL5^{Vif-CBF β} was pre-NEDD8ylated in conditions that included: 50 mM NaCl, 50 mM Tris-Cl pH 7.6, 2.5 mM MgCl₂, 2 mg/ml BSA, 2 mM ATP, 100 nM NEDD8 activating enzyme (NAE), 2 μ M UBE2F, 30 μ M NEDD8 and 4 μ M Vif E3 ligase. After 1 hr, the NEDD8 reaction mixture was diluted ~6 fold upon the addition of the ubiquitin activating system and substrate. The ubiquitination reactions were quenched after 1 hr by the addition

of 2x SDS loading dye. UBE1, NEDD8, and ubiquitin variants were purchased from Boston Biochem. Ubiquitinated A3 proteins were detected using a monoclonal anti-c-Myc antibody (Sigma).

Protein expression and Purification

All constructs and mutations were generated by standard PCR and restriction-based cloning methods unless otherwise noted. HIS₆-tagged UBE2F full-length or residues 26-185 (UBE2F_{core}), GST-tagged UBE2M, HIS₆-UBE2R1, HIS₆-GB1-tagged RBX2_{RING} (44-113) were expressed in *E. coli*. HIS₆-GB1-tagged CUL5-RBX2 was co-expressed in *E. coli* from a pRSF-Duet plasmid. All tags were removed by TEV protease or thrombin (Sigma). All proteins were subjected to size exclusion chromatography for the final purification. The RBX2(Swap4) mutant was obtained by custom cDNA synthesis (Gene Art). All constructs were verified by sequencing of the entire open reading frame.

For expression, plasmids encoding UBE2F, RBX2_{RING} and CUL5/RBX2, were transformed into either *E. coli* BL21(DE3)-Star or BL21(DE3) (Invitrogen) cells and grown at 37 °C to an optical density of 0.4-0.6, incubated at 17 °C until an optical density of 1.2 was reached and induced with 0.5 mM IPTG overnight. 100 µM ZnCl₂ was added to cultures harboring RING-containing constructs approximately one hour prior to induction. Unlabelled, ¹⁵N- or ¹³C-labelled proteins were expressed in cells grown in LB media, M9 media supplemented with 1 gram of ¹⁵N NH₄Cl, or M9 media supplemented with 2 grams of ¹³C-glucose, respectively.

Unless otherwise noted, all proteins were purified at 4 °C according to the following protocol. 10 μ M ZnCl₂ was included in the buffers for all proteins containing a RING-domain. Cells from 1L of culture were resuspended in 20 mL lysis buffer (20 mM HEPES pH=7.6, 500 mM NaCl, 10 mM imidazole, 0.1 % NP-40, 10% glycerol, 10 mM β -mercaptoethanol, 1 mg/mL lysozyme (Sigma), 0.2 tablet EDTA-free complete protease-inhibitor cocktail (Roche)), and incubated on ice for 20 minutes followed by sonication and high-speed centrifugation. The soluble fraction was incubated with Ni-NTA resin (Qiagen) for 1 h, and loaded onto a gravity column. The resin was then extensively washed with at least 30 column volumes (CV) Lysis Buffer and 30 CV Wash Buffer (20 mM HEPES pH=7.6, 500 mM NaCl, 20 mM imidazole, 10 % glycerol 10 mM β -mercaptoethanol). Specifically bound proteins were eluted with 20 mL Elution Buffer (20 mM HEPES pH=7.6, 500 mM NaCl, 250 mM imidazole, 10 % glycerol 10 mM β -mercaptoethanol) per 5 grams cell pellet. Tags were removed by incubation with TEV protease overnight during dialysis against Dialysis Buffer (20 mM HEPES pH=7.6, 500 mM NaCl, 10 % glycerol, 1 mM DTT). Cleaved tags, uncleaved proteins, and TEV protease were removed by two passages through a Ni-NTA gravity column. Size exclusion chromatography into buffer (20 mM HEPES pH=7.6, 150 mM NaCl, 1 mM DTT) was used as a final purification step. Proteins >95 % pure were then concentrated and used as-is, or aliquoted into single-use portions and flash-frozen in liquid nitrogen. The NEDD8 E1 (NAE), NEDD8 containing an N-terminal PKA-site and GST-UBE2M were prepared as previously described [52]. Purified 6-protein CRL5^{Vif-CBF β}

complex was obtained as described previously [12]. Recombinant A3A- and A3G-myc-His₆ were purified from HEK293T cells as described [53,54].

NMR Spectroscopy

All spectra were recorded at 20 °C on Bruker spectrometers equipped with cryoprobes and processed with NMRPipe [55]. Backbone resonance assignments of UBE2F_{core} and RBX2_{RING} were obtained using standard triple resonance methodology [56]. Titration data were collected on a Bruker 800 MHz spectrometer outfitted with a cryoprobe using 50 µM ¹⁵N-labelled protein and increasing amounts of unlabelled ligand in a standard buffer (100 mM NaCl, 1 mM DTT and 25 mM HEPES, pH=7.5). Chemical shift changes in titration series were analyzed using CCPNMR [57] and fit to standard ligand-binding curves in SigmaPlot.

Stable knockdown of RBX1 and 2 in CD4+ T-cell lines and assay of viral spread

Stable knockdown of RBX1 or RBX2 in H9 and SupT1 CD4+ T-lymphoblastoid cell lines was performed via VSV-G pseudotyped lentiviral transduction employing the pGIPz shRNAmir lentiviral vector system from Open Biosystems. Cells were obtained from the National Institutes of Health AIDS Reagent Program and maintained in RPMI + 11.5% fetal calf serum (Hyclone) at 37°C, 5% CO₂. The following shRNAmir constructs were utilized: RBX1, V3LHS_637679 and V3LHS_637677; RBX2, V2LHS_197071, V3LHS_408994,

and V3LHS_408992; Non-silencing scrambled control, RHS 4346. VSV-G pseudotyped lentiviruses were produced in HEK293T cells as described above for pLKO.I lentiviral vectors. Infectious titers (TU/mL) of pGIPz-derived pseudotyped lentiviruses were determined via serial dilution of virus over HEK293T cells followed by flow cytometric analysis for cellular green fluorescent protein (GFP) expression (visual indicator incorporated into the integrated pGIPz transgene cassette) 3 days following transduction. H9 and SupT1 cells were transduced with 20 TU/cell via centrifugal inoculation at 1200 x g at 37°C for 2 hours in media containing 8 µg/mL polybrene. Input inoculum was then removed, the cells washed once with phosphate-buffered saline (PBS), and the media replaced. Five to seven days following transduction, when T-cells exhibited strong transgene-driven GFP expression, puromycin (Invitrogen) selection was initiated at 2 µg/mL for 7 days and afterward reduced at 0.5 µg/mL to maintain transgene expression. Knockdown efficiency was determined 14 days following the initiation of puromycin selection via RT-qPCR.

HIV_{NL4-3} and HIV_{NL4-3}ΔVif (start codon deleted and tandem stop codons introduced downstream) were generated via transient transfection of HEK293T cells using Polyjet lipofection reagent (SignaGen) per manufacturer's protocol. Three days following transfection, virus-laden culture supernatant was harvested, DNase-treated with 20 µg/mL DNase (Roche), 0.45 µm filtered, aliquoted, and stored at -80°C. Virus titers were determined via p24 ELISA as described above.

HIV spreading assays were performed via inoculation of 250K transduced H9 or SupT1 T-cells with 25 ng of HIV (corresponding to a multiplicity of infection of 0.1) in 250 μ L culture media in triplicate sets of wells in 96-well microtiter plates. Twenty-four hours post inoculation, input virus was aspirated, the cells washed with PBS, and the media replaced. The infections were then monitored in 48-72 hour intervals via immunofluorescence assay for cellular HIV antigen synthesis and via p24 ELISA in the culture supernatant for progeny virus production.

RT-qPCR

Transduced cells were lysed with QIAshredder columns (QIAGEN) and total RNA was isolated using RNeasy Mini Kit (QIAGEN). On-column DNase digestion was performed using RNase-Free DNase Set (QIAGEN). Total RNA was reverse transcribed with iScript Reverse Transcription Supermix (BIO-RAD), using a mix of oligodT and random primers in a 20 μ L reaction according to the manufacturer's protocol. Salt-free primers for RNAi target gene (RBX2: forward primer ACG TGG AGT GCG ATA CGT G; reverse primer ACA TTC TCC CCA GAC CAC AA, RBX1: forward primer TGC AGG AAC CAC ATT ATG GA; reverse primer GCG AGA GAT GCA GTG GAA GT) and reference gene (RPLP0: forward primer GCT GCT GCC CGT GCT GGT G; reverse primer TGG TGC CCC TGG AGA TTT TAG TGG) were generated (Integrated DNA Technologies) and cDNA levels were compared by quantitative PCR using SsoAdvanced SYBR Green Supermix (BIO-RAD) and CFX Connect Real-Time PCR Detection System (BIO-

RAD). All reactions were performed in triplicate and individual samples were normalized to the human gene RPLP0. Relative gene expression was calculated using the $\Delta\Delta C_q$ method as described by Livak and Schmittgen [58].

NEDD8ylation assays

200 μM NEDD8 containing N-terminal PKA site was radiolabeled with 2,500 units of PKA (NEB) and 7 ml of $^{32}\text{P}(\gamma)\text{-ATP}$ (specific activity of 6000Ci/mmol) in a total reaction volume of 50 ml of PKA reaction buffer (NEB). Pulse chase assays were performed at room temperature as previously described [22], with the following changes: the final concentration of E2 and CUL5 were 100 nM and 500 nM respectively. Reactions were visualized by phosphorimaging (Typhoon) after fractionation on 8-12% SDS-PAGE gels (Biorad), that were then dried and exposed to a storage phosphor screen overnight. Data were quantified as a ratio of product (NEDD8ylated CUL5) to the total of substrate and product (NEDD8ylated CUL5 and UBE2~N8) using ImageQuant. Initial rates were determined as described previously [41].

Assays for inhibition of UBE2F charging were performed by pre-mixing NEDD8 E1 and MLN4924 in for 10 minutes, and adding this to a second solution to give a final concentration of 12 μM UBE2F, 5 nM NEDD8 E1, 1.5 μM ^{32}P -labelled NEDD8, 50 μM ATP and a variable concentration of inhibitor in 10 μL of 1X reaction buffer (same as above). Reactions were stopped after 3 minutes by the addition of 1 equivalent of non-reducing SDS-PAGE loading dye containing 10 mM EDTA. Gels were visualized as above. Bands were quantified by

comparison to a simultaneously exposed dilution series of a known concentration of ^{32}P -NEDD8. Data from multiple independent experiments was fit to a 4-parameter logistic equation, yielding an IC50 of 38 ± 4.3 n.

Modeling

The model of UBE2F/RBX2 was created using NMR chemical shift perturbations as HADDOCK restraints using PDB codes 2ECL and 2EDI as inputs [59]. The model of CUL5/RBX2/UBE2F was generated using the ALIGN command of PyMol and PDB codes 2ECL, 2EDI, 3RTR and 3EB6 as inputs [33,60].

ACKNOWLEDGEMENTS: We thank Takanori Kigawa and Mikako Shirouzu for sample preparation and help with the screening data of the human UBE2F; Matt Jacobson and Adam Steeves for insightful discussions; and Dr. Brenda Schulman (St. Jude's Medical Center) for sharing expression constructs for GST-NAE1-UBA3 and GST-NEDD8.

REFERENCES

1. Ott M, Geyer M, Zhou Q (2011) The control of HIV transcription: keeping RNA polymerase II on track. *Cell Host Microbe* 10: 426-435.
2. von Schwedler UK, Stuchell M, Muller B, Ward DM, Chung HY, et al. (2003) The protein network of HIV budding. *Cell* 114: 701-713.
3. Suhasini M, Reddy TR (2009) Cellular proteins and HIV-1 Rev function. *Curr HIV Res* 7: 91-100.
4. Namy O, Moran SJ, Stuart DI, Gilbert RJ, Brierley I (2006) A mechanical explanation of RNA pseudoknot function in programmed ribosomal frameshifting. *Nature* 441: 244-247.
5. Malim MH, Emerman M (2008) HIV-1 accessory proteins--ensuring viral survival in a hostile environment. *Cell Host Microbe* 3: 388-398.
6. Jäger S, Cimermancic P, Gulbahce N, Johnson JR, McGovern KE, et al. (2012) Global landscape of HIV-human protein complexes. *Nature* 481: 365-370.
7. Sheehy AM, Gaddis NC, Choi JD, Malim MH (2002) Isolation of a human gene that inhibits HIV-1 infection and is suppressed by the viral Vif protein. *Nature* 418: 646-650.
8. Malim MH (2009) APOBEC proteins and intrinsic resistance to HIV-1 infection. *Philos Trans R Soc Lond B Biol Sci* 364: 675-687.
9. Harris RS, Bishop KN, Sheehy AM, Craig HM, Petersen-Mahrt SK, et al. (2003) DNA deamination mediates innate immunity to retroviral infection. *Cell* 113: 803-809.
10. Zheng YH, Irwin D, Kurosu T, Tokunaga K, Sata T, et al. (2004) Human APOBEC3F is another host factor that blocks human immunodeficiency virus type 1 replication. *J Virol* 78: 6073-6076.
11. Yu X, Yu Y, Liu B, Luo K, Kong W, et al. (2003) Induction of APOBEC3G ubiquitination and degradation by an HIV-1 Vif-Cul5-SCF complex. *Science* 302: 1056-1060.
12. Jäger S, Kim DY, Hultquist JF, Shindo K, LaRue RS, et al. (2012) Vif hijacks CBF-beta to degrade APOBEC3G and promote HIV-1 infection. *Nature* 481: 371-375.
13. Zhang WY, Du J, Evans SL, Yu YK, Yu XF (2012) T-cell differentiation factor CBF-beta regulates HIV-1 Vif-mediated evasion of host restriction. *Nature* 481: 376-U159.
14. Wong WF, Kohu K, Chiba T, Sato T, Satake M (2011) Interplay of transcription factors in T-cell differentiation and function: the role of Runx. *Immunology* 132: 157-164.
15. Hultquist JF, Binka M, Larue RS, Simon V, Harris RS (2012) Vif Proteins of Human and Simian Immunodeficiency Viruses Require Cellular CBFbeta To Degrade APOBEC3 Restriction Factors. *J Virol* 86: 2874-2877.
16. Pickart CM (2001) Mechanisms underlying ubiquitination. *Annu Rev Biochem* 70: 503-533.

17. Mehle A, Strack B, Ancuta P, Zhang C, McPike M, et al. (2004) Vif overcomes the innate antiviral activity of APOBEC3G by promoting its degradation in the ubiquitin-proteasome pathway. *J Biol Chem* 279: 7792-7798.
18. Deshaies RJ, Emberley ED, Saha A (2010) Control of cullin-ring ubiquitin ligase activity by nedd8. *Subcell Biochem* 54: 41-56.
19. Petroski MD, Deshaies RJ (2005) Function and regulation of cullin-RING ubiquitin ligases. *Nat Rev Mol Cell Biol* 6: 9-20.
20. Soucy TA, Smith PG, Milhollen MA, Berger AJ, Gavin JM, et al. (2009) An inhibitor of NEDD8-activating enzyme as a new approach to treat cancer. *Nature* 458: 732-736.
21. Brownell JE, Sintchak MD, Gavin JM, Liao H, Bruzzese FJ, et al. (2010) Substrate-assisted inhibition of ubiquitin-like protein-activating enzymes: the NEDD8 E1 inhibitor MLN4924 forms a NEDD8-AMP mimetic in situ. *Mol Cell* 37: 102-111.
22. Huang DT, Ayrault O, Hunt HW, Taherbhoy AM, Duda DM, et al. (2009) E2-RING expansion of the NEDD8 cascade confers specificity to cullin modification. *Mol Cell* 33: 483-495.
23. Kamura T, Maenaka K, Kotoshiba S, Matsumoto M, Kohda D, et al. (2004) VHL-box and SOCS-box domains determine binding specificity for Cul2-Rbx1 and Cul5-Rbx2 modules of ubiquitin ligases. *Genes Dev* 18: 3055-3065.
24. Yu Q, Konig R, Pillai S, Chiles K, Kearney M, et al. (2004) Single-strand specificity of APOBEC3G accounts for minus-strand deamination of the HIV genome. *Nat Struct Mol Biol* 11: 435-442.
25. Zhang H, Yang B, Pomerantz RJ, Zhang C, Arunachalam SC, et al. (2003) The cytidine deaminase CEM15 induces hypermutation in newly synthesized HIV-1 DNA. *Nature* 424: 94-98.
26. Mangeat B, Turelli P, Caron G, Friedli M, Perrin L, et al. (2003) Broad antiretroviral defence by human APOBEC3G through lethal editing of nascent reverse transcripts. *Nature* 424: 99-103.
27. Refsland EW, Hultquist JF, Harris RS (2012) Endogenous origins of HIV-1 G-to-A hypermutation and restriction in the nonpermissive T cell line CEM2n. *PLoS Pathog* 8: e1002800.
28. DeHart JL, Bosque A, Harris RS, Planelles V (2008) Human immunodeficiency virus type 1 Vif induces cell cycle delay via recruitment of the same E3 ubiquitin ligase complex that targets APOBEC3 proteins for degradation. *J Virol* 82: 9265-9272.
29. Huthoff H, Malim MH (2007) Identification of amino acid residues in APOBEC3G required for regulation by human immunodeficiency virus type 1 Vif and Virion encapsidation. *J Virol* 81: 3807-3815.
30. Refsland EW, Stenglein MD, Shindo K, Albin JS, Brown WL, et al. (2010) Quantitative profiling of the full APOBEC3 mRNA repertoire in lymphocytes and tissues: implications for HIV-1 restriction. *Nucleic Acids Res* 38: 4274-4284.

31. Kamura T, Burian D, Yan Q, Schmidt SL, Lane WS, et al. (2001) Muf1, a novel Elongin BC-interacting leucine-rich repeat protein that can assemble with Cul5 and Rbx1 to reconstitute a ubiquitin ligase. *J Biol Chem* 276: 29748-29753.
32. Kobayashi M, Takaori-Kondo A, Miyauchi Y, Iwai K, Uchiyama T (2005) Ubiquitination of APOBEC3G by an HIV-1 Vif-Cullin5-Elongin B-Elongin C complex is essential for Vif function. *J Biol Chem* 280: 18573-18578.
33. Calabrese MF, Scott DC, Duda DM, Grace CR, Kurinov I, et al. (2011) A RING E3-substrate complex poised for ubiquitin-like protein transfer: structural insights into cullin-RING ligases. *Nat Struct Mol Biol* 18: 947-949.
34. Randow F, Lehner PJ (2009) Viral avoidance and exploitation of the ubiquitin system. *Nat Cell Biol* 11: 527-534.
35. Saha A, Deshaies RJ (2008) Multimodal activation of the ubiquitin ligase SCF by Nedd8 conjugation. *Mol Cell* 32: 21-31.
36. Duda DM, Borg LA, Scott DC, Hunt HW, Hammel M, et al. (2008) Structural insights into NEDD8 activation of cullin-RING ligases: conformational control of conjugation. *Cell* 134: 995-1006.
37. Donaldson TD, Noureddine MA, Reynolds PJ, Bradford W, Duronio RJ (2004) Targeted disruption of *Drosophila* Roc1b reveals functional differences in the Roc subunit of Cullin-dependent E3 ubiquitin ligases. *Mol Biol Cell* 15: 4892-4903.
38. Tron AE, Arai T, Duda DM, Kuwabara H, Olszewski JL, et al. (2012) The glomovenous malformation protein Glomulin binds Rbx1 and regulates cullin RING ligase-mediated turnover of Fbw7. *Mol Cell* 46: 67-78.
39. Kurz T, Ozlu N, Rudolf F, O'Rourke SM, Luke B, et al. (2005) The conserved protein DCN-1/Dcn1p is required for cullin neddylation in *C. elegans* and *S. cerevisiae*. *Nature* 435: 1257-1261.
40. Kurz T, Chou YC, Willems AR, Meyer-Schaller N, Hecht ML, et al. (2008) Dcn1 functions as a scaffold-type E3 ligase for cullin neddylation. *Mol Cell* 29: 23-35.
41. Scott DC, Monda JK, Grace CR, Duda DM, Kriwacki RW, et al. (2010) A dual E3 mechanism for Rub1 ligation to Cdc53. *Mol Cell* 39: 784-796.
42. Smith JL, Bu W, Burdick RC, Pathak VK (2009) Multiple ways of targeting APOBEC3-virion infectivity factor interactions for anti-HIV-1 drug development. *Trends Pharmacol Sci* 30: 638-646.
43. Cao J, Isaacson J, Patick AK, Blair WS (2005) High-throughput human immunodeficiency virus type 1 (HIV-1) full replication assay that includes HIV-1 Vif as an antiviral target. *Antimicrob Agents Chemother* 49: 3833-3841.
44. Nathans R, Cao H, Sharova N, Ali A, Sharkey M, et al. (2008) Small-molecule inhibition of HIV-1 Vif. *Nat Biotechnol* 26: 1187-1192.
45. Cen S, Peng ZG, Li XY, Li ZR, Ma J, et al. (2010) Small molecular compounds inhibit HIV-1 replication through specifically stabilizing APOBEC3G. *J Biol Chem* 285: 16546-16552.

46. Xiao Z, Ehrlich E, Luo K, Xiong Y, Yu XF (2007) Zinc chelation inhibits HIV Vif activity and liberates antiviral function of the cytidine deaminase APOBEC3G. *FASEB J* 21: 217-222.
47. Hultquist JF, Lengyel JA, Refsland EW, LaRue RS, Lackey L, et al. (2011) Human and rhesus APOBEC3D, APOBEC3F, APOBEC3G, and APOBEC3H demonstrate a conserved capacity to restrict Vif-deficient HIV-1. *J Virol* 85: 11220-11234.
48. Ceccarelli DF, Tang X, Pelletier B, Orlicky S, Xie W, et al. (2011) An allosteric inhibitor of the human cdc34 ubiquitin-conjugating enzyme. *Cell* 145: 1075-1087.
49. Sarbassov DD, Guertin DA, Ali SM, Sabatini DM (2005) Phosphorylation and regulation of Akt/PKB by the rictor-mTOR complex. *Science* 307: 1098-1101.
50. Gijssbers R, Ronen K, Vets S, Malani N, De Rijck J, et al. (2010) LEDGF hybrids efficiently retarget lentiviral integration into heterochromatin. *Mol Ther* 18: 552-560.
51. Russell RA, Moore MD, Hu WS, Pathak VK (2009) APOBEC3G induces a hypermutation gradient: purifying selection at multiple steps during HIV-1 replication results in levels of G-to-A mutations that are high in DNA, intermediate in cellular viral RNA, and low in virion RNA. *Retrovirology* 6: 16.
52. Huang DT, Schulman BA (2005) Expression, purification, and characterization of the E1 for human NEDD8, the heterodimeric APPBP1-UBA3 complex. *Methods Enzymol* 398: 9-20.
53. Stenglein MD, Burns MB, Li M, Lengyel J, Harris RS (2010) APOBEC3 proteins mediate the clearance of foreign DNA from human cells. *Nat Struct Mol Biol* 17: 222-229.
54. Shlyakhtenko LS, Lushnikov AY, Li M, Lackey L, Harris RS, et al. (2011) Atomic force microscopy studies provide direct evidence for dimerization of the HIV restriction factor APOBEC3G. *J Biol Chem* 286: 3387-3395.
55. Delaglio F, Grzesiek S, Vuister GW, Zhu G, Pfeifer J, et al. (1995) NMRPipe: a multidimensional spectral processing system based on UNIX pipes. *J Biomol NMR* 6: 277-293.
56. Sattler M, Schleucher J, Griesinger C (1999) Heteronuclear multidimensional NMR experiments for the structure determination of proteins in solution employing pulsed field gradients. *Progress in Nuclear Magnetic Resonance Spectroscopy* 34: 93-158.
57. Vranken WF, Boucher W, Stevens TJ, Fogh RH, Pajon A, et al. (2005) The CCPN data model for NMR spectroscopy: development of a software pipeline. *Proteins* 59: 687-696.
58. Livak KJ, Schmittgen TD (2001) Analysis of relative gene expression data using real-time quantitative PCR and the 2^{-Delta Delta C(T)} Method. *Methods* 25: 402-408.

59. Dominguez C, Boelens R, Bonvin AM (2003) HADDOCK: a protein-protein docking approach based on biochemical or biophysical information. *Journal of the American Chemical Society* 125: 1731-1737.
60. Mace PD, Linke K, Feltham R, Schumacher FR, Smith CA, et al. (2008) Structures of the cIAP2 RING domain reveal conformational changes associated with ubiquitin-conjugating enzyme (E2) recruitment. *J Biol Chem* 283: 31633-31640.
61. Albin JS, Hache G, Hultquist JF, Brown WL, Harris RS (2010) Long-term restriction by APOBEC3F selects human immunodeficiency virus type 1 variants with restored Vif function. *J Virol* 84: 10209-10219.

FIGURE LEGENDS

Fig. 1. Pharmacological Inhibition of NEDD8 E1 by MLN4924 blocks the ability of Vif to counteract A3G

A, Single-cycle infectivity assay of HIV_{NL4-3} produced in HEK293T cells transfected with empty vector control (white bars) or V5-tagged A3G (black bars, 120 ng), 1 µg of NL4-3 proviral DNA and treated with indicated concentrations of MLN4924. **B**, Parallel immunoblots indicating MLN4924 restores steady-state levels of A3G in cells and packaging in virions. **C**, Quantitation of G to A mutations in gDNA sequences from virions produced in cells treated with either DMSO or 500 nM MLN4924.

Fig. 2. Vif requires the NEDD8 E2, UBE2F, to degrade A3G and mediate HIV Infectivity

A, Knockdown of UBE2F but not UBE2M impairs viral infectivity. HEK293T cells stably depleted for UBE2M (grey bars), UBE2F (white bars) or in non-silencing control shRNA (black bars) were transfected with 1 µg proviral DNA (NL4-3), 340 ng A3G or empty vector and infectivity of produced virions was measured. Mean and 1 SD of duplicate experiments are graphed. **B**, Immunoblots corresponding to experiments shown in panel **A** show an increase in A3G stability in cells treated with UBE2F shRNAs relative to cells treated with UBE2M or scramble shRNAs. **C**, HIV requires Vif and UBE2F to fully neutralize A3G. Single-cycle infectivity assay of HIV_{NL4-3}ΔVif produced in HEK293T cells stably

depleted for UBE2M (grey bars), UBE2F (white bars) or non-silencing control shRNA (black bars). A3G (500ng) or empty vector was co-transfected with 1 μ g HIV_{NL4-3} Δ Vif and increasing amounts of Vif-FLAG (0, 15, 100, or 350 ng). Values were normalized to the infectivity in absence of A3G and mean and 1 SD of duplicate experiments are graphed. **D**, Immunoblots corresponding to samples in panel **C** without Vif and with the highest amount of Vif, indicating reduction of cellular and virally packaged A3G depends on Vif and UBE2F but not UBE2M. **E**, Infectivity of HIV_{NL4-3} Δ Vif produced in HEK293T cells stably depleted for UBE2F (white bars), or non-silencing control shRNA (black bars) in the presence of transfected HIV_{NL4-3} Δ Vif (1 μ g), A3G-V5 (500 ng), Vif-FLAG (+Vif, 100 ng), RNAi-immune UBE2F-myc (+UBE2F, 10 ng) or empty vector controls indicated by -Vif and -UBE2F. Mean and 1 SD of duplicate experiments are graphed. The presence of the RNAi-immune UBE2F vector in +Vif cells yielded a partial recovery of infectivity relative to control cells, but not in -Vif cells. Partial complementation may be due to the confounding effects of a mixed pool of knockdown cells and the observation that transfection of larger amounts of UBE2F inhibit virus production (data not shown). **F**, Immunoblots of cell lysates and virus particles corresponding to panel **E**. The ability of Vif to promote degradation and reduce packaging of A3G is strongly reduced in UBE2F KD cells (lanes 1, 2, 5, 6), and partially recovered in the presence of transfected RNAi-immune UBE2F (lanes 3, 4, 7, 8). The asterisk indicates the observed band for endogenous UBE2F. Long and short exposure times for the immunoblots are indicated.

Fig. 3. UBE2F is required for activation of CRL5^{Vif-CBF β} *in vitro*

A, Diagram of the ubiquitination protocol used in panel **B**. **B**, *In vitro* ubiquitination of A3G by recombinant CRL5^{Vif-CBF β} with UBE2R1 as ubiquitin conjugating enzyme requires UBE2F. Immunoblots of ubiquitination reactions containing myc-tagged A3G as the substrate show high-molecular weight polyubiquitin chains, require all protein components of the ubiquitin and NEDD8 activating systems and are only observed when UBE2F (lane 9) but not when UBE2M (lane 10) is used as NEDD8 conjugating enzyme. A3A is not susceptible to Vif and was used as a negative control. **C**, Coomassie-stained SDS-PAGE of NEDD8ylation “pulse” reaction indicates that under conditions used in panel **B** indicate CUL5 is completely NEDD8ylated by UBE2F; only a minor fraction (<5%) is NEDD8ylated by UBE2M. **D**, ¹⁵N-HSQC spectral overlays of RBX2_{RING} in the presence and absence of ~100 μ M, unlabeled full-length UBE2M (top) or UBE2F (bottom).

Fig. 4. RBX2 is required for viral spread through non-permissive CD4+ H9 T-cells

A, HIV multiple round replication assays are shown for indicated viruses in Vif-permissive (SupT1) or Vif non-permissive (H9) cell lines transduced with viruses producing either control (shSCR) or RBX2-specific (shRBX2-5) shRNAs. Blue circles indicate shSCR treated cells infected with NL4-3 virus, yellow triangles indicate shSCR treated cells infected with NL4-3 virus lacking Vif, and red diamonds indicate shRBX2-5

treated cells infected with NL4-3 virus. Points are the mean of three independent biological replicates, error bars indicate 1 SD. **B**, Relative RBX2 mRNA knockdown normalized to non-silencing shSCR control as determined by RT-qPCR for the cell lines shown in panel **A**. Bars indicate the average of triplicate measurements, error bars are 1 SD.

Fig. 5. Structural basis for discrimination between NEDD8 pathways

A, Surface representations of RBX1_{RING} and RBX2_{RING} with divergent surface residues (Swap4) targeted for substitution analysis. Coordinates for RBX1, RBX2 were from PDB files 2EDI and 3DQV, respectively. **B**, Time courses of NEDD8 transfer from UBE2M to indicated CUL5/RBX complexes and **C**, relative initial rates for NEDD8ylation normalized to CUL5/RBX1. Error bars indicate standard deviation between at least two experiments. **D**, Excerpts from ¹⁵N-HSQC spectra of RBX2 titrated with increasing concentrations of unlabelled wild-type or mutant UBE2F. **E**, Time courses for NEDD8 transfer from wild-type and UBE2F mutants to CUL5/RBX2. Error bars indicate standard deviation between at least two experiments. **F**, Relative initial rates for NEDD8ylation of CUL5/RBX2 normalized by wild-type UBE2F. Error bars indicate standard deviation between at least two experiments. **G**, Model of CUL5/RBX2/UBE2F complex based on CUL1/RBX1 crystal structure (3RTR) and cIAP2/UBE2D2 crystal structure (3EB6) [33,60]. UBE2F, RBX2 and CUL5 are shown in white, grey, and green respectively. The catalytic cysteine of UBE2F and the NEDD8 acceptor lysine of CUL5 (K724) are shown in orange; the unique loop insertion of UBE2F, blue; Asn92 of UBE2F,

yellow sticks; and residues of RBX2 targeted for Swap4 mutation, red. Details of modeling can be found in the Experimental Procedures.

Fig. 6. The UBE2F loop insertion is required for efficient viral infectivity

A, Single-cycle infectivity assay of HIV_{NL4-3}ΔVif produced from HEK293T cells stably depleted for UBE2F (white bars), or non-silencing control shRNA (black bars) in the presence of transfected HIV_{NL4-3}ΔVif (1 μg), A3G-V5 (500 ng), Vif-FLAG (100 ng), and increasing amounts of RNAi-immune wild-type or ΔLoop UBE2F-myc (0.2, 1, 3 or 10 ng), a catalytic mutant of UBE2F harboring a cysteine to alanine change at position 116 (10 ng), or empty vector control (10 ng). Mean and +-SD of duplicate experiments are graphed. **B**, Immunoblots of cell lysates and virus particles corresponding to panel **A**. A3G levels in cellular lysates and virus particles in UBE2F KD cells transfected with increasing amounts of RNAi-immune UBE2F (compare lanes 3-6, left and right), catalytic mutant UBE2F (C116A) or increasing amounts of UBE2F (ΔLoop) (lanes 1, 2, 7-10 left and right). To discern A3G levels in the virion in the shSCR lanes the immunoblots were exposed longer and non-specific bands from the protein ladder became apparent, as indicated by an asterisk.

Fig. 7. A model illustrating how inhibition of CUL5 NEDD8ylation leads to reduced infectivity of HIV

Two enzymatic steps must take place in order for CRL5^{Vif-CBFβ} to be properly activated by NEDD8 conjugation, and therefore for A3G-degradation to take

place, in cells infected with HIV. First, NEDD8 is loaded onto the E2 UBE2F by NAE. The small molecule MLN4924 is able to inhibit this step, blocking degradation of A3G and thereby reducing viral infectivity. Second, UBE2F is recognized by the RBX2 subunit of CRL5^{Vif-CBF β} , and transfers NEDD8 to CUL5.

SUPPORTING INFORMATION

Fig. S1. Effects of MLN4924 on A3G activity, cell viability and charging of UBE2F

A, Alternative representation of data from **Fig. 1C** as percentages of sequences containing the indicated range of G to A mutations. **B**, Toxicity of MLN4924 in SupT11 CD4+ T-cell lines, a subclone of SupT1 [61]. The CT50 of MLN4924 was determined via serial dilution of compound over 250K SupT1 cells in triplicate sets of cultures. Residual cellular viability was determined via colorimetric (3-(4,5-Dimethylthiazol-2-yl)-2,5-diphenyltetrazolium bromide (MTT) metabolic assay after three days of cell culture with compound. Percent viable cells is calculated via comparison to drug-naïve (100% viable) and media (0% viable) controls. Error bars are 1 SD. The vertical dashed line denotes the 50% cellular viability value at 120 nM MLN4924. **C**, Charging of UBE2F by the NEDD8 E1 is inhibited *in vitro* by MLN4924. Formation of NEDD8~UBE2F conjugates was monitored by following ³²P-NEDD8 after incubation with NEDD8 activating system and E2. Percent inhibition is graphed, where error bars indicate the standard deviation for two independent experiments.

Fig. S2. Knockdown of UBE2F reduces CUL5 NEDD8ylation

Immunoblots of CUL5 in extracts of virus producing HEK293T cells treated with shRNA for UBE2M, UBE2F and non-silencing control indicate the fraction of

NEDD8ylated CUL5 is reduced by shUBE2F but not shUBE2M or non-silencing control.

Fig. S3. Specificity of CRL5^{Vif-CBF β} ubiquitin ligase for substrate and NEDD8 conjugating enzymes.

A, *In vitro* ubiquitination of A3G by recombinant CRL5^{Vif-CBF β} is blocked in the double-mutant A3G(D128K,D130K). Immunoblots of ubiquitination reactions containing myc-tagged wild-type or mutant A3G as the substrate and using wild-type and ubiquitin variants (Me-Ub or K48R) are shown. The pattern for Me-Ub and K48R is similar, consistent with previous studies showing CRL5^{Vif-CBF β} can form K48 chains on Vif susceptible A3 substrates when UBE2R1 is used as E2 [12]. The asterisk indicates a non-specific band present in preparation of A3 proteins. **B**, Coomassie-stained SDS-PAGE of NEDD8ylation “pulse” reaction indicates that under conditions used in panel **A** indicate CUL5 is completely NEDD8ylated in the reactions shown. **C**, RBX2_{RING} is shown, colored by chemical shift perturbation upon addition of UBE2F_{core} (top), and including RBX1/2 conservation data, as cyan surface (bottom). **D**, Conservation between RBX2 (top) and RBX1 (bottom) is mapped in cyan onto the respective NMR or crystal structure. **E**, Plot of composite chemical shifts upon addition of UBE2F_{core} to RBX2_{RING}, as calculated by $\sqrt{((\delta H_{apo} - \delta H_{bound})^2 + ((\delta N_{apo} - \delta N_{bound})/5)^2)}$. Horizontal lines indicate the mean chemical shift perturbation (black) or the mean plus one standard deviation (red). Columns colored cyan indicate

conservation between RBX1 and RBX2. Green coloration indicates positions chosen for swap mutations made in RBX2(Swap4). Assigned secondary structure and domain organization is shown above. Coordinates for UBE2F, RBX1 and RBX2 were derived from 2EDI, 3DQV and 2ECL respectively. **F**, Raw kinetic data from pulse-chase NEDD8ylation experiments following transfer of ³²P-labelled NEDD8 from UBE2M onto various constructs as graphed in Fig. 5B. **G**, Kinetic data from pulse-chase NEDD8ylation experiments following transfer of ³²P-labelled NEDD8 from UBE2F onto CUL5/RBX1, CUL5/RXB2 and CUL5/RBX(Swap4) indicating the Swap4 substitution does not significantly affect function with UBE2F. **H**, Plots of data from **G**. (CUL5/RBX1, black circles; CUL5/RBX2(Swap4), green triangles; CUL5/RBX2, white squares) Error bars indicate standard deviation of measured P/(S+P) ratios for at least two independent experiments. **I**, Relative initial rates for NEDD8ylation are shown as fit by solid lines in **H**. Values are normalized to the rate of CUL5-RBX1. Error bars indicate standard deviation between at least two experiments.

Fig. S4. RBX2 knockdown efficiency has a reciprocal correlation with the ability of HIV to spread through non-permissive H9 T-cells.

A, Spreading assays are shown for HIV_{NL4-3} viruses in Vif non-permissive (H9) cells stably expressing non-silencing shSCR control (blue circles) or RBX2-specific shRNAs (green triangles, red squares, and purple diamonds). Points are the average of three independent biological replicates, error bars are 1 SD. **B**, Relative RBX2 mRNA

expression determined by RT-qPCR is shown for the cell lines shown in **A**. Error bars indicate the standard deviation calculated as described in Materials and Methods. **C**, shRNA targeting RBX2 does not have an off-target effect on RBX1. Relative RBX1 gene expression determined by RT-qPCR is shown for the cell lines shown in **Fig. 4A**, indicating expression level of RBX1 mRNA in H9 or SupT1 cells treated with RBX2-specific shRNAs. The replication delay observed in H9 cells knocked-down for RBX2 is not due to adventitious knockdown of RBX1, as little to no change in RBX1 mRNA levels was observed in H9 or SupT1 cell lines stably expressing shRBX2-5 relative to the control. Error bars indicate the standard deviation calculated as described in Materials and Methods.

Fig. S5. NMR analysis of UBE2F-RBX2 binding

A, A model of the RBX2_{RING}-UBE2F_{core} complex is shown, based on chemical shift-derived restraints. The model was created using the HADDOCK software package [59]. The RBX2_{RING} surface is shown in white and UBE2F_{core} is shown as a cartoon colored by chemical shift perturbation upon addition of RBX2_{RING}. Low and high chemical shift perturbations correspond with grey and red coloration respectively. The Cys116 side chain of UBE2F is shown in stick representation, with a yellow sphere representing the sulphur atom. **B**, HSQC spectral overlays are shown for UBE2F_{core} alone (black), or with the addition of 384 μ M RBX2_{RING} (red). **C**, Plot of composite chemical shifts upon addition of RBX2_{RING} to ¹⁵N-labelled UBE2F_{core}, as calculated by $\sqrt{((\delta H_{apo} - \delta H_{bound}))^2 + ((\delta N_{apo} -$

$\delta N_{\text{bound}}/5)^2$). Horizontal lines indicate the mean chemical shift perturbation (black) or the mean plus one standard deviation (red). Columns colored blue indicate the perturbed loop residues, ${}_{124}\text{SIDGTG}_{129}$. Blue coloration indicates the unique loop residues, and yellow indicates Asn96. Assigned secondary structure is shown above. **D**, Raw time course data for **Fig. 5E**, as described in main text. **E**, Quantification of UBE2F/RBX2 dissociation constant by NMR titrations. Data points and fitted curves are shown for the titration of ${}^{15}\text{N}$ -labelled $\text{RBX2}_{\text{RING}}$ with either UBE2F (black) UBE2F(Δ Loop) (blue) or UBE2F(N92A) (yellow). The D48 resonance is followed, as it is less broadened than more significantly perturbed residues in the interface.

Figure 1

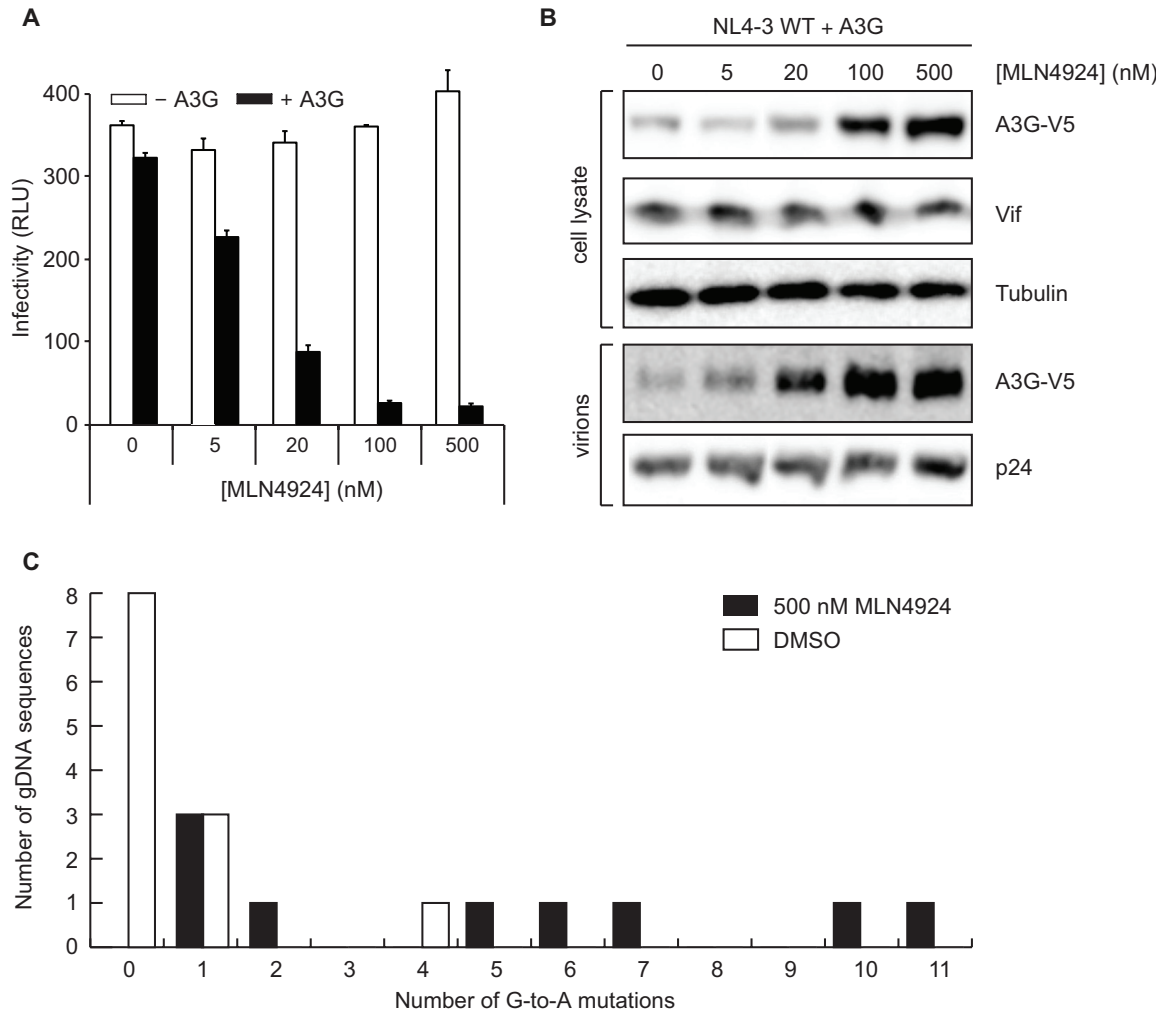


Figure 2

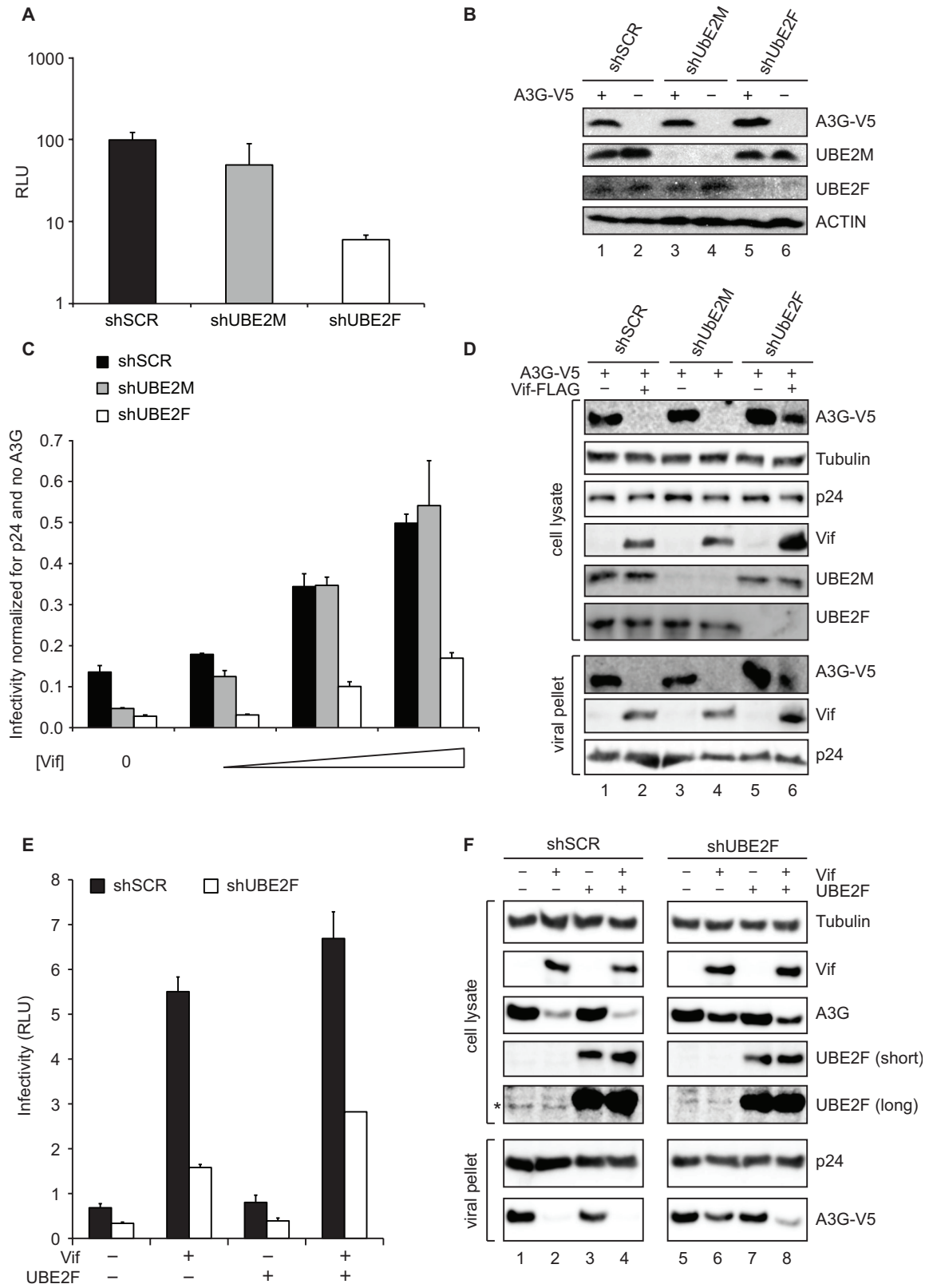


Figure 3

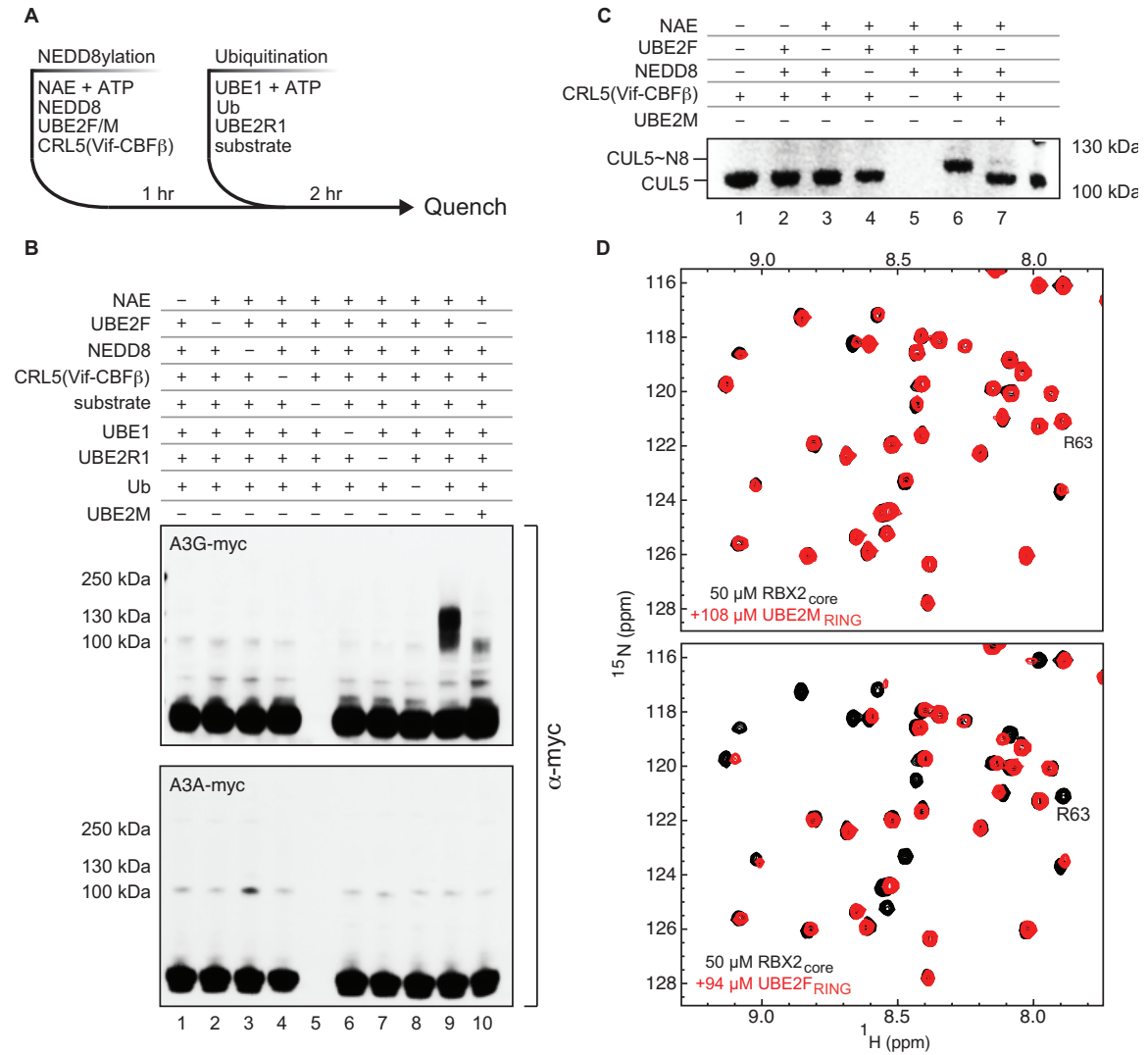


Figure 4

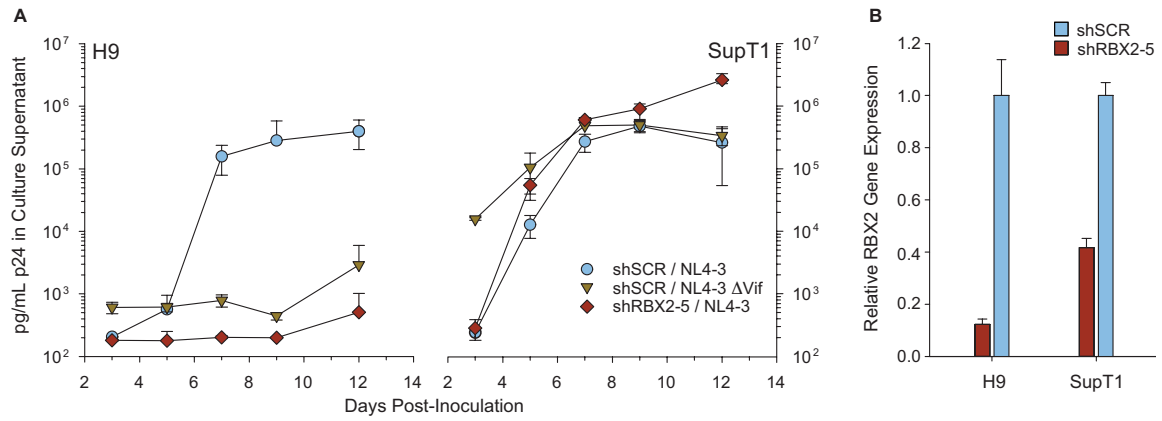


Figure 5

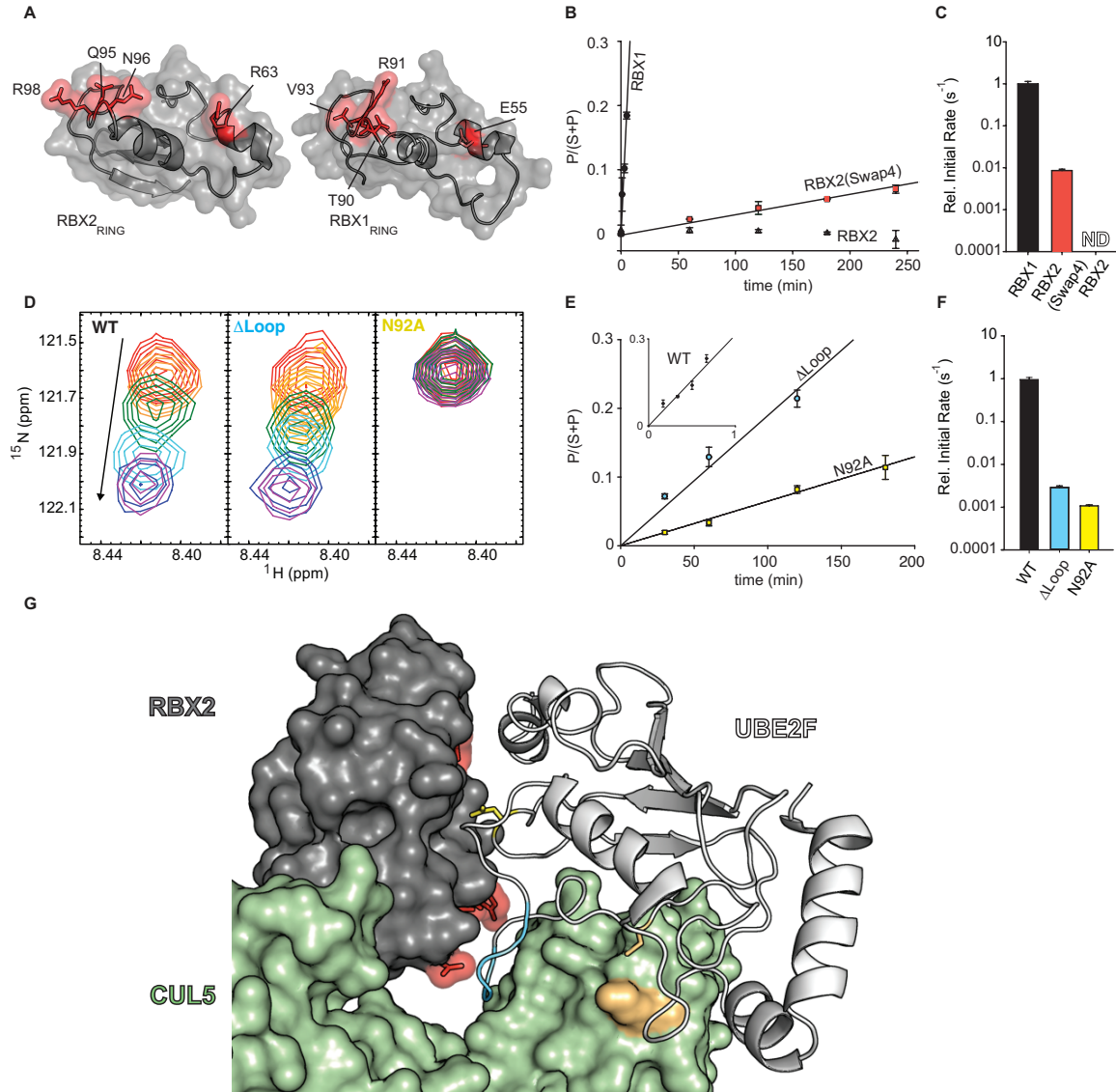


Figure 6

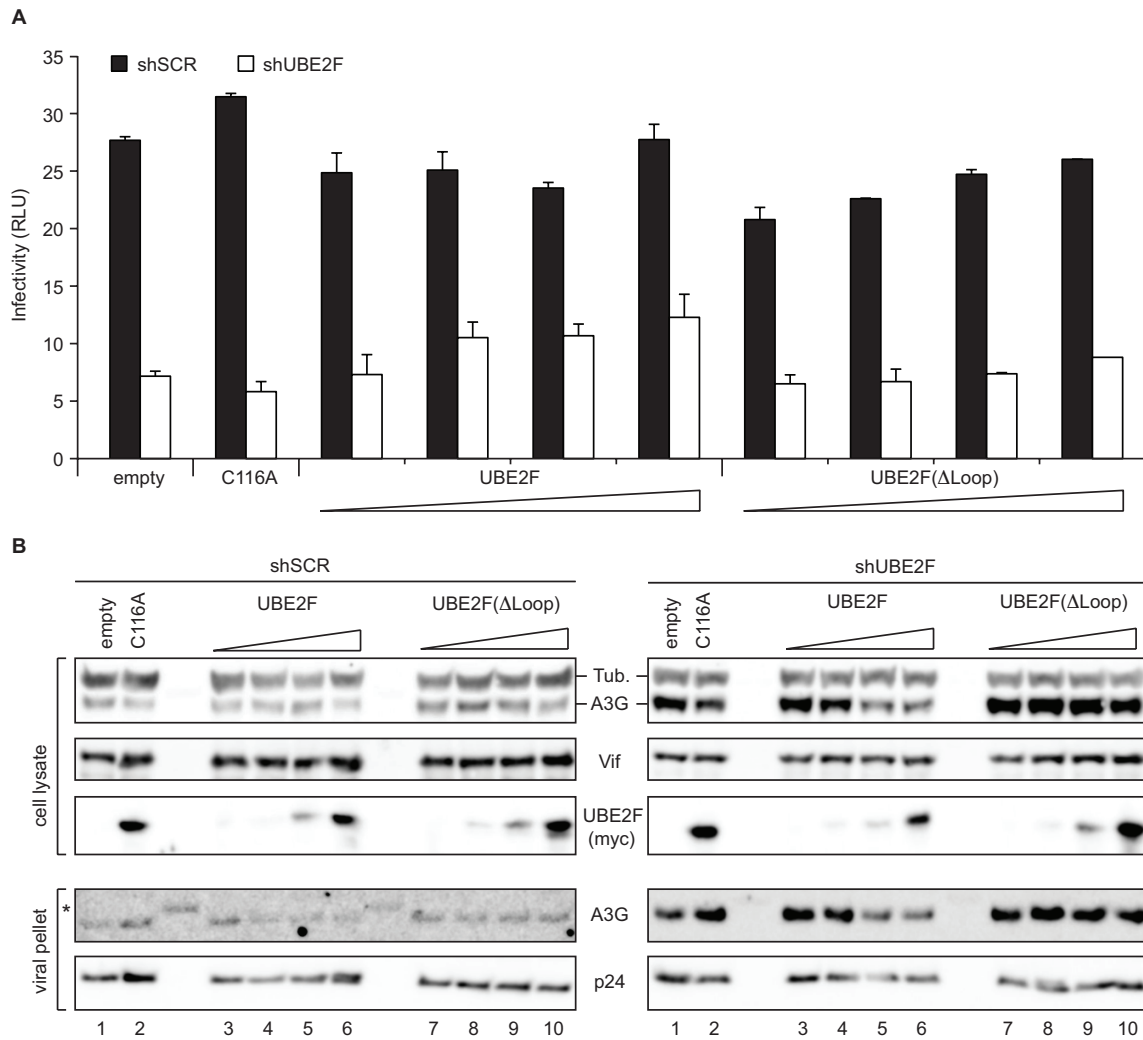
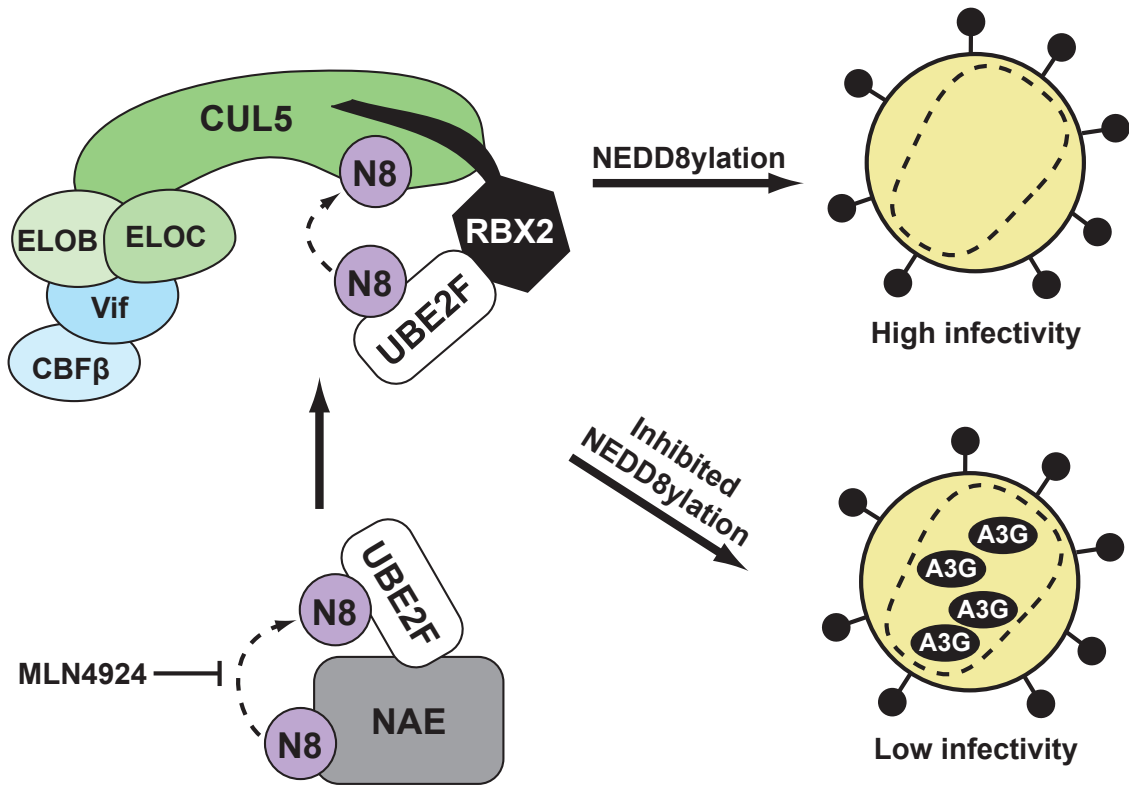
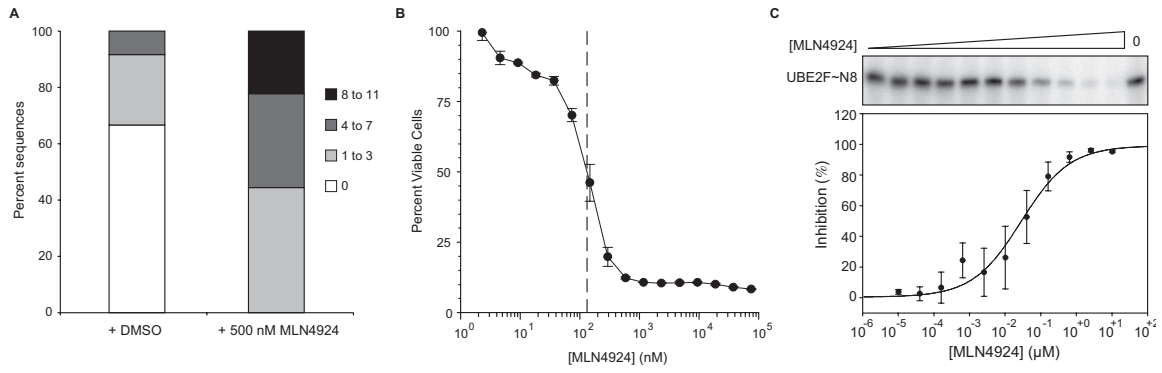


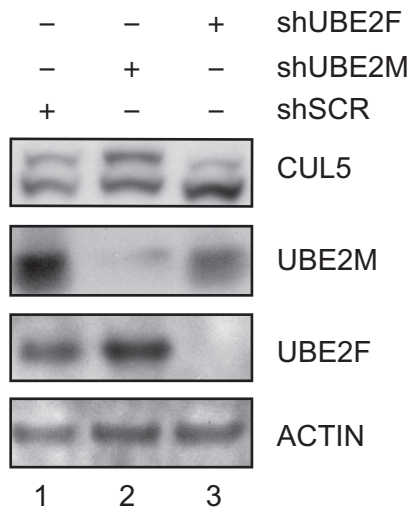
Figure 7



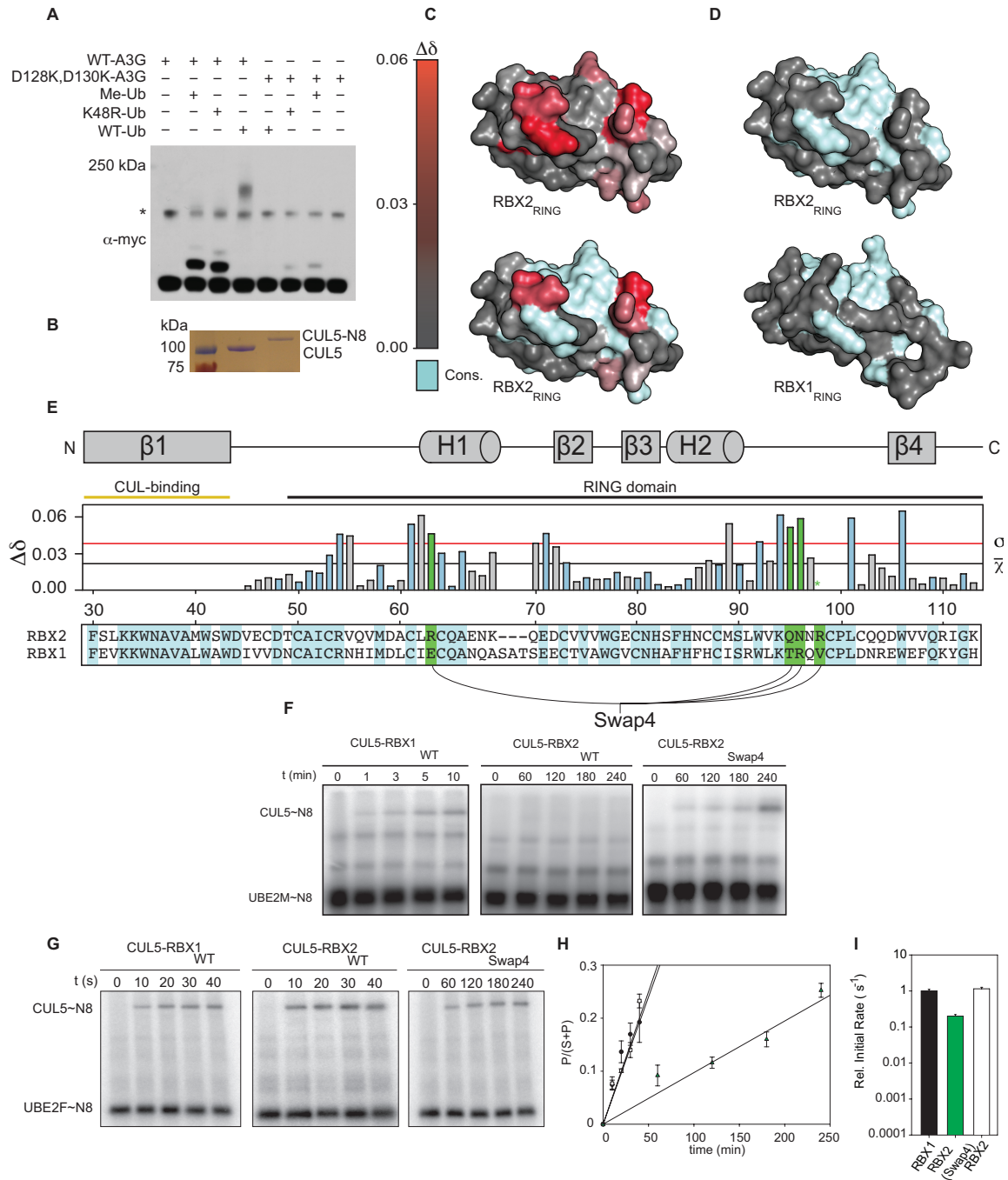
Supplementary Figure 1



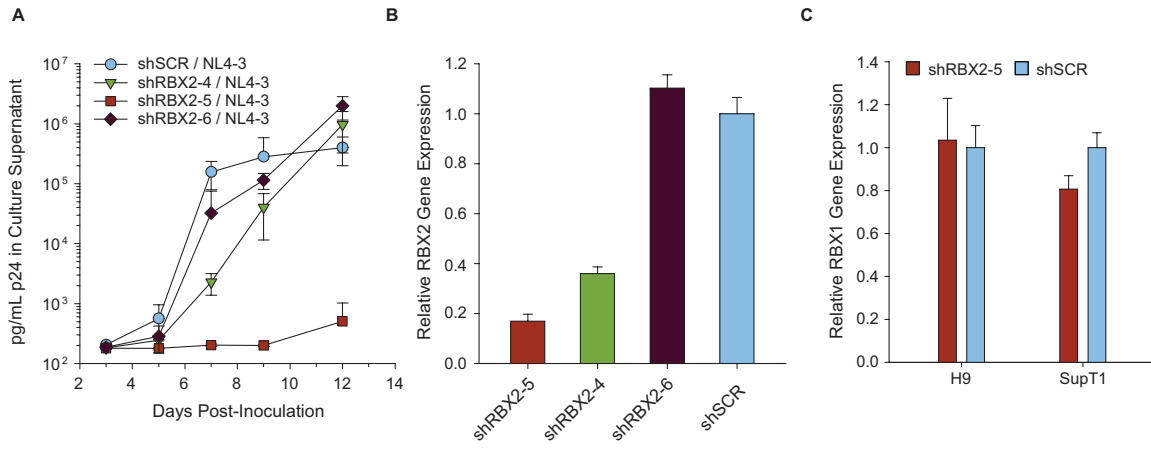
Supplementary Figure 2



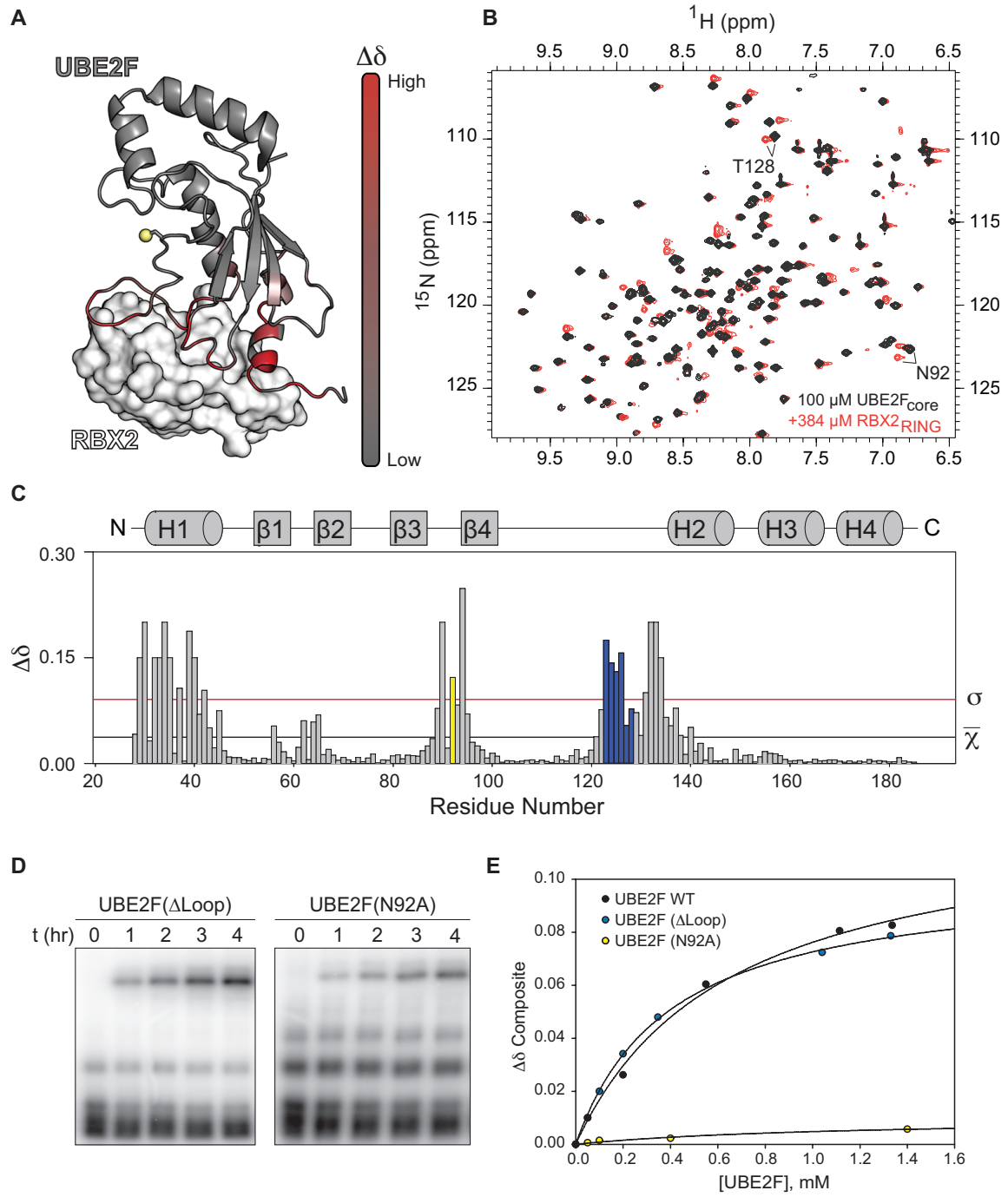
Supplementary Figure 3



Supplementary Figure 4



Supplementary Figure 5



CHAPTER 3

A role for lysine acetylation in regulation of NEDD8ylation?

David J. Stanley^{1,2}, and John D. Gross^{1,3}

¹Graduate Program in Biophysics, UCSF, 600 16th Street, San Francisco, CA 94158, USA

²Dept. of Pharmaceutical Chemistry, UCSF, 600 16th Street, San Francisco, CA 94158, USA

³California Institute for Quantitative Biosciences, QB3, UCSF, 600 16th Street, San Francisco, CA 94158, USA

Abstract

Modification of Cullin-RING ubiquitin ligases (CRLs) with NEDD8 is strictly required for efficient polyubiquitylation of substrates. This process requires the involvement of a DCN protein, which binds both NEDD8 E2 and Cullin substrate and promotes the transfer of NEDD8 in an E3-like manner. In humans there are five “DCN-like” proteins (DCNL1-5), and although the physical interactions within all possible DCNL-CUL-E2 pairs have been systematically studied, it remains unclear whether DCN-CRL specificity is a general principle of CRL regulation. We set out to better understand DCN-CRL interactions by asking whether lysine acetylation sites in the N-terminal tails of the NEDD8 E2s identified by recent proteome-wide studies have any role in regulating NEDD8ylation of CRLs. Protein semi-synthesis was used to construct full-length UBE2F containing specified lysine and/or N-terminal acetylation modifications. Measurement of Ac-UBE2F-DCNL affinities by surface plasmon resonance generally agreed with prior work. Small perturbations of measured affinities were observed in the cases of Ac-UBE2F(K7Ac) or Ac-UBE2F(K9Ac), suggesting a small role if any for lysine acetylation in the regulation of E2-DCN interactions.

INTRODUCTION

Proteasomal turnover of proteins is a central process in cells that displays both ubiquity and substrate specificity (5, 11, 23). The key to the co-existence of these qualities lies in the hierarchical organization of the ubiquitylation machinery. At each level of the E1-E2-E3 cascade, an exponentially increasing number of enzymes make up the branching pathways that serve to pass ubiquitin from one of two E1 ubiquitin-activating enzymes to one of several thousand substrates, comprising approximately 40% of the proteome (3, 10, 14). Each edge of this network presents an opportunity for regulation. The diversity in mechanism by which regulation of ubiquitylation is achieved is broad; non-ubiquitin post-translational modifications (PTMs), localization, conformational control and finely tuned temporal dynamics are all well represented (4, 15, 18).

One large and particularly regulated family of ubiquitin ligases is the Cullin-RING ligases, or CRLs (21, 22). The stability of roughly 10% of cellular proteins, or 25% of proteasome substrates, is controlled directly by CRLs (28). Modularity in CRL composition, similarly to the hierarchy of the overall ubiquitin cascade, allows a small set of Cullin scaffold proteins to direct the assembly of a vast array of holoenzymes consisting of substrate receptor (SR), adaptor, and RING-protein subunits in addition to the scaffold.

A principle that has emerged in the last decade is that CRLs are continually undergoing a 'NEDD8 cycle', through which efficient sampling of the current pool of SR subunits is promoted (24). NEDD8 is a small ubiquitin-like protein that over the course of the NEDD8 cycle is conjugated to CRLs by a NEDD8-specific E1-E2-E3 pathway, and removed through interaction with the Cop9 Signalosome (CSN) (25). In the yeast *S. cerevisiae*, the Defective in Cullin Nedd8ylation (Dcn) protein promotes the conjugation step by binding both Cullin and N-terminally acetylated E2 tail, and is required for efficient substrate turnover (12, 13, 26, 27). The human DCN-like (DCNL) family consists of five family members with significant sequence homology to the yeast protein, and is tentatively thought to impart a layer of specificity to CRL NEDD8ylation (15, 16).

Recent proteome-wide studies of lysine acetylation identified sites near the N-termini of both NEDD8 E2s (2). The N-termini of NEDD8 E2s are important for both their interaction with E1 and DCN (8, 26). Furthermore, examination of crystal structures of DCNL proteins with E2 N-terminal peptides suggests that hydrogen-bonding between UBE2F K7 and DCNL3 E194 Lysine acetylation is possible (**Fig. S1**) (16). Regulation through lysine acetylation has to date been primarily studied as it relates to the modification of histone tails, wherein it contributes to the epigenetic code, prompting us to ask whether the acetylation state of lysine residues in the N-terminal tails of NEDD8 E2s influences the NEDD8ylation process (9).

Only a subset of PTMs found in cells are expected to modify protein function (1). In order to interrogate whether lysine acetylation can perturb the physical interactions between NEDD8 E2s and other pathway components, we used a protein semisynthesis approach to construct full-length UBE2F containing specified N-terminal and/or (ϵ)-lysine acetylation modifications (29). Ambiguity remains in whether K7 or K9 of UBE2F was previously detected, as the sequence resolution obtained by IP/MS approaches is limited by the size of the detected peptide, and both lysines appear conserved in higher eukaryotes; therefore, both possible modifications were included in this analysis (**Fig. S2**) (2, 6). Synthesized proteins containing a C-terminal biotin moiety were linked to streptavidin-coated surfaces, and binding constants for all E2-DCNL pairs were measured by surface plasmon resonance (SPR). Although small differences in affinity were detected between that of WT and acetylated lysine-containing complexes, the greatest change was less than three-fold, indicating that lysine acetylation is likely not a key regulator of this interaction. A subset of peptides used for the semisynthesis ligation reaction had weak reaction kinetics, and produced a mixture of full-length and un-ligated protein that was not separable by ion exchange or size exclusion chromatography. While these mixtures were acceptable for use in the SPR assay, as only full-length protein can interact with DCNLs, they were not suitable for biochemical assays of NEDD8 E1 charging activity. The scope of this study is therefore limited to only one of two possible enzymatic steps at which lysine acetylation could influence NEDD8ylation of CRLs.

RESULTS & DISCUSSION

Semi-synthesis of Ac-UBE2F containing acetyl-lysine at specified positions

A major shortcoming, and in some cases virtue, of the heterologous expression of eukaryotic proteins in *E. coli* is the lack of endogenous systems in place for the modification of target proteins with PTMs that would normally be found on a protein in its true native state. In some cases, it is possible to co-express an appropriate enzyme along with the target protein and achieve satisfactory homogeneity of purified protein, but this requires a working knowledge of enzyme-substrate relationships that is typically lacking (26). Engineered orthogonal pyrrolysyl-tRNA synthetase / tRNA pairs have been recently reported that enable the incorporation of unnatural amino acids into proteins during bacterial expression (19). While useful in cases in which a single modification is required, the number of plasmids and overall complexity of the system needed for the *in vivo* modification state increases when multiple unrelated modifications are desired. Therefore, we chose to use a semi-synthetic strategy to produce di-acetylated UBE2F.

Peptides corresponding to the amino-acetylated N-terminal 16 residues of UBE2F containing a C-terminal thioester were synthesized, and ligated through a transthioesterification reaction to residues 17-185, to form the full-length protein after S-to-N acyl shift (17, 20, 29) (**Fig. 2a**). An S17C mutation was necessary to enable chemistry, by leaving an N-terminal cysteine following removal of an N-terminal 6xHis-GST tag used for initial affinity purification. Cysteine is not the optimal residue in the

P1 site for TEV protease, but in this case is accommodated by the protease. A 1-3 hr period of TEV protease treatment was sufficient to cleave substantial quantities of 6xHis-GST-UBE2F, while avoiding the production of multiple protease products as observed in longer 15 hr time points by SDS-PAGE (**Fig. 1a**). Separation of TEV protease products was achieved by size exclusion chromatography (**Fig. 1b,c**) followed by glutathione affinity chromatography to remove lingering 6xHis-GST contaminants. Electrospray mass spectrometry (ES-MS) confirmed the purity and correct mass of UBE2F₁₇₋₁₈₅(S17C)~biotin (**Fig. 2b, black**). The appearance of two distinct peaks with a mass difference of 226 Daltons is indicative of a mixed population of protein either ligated to biotin or not, due to imperfect *in vivo* ligation efficiency. Incubation of the purified protein with 1 mM Ac-MLTLASKLKRDDGLKG peptide-thioester and 10 mM MESNA for 6 hours yielded fully ligated protein (**Fig. 2b, orange**). Other peptides ((Ac)MLTLASK(Ac)LKRDDGLKG or (Ac)MLTLASK(Ac)LKRDDGLKG) yielded mixed populations of roughly 50-80% ligated protein (data not shown).

We originally intended to utilize ligated proteins for both E3 (DCNL) and E1 (NAE1) interactions, but experiments with E1 were precluded by ligation product heterogeneity. Although up to four species were present in some ligation products (+/- peptide, +/- biotin), these products are still useful for SPR experiments. Protein lacking either peptide or biotin will not interact with DCNLs or the Streptavidin-coated SPR chip surface, respectively.

Lysine acetylation has only a small effect on UBE2F-DCNL affinity

To examine whether lysine acetylation in the N-terminal tail of UBE2F controls the interaction with DCNLs, we used measured affinities between semi-synthetic UBE2F variants acetylated at the N-terminus and either K7, K9, or lacking lysine acetylation, (referred to as UBE2F^{NAc}, UBE2F^{NAc,K7Ac}, or UBE2F^{NAc,K9Ac} hereafter). Purified proteins containing a C-terminal biotin moiety were non-covalently deposited on a Straptavidin-coated chip surface (Xantac), and increasing concentrations of DCNL core domains were flowed over the chip. Initial experiments displayed good signal stability, and produced binding curves that fit very well to a single-site binding model (**Fig. 3**). Some increase in the baseline sensorgram signal was observed after several repeated experiments, that led to an overall decrease in the dynamic range of signal observed, but did not affect affinities measured at the beginning or end of a run. Regardless, further purification of the DCNL proteins by ion exchange chromatography largely resolved this issue and allowed the collection of datasets over multiple days.

Multiple data sets were collected for all 15 UBE2F-DCNL pairs, and yielded good fits over the analyte concentration range of $<10^{-6}$ M to $\sim 10^{-3}$ M (**Fig. 4**). The UBE2F^{NAc} dataset was roughly in agreement with that reported by the Schulman group (16), with the the following exceptions: firstly, we report K_d values for UBE2F^{NAc}-DCNL4 and UBE2F^{NAc}-DCNL5, of ~ 80 μ M and 160 μ M respectively, whereas no value was previously reported. Secondly, we find that although the trend for UBE2F^{NAc}-DCNL(1-3) interactions is the same with DCNL3 being the strongest interactor, the equilibrium constants measured are 10-fold greater than reported. It is conceivable that the S17C

mutation in UBE2F, although distant from side chains directly contacting the DCNL partner, could inhibit the interaction in some manner, possibly by disfavoring the α -helical conformation of the tail observed in E2-DCNL structures (16).

The UBE2F^{N_{Ac},K7_{Ac}} and UBE2F^{N_{Ac},K9_{Ac}} datasets did not significantly deviate from that of UBE2F^{N_{Ac}}, although some small changes were observed (**Figs. 4, S3**). The overall trend was of slightly higher K_d values in the case of lysine acetylation. Interestingly, the strongest effect was found to be for UBE2F^{N_{Ac},K7_{Ac}} and UBE2F^{N_{Ac},K9_{Ac}} with DCNL3, where 2- and 3-fold increases in K_d were measured, respectively. Lysine acetylation perturbed the equilibrium constants for all other DCNL complexes only weakly, with no change in K_d greater than 2-fold observed. As lysine acetylation did not appear to strongly contribute to regulation of UBE2F-DCNL interaction, this line of inquiry was not pursued further.

It remains entirely possible that acetylation of lysines in the N-terminal tails of NEDD8 E2s could regulation CRL NEDD8ylation. Importantly, in this study we have only queried the effect of lysine acetylation on UBE2F-DCNL interactions, whereas K3 of UBE2M was also found in an acetylated state by IP/MS (2). Furthermore, due to heterogeneity of ligated protein products we were not able to conduct experiments to ask if the E1 step is affected by lysine acetylation. An obvious future direction is to use alternative methods such as unnatural amino acid incorporation to produce homogeneously acetylated for use in E1 biochemistry (**Fig. S4**), where unlike interaction with DCNLs, N-terminal acetylation is not important.

Materials and Methods

Protein expression and purification

All proteins described herein were expressed in *E. coli* BL21(DE3)-Star cells. Cells were grown at 37 deg. C to an optical density of $A_{600}=1$, and chilled at 4 deg. C for 30 minutes prior to induction at 16 deg. C for roughly 15 hours using a final IPTG concentration of 0.1-0.5 mM. UBE2F_{S17C}(17-185) included a c-terminal biotinylation signal 'GLNDIFEAQKIEWHE' and was coexpressed with the biotin ligase and supplemented with 10 mM biotin.

UBE2F_{S17C}(17-185)-biotin was expressed with an N-terminal 6xHis-GST fusion and purified by glutathione affinity chromatography, followed by partial removal of the fusion partner by TEV protease treatment for 1-3 hours and size exclusion chromatography immediately thereafter. A second glutathione affinity step was used to remove remaining fusion partner. Flow through at this stage was collected and concentrated and analyzed by SDS-PAGE and ESI-MS for purity and correct mass. 1X PBS pH=7.5 was used as a buffer throughout the purification.

Core domains of DCNL1-5 corresponding to the conserved PONY domain were cloned and expressed with either an N-terminal 6xHis or 6xHis-GST fusion, and purified similarly to above with the following exceptions: TEV protease treatment was for 15h in order to completely remove fusion tags, and the following buffers were used for proteins not tagged with GST. Lysis buffer (20 mM HEPES pH=7.6, 500 mM NaCl, 10

mM imidazole, 0.1 % NP-40, 10% glycerol, 1 mM DTT), Wash Buffer (20 mM HEPES pH=7.6, 500 mM NaCl, 20 mM imidazole, 10 % glycerol, 1 mM DTT), Elution Buffer (20 mM HEPES pH=7.6, 500 mM NaCl, 250 mM imidazole, 10 % glycerol, 1mM DTT), and Sizing Buffer (20 mM HEPES pH=7.6, 150 mM NaCl, 1mM DTT). A final anion exchange step was used to prepare DCNL proteins for SPR experiments (HiTrap Q HP, GE).

Native chemical ligation

Lyophilized peptides were resolubilized to a concentration of 1-3 mM in small volumes of 1X PBS buffer (100-200 μ L) with 20 mM MESNA. Neutral pH was confirmed by the use of pH paper. Solubility was good for the Ac-MLTLASKLKRDDGLKG peptide, but some insoluble material remained after resuspension for the acetyl-lysine peptides. This material was removed by centrifugation.

The solution described above was mixed with an equal volume of 200-300 μ M UBE2F_{S17C}(17-185), to give a final concentration of ~1 mM peptide, 10 mM MESNA, 100-200 μ M protein, in 1 X PBS pH=7.5. Reactions were allowed to proceed for 24 hours, with time points being taken at 3, 6 and 24 hours. Products were buffer exchanged into 1X PBS pH=7.5, 1 mM DTT by two passages through a PD-10 column (Bio-Rad). ESI-MS was used to analyze the reaction products, and successfully ligated products were stocked in aliquots at 20 μ M.

Surface plasmon resonance

Biotinylated proteins were deposited on a streptavidin-coated carboxymethyl dextran sensor chip (Xantec) using a Biacore 2000 system (GE Healthcare). Signals were stable after several hours of buffer flow (150 mM NaCl, 1 mM DTT, 25 mM HEPES pH = 7.5). Increasing concentrations of DCNL proteins in the above buffer were flowed over the sensor chip, interspersed with buffer only. Triplicate or duplicate data sets for each ligand-analyte pair were processed in MATLAB with scripts based on prior work (K. Kuchenbecker, personal communication) and fit to a single site saturation binding model using a least squares algorithm.

Figure Legends

Figure 1

A, SDS-PAGE analysis of products following treatment of 6xHis-GST-UBE2F_{S17C}(17-185) with TEV protease. Varying degrees of cleavage are observed, depending on time (1 or 15 hours) and protein:protease molar ratio (1:60, 40, or 20). **B**, Size exclusion chromatography of products resulting from cleavage of 6xHis-GST-UBE2F_{S17C}(17-185) with TEV protease. Fractions analyzed in **C** are marked 'SDS-PAGE', and fractions pooled for further purification are marked 'Coll'. **C**, SDS-PAGE analysis of fractions as indicated in **B**.

Figure 2

A, Schematic of the native chemical ligation reaction used to ligate acetylated peptides to UBE2F_{S17C}(17-185). **B**, ESI-MS spectrums of purified of pre-ligation UBE2F_{S17C}(17-185) (black) and post-ligation Ac-UBE2F_{S17C} (orange). Double peaks are observed in each, indicated a mass difference of 226 Daltons, due to inefficiency in *in vivo* biotin ligation.

Figure 3

A, Raw SPR sensorgram data for increasing concentrations of DCNL2 against NoKAc. Sensorgram curves are colored from black to blue, representing a concentration range from 350 nM to 450 μ M. **B**, Equilibrium response values from multiple experiments are scaled and plotted individually as blue dots. Orange circles

indicate the fitted curve. Residuals from the average response value compared with the fit are shown as inset.

Figure 4

K_d values are shown for all E2-DCNL pairs. NoKAc, 7KAc, and 9KAc are represented by blue, green, or red bars respectively.

SUPPLEMENTARY FIGURE LEGENDS

Supplementary Figure 1

K7 of UBE2F (orange) approaches E194 of DCNL3 (grey). Side chains are shown as sticks (PDB: 4GBA) (16).

Supplementary Figure 2

K7 and K9 of UBE2F are conserved across many eukaryotic species. PHOSIDA database conservation information is shown (6).

Supplementary Figure 3

Fits used to determine all K_d values shown in **Fig. 4** are shown. NoKAc, 7KAc, and 9KAc data are shown in blue, green, or red respectively.

Supplementary Figure 4

Modelling of the UBE2F sequence onto the crystal structure of Ubc12-APPBP1-UBA3-NEDD8-MgATP (PDB ID: 2NVU) suggests that K7 of UBE2F could potentially be poised to interact with NAE1 (7).

Figure 1

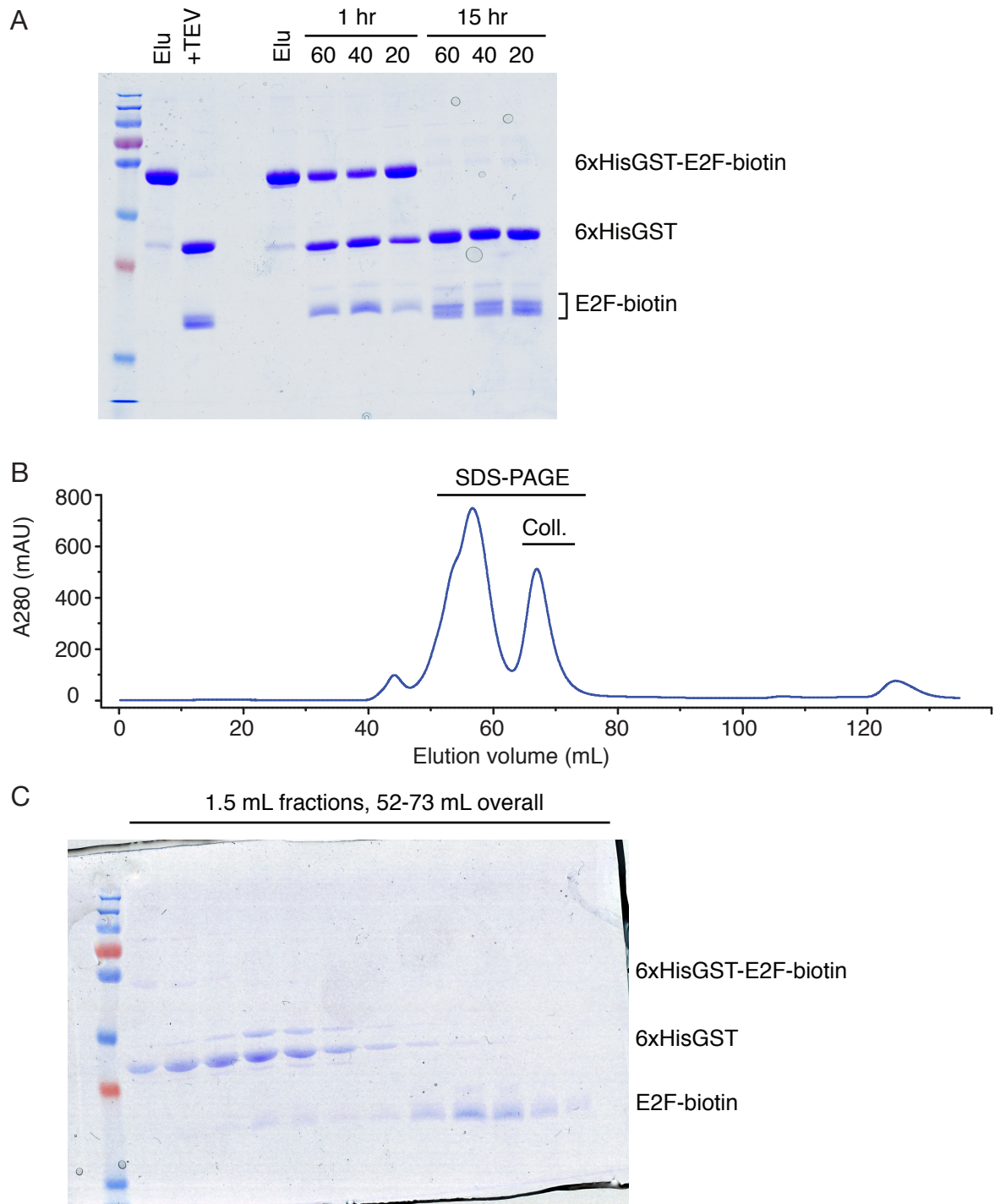
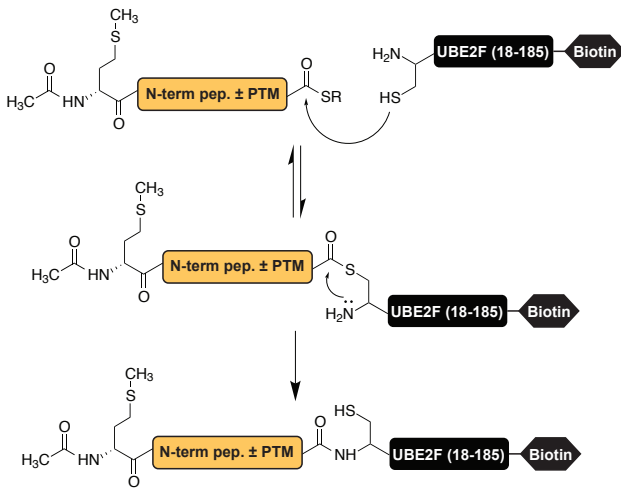


Figure 2

A



B

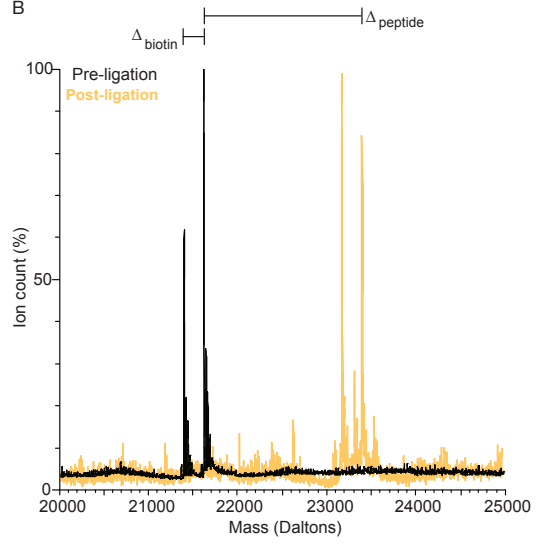


Figure 3

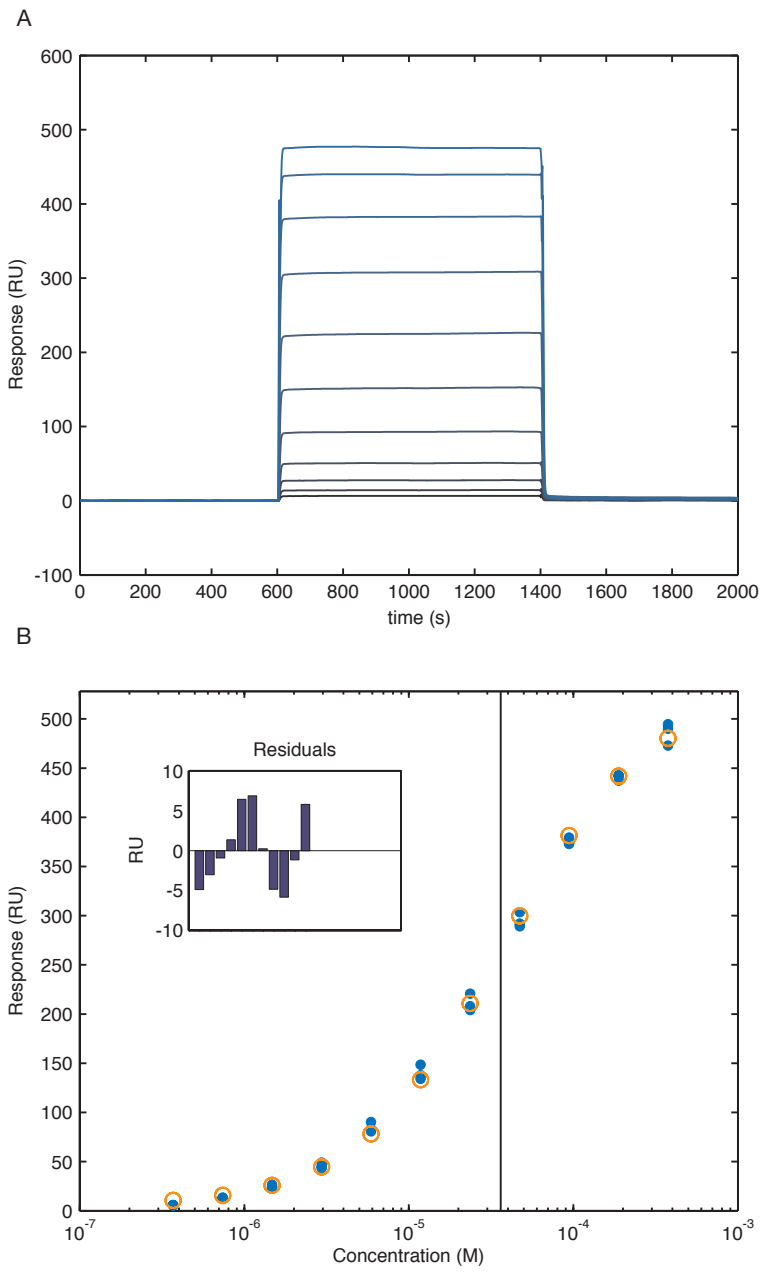
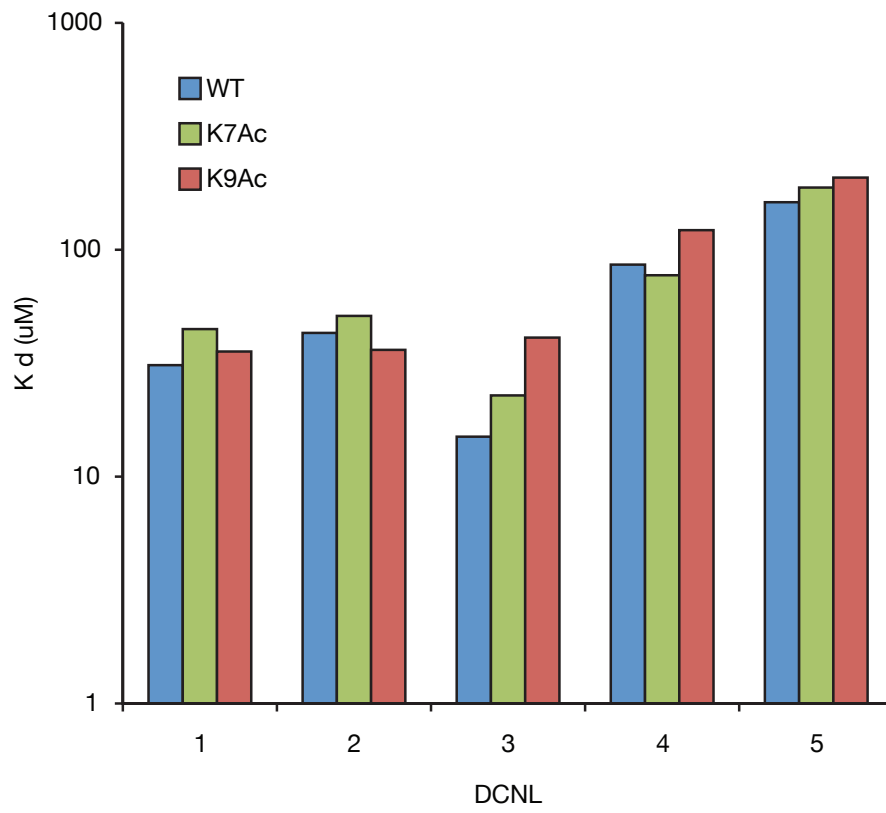
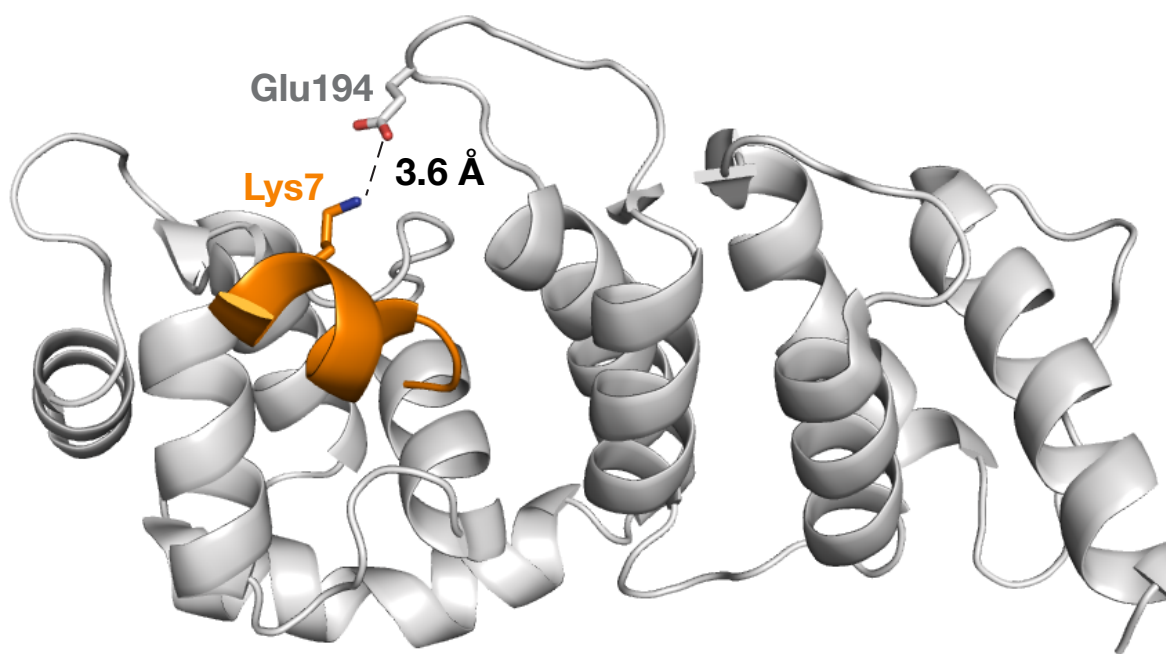


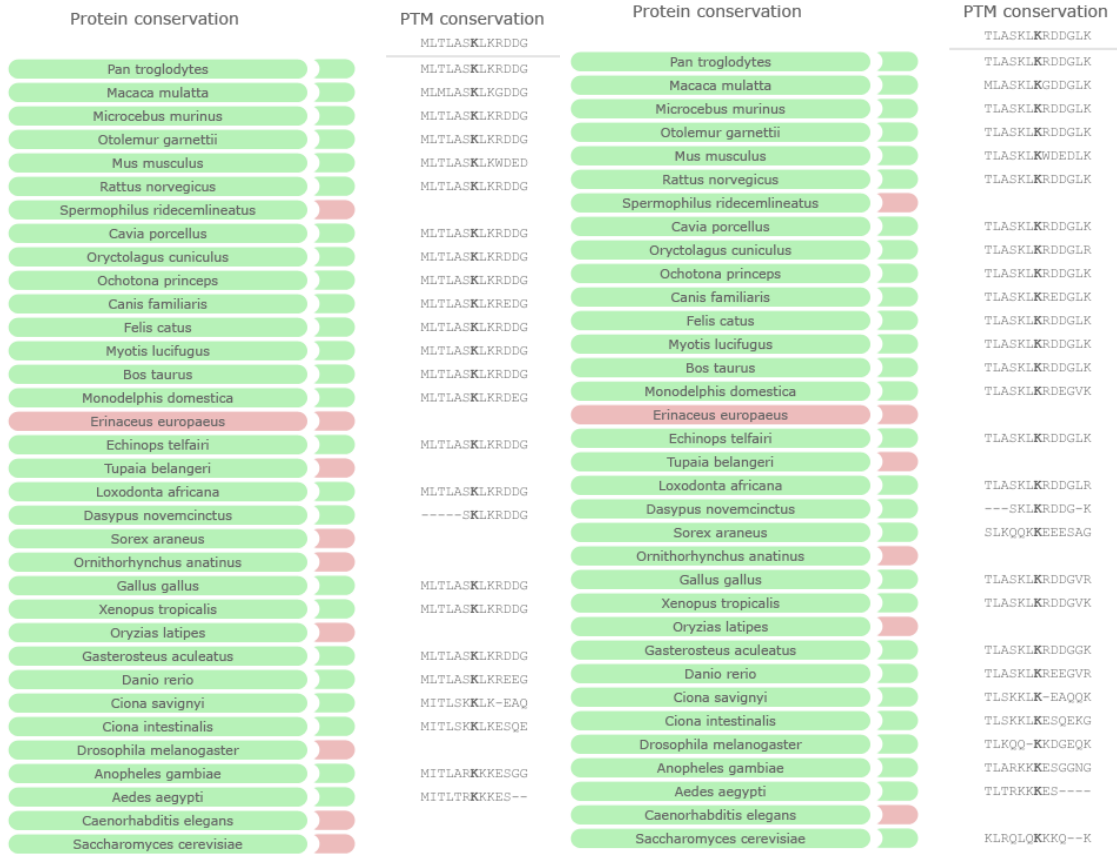
Figure 4



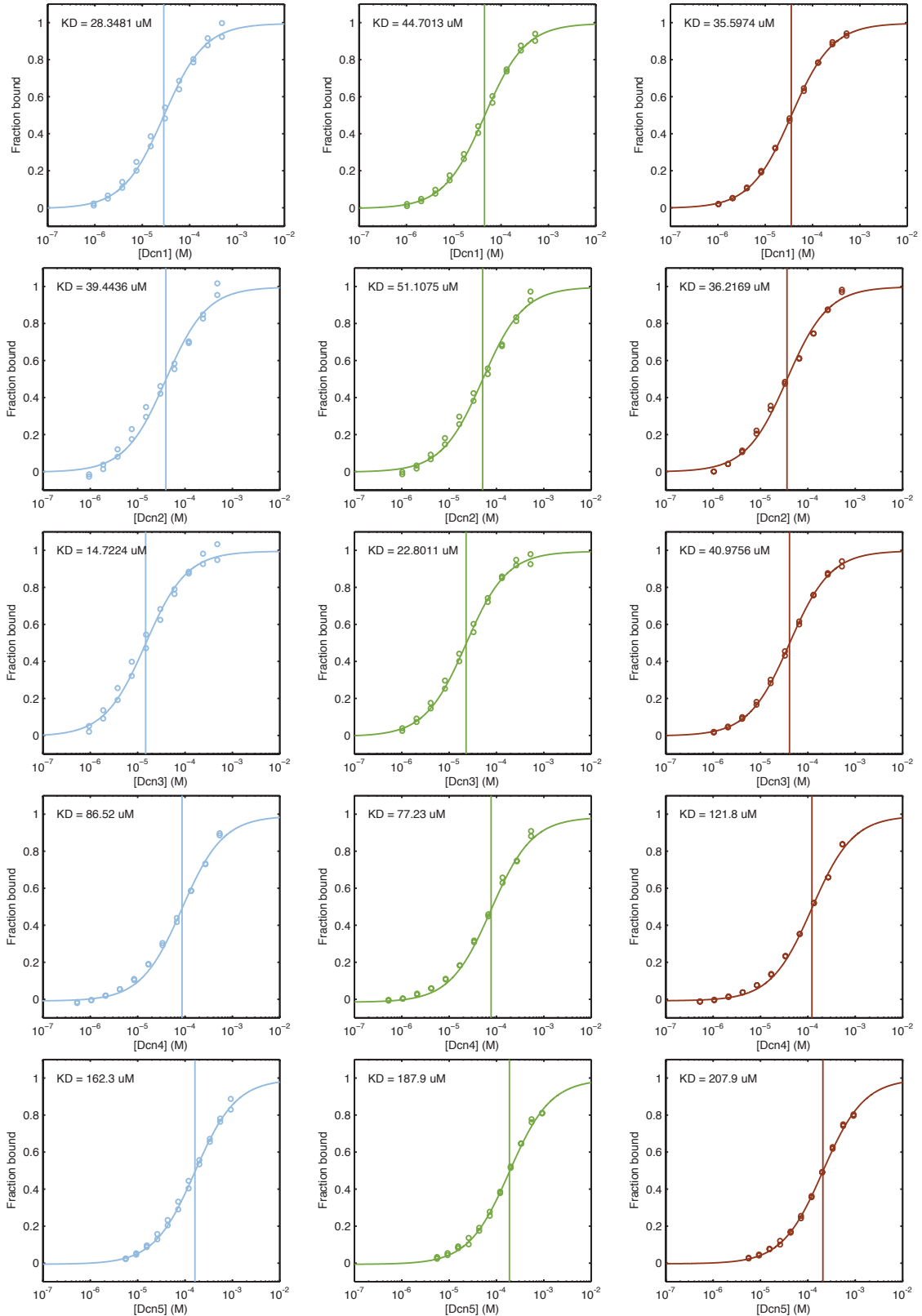
Supplemental Figure 1



Supplemental Figure 2

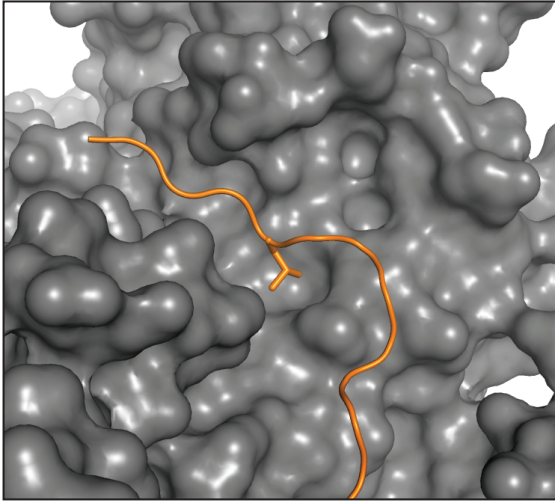


Supplemental Figure 3

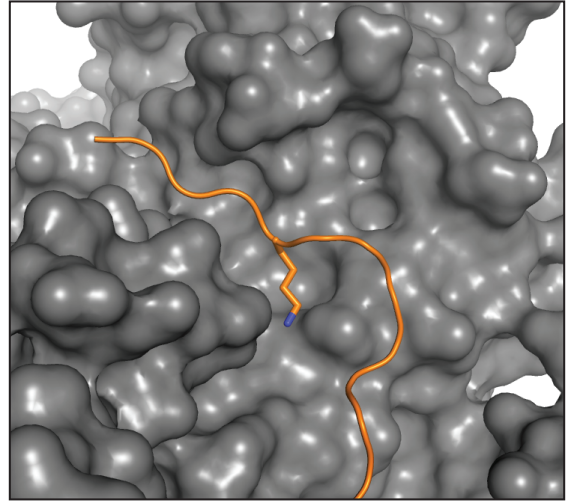


Supplemental Figure 4

A



B



REFERENCES

1. **Beltrao, P., V. Albanese, L. R. Kenner, D. L. Swaney, A. Burlingame, J. Villen, W. A. Lim, J. S. Fraser, J. Frydman, and N. J. Krogan.** 2012. Systematic functional prioritization of protein posttranslational modifications. *Cell* **150**:413-25.
2. **Choudhary, C., C. Kumar, F. Gnad, M. L. Nielsen, M. Rehman, T. C. Walther, J. V. Olsen, and M. Mann.** 2009. Lysine acetylation targets protein complexes and co-regulates major cellular functions. *Science* **325**:834-40.
3. **Deshais, R. J., and C. A. Joazeiro.** 2009. RING domain E3 ubiquitin ligases. *Annu Rev Biochem* **78**:399-434.
4. **Duda, D. M., L. A. Borg, D. C. Scott, H. W. Hunt, M. Hammel, and B. A. Schulman.** 2008. Structural insights into NEDD8 activation of cullin-RING ligases: conformational control of conjugation. *Cell* **134**:995-1006.
5. **Dye, B. T., and B. A. Schulman.** 2007. Structural mechanisms underlying posttranslational modification by ubiquitin-like proteins. *Annu Rev Biophys Biomol Struct* **36**:131-50.
6. **Gnad, F., S. Ren, J. Cox, J. V. Olsen, B. Macek, M. Oroshi, and M. Mann.** 2007. PHOSIDA (phosphorylation site database): management, structural and evolutionary investigation, and prediction of phosphosites. *Genome Biol* **8**:R250.
7. **Huang, D. T., H. W. Hunt, M. Zhuang, M. D. Ohi, J. M. Holton, and B. A. Schulman.** 2007. Basis for a ubiquitin-like protein thioester switch toggling E1-E2 affinity. *Nature* **445**:394-8.
8. **Huang, D. T., D. W. Miller, R. Mathew, R. Cassell, J. M. Holton, M. F. Roussel, and B. A. Schulman.** 2004. A unique E1-E2 interaction required for optimal conjugation of the ubiquitin-like protein NEDD8. *Nat Struct Mol Biol* **11**:927-35.
9. **Jenuwein, T., and C. D. Allis.** 2001. Translating the histone code. *Science* **293**:1074-80.
10. **Jin, J., X. Li, S. P. Gygi, and J. W. Harper.** 2007. Dual E1 activation systems for ubiquitin differentially regulate E2 enzyme charging. *Nature* **447**:1135-8.
11. **Kerscher, O., R. Felberbaum, and M. Hochstrasser.** 2006. Modification of proteins by ubiquitin and ubiquitin-like proteins. *Annu Rev Cell Dev Biol* **22**:159-80.
12. **Kurz, T., Y. C. Chou, A. R. Willems, N. Meyer-Schaller, M. L. Hecht, M. Tyers, M. Peter, and F. Sicheri.** 2008. Dcn1 functions as a scaffold-type E3 ligase for cullin neddylation. *Mol Cell* **29**:23-35.
13. **Kurz, T., N. Ozlu, F. Rudolf, S. M. O'Rourke, B. Luke, K. Hofmann, A. A. Hyman, B. Bowerman, and M. Peter.** 2005. The conserved protein DCN-1/Dcn1p is required for cullin neddylation in *C. elegans* and *S. cerevisiae*. *Nature* **435**:1257-61.

14. **Lee, J. E., M. J. Sweredoski, R. L. Graham, N. J. Kolawa, G. T. Smith, S. Hess, and R. J. Deshaies.** 2011. The steady-state repertoire of human SCF ubiquitin ligase complexes does not require ongoing Nedd8 conjugation. *Mol Cell Proteomics* **10**:M110 006460.
15. **Meyer-Schaller, N., Y. C. Chou, I. Sumara, D. D. Martin, T. Kurz, N. Katheder, K. Hofmann, L. G. Berthiaume, F. Sicheri, and M. Peter.** 2009. The human Dcn1-like protein DCNL3 promotes Cul3 neddylation at membranes. *Proc Natl Acad Sci U S A* **106**:12365-70.
16. **Monda, J. K., D. C. Scott, D. J. Miller, J. Lydeard, D. King, J. W. Harper, E. J. Bennett, and B. A. Schulman.** 2013. Structural conservation of distinctive N-terminal acetylation-dependent interactions across a family of mammalian NEDD8 ligation enzymes. *Structure* **21**:42-53.
17. **Muir, T. W., D. Sondhi, and P. A. Cole.** 1998. Expressed protein ligation: a general method for protein engineering. *Proc Natl Acad Sci U S A* **95**:6705-10.
18. **Nash, P., X. Tang, S. Orlicky, Q. Chen, F. B. Gertler, M. D. Mendenhall, F. Sicheri, T. Pawson, and M. Tyers.** 2001. Multisite phosphorylation of a CDK inhibitor sets a threshold for the onset of DNA replication. *Nature* **414**:514-21.
19. **Neumann, H., S. Y. Peak-Chew, and J. W. Chin.** 2008. Genetically encoding N(epsilon)-acetyllysine in recombinant proteins. *Nat Chem Biol* **4**:232-4.
20. **Nilsson, B. L., M. B. Soellner, and R. T. Raines.** 2005. Chemical synthesis of proteins. *Annu Rev Biophys Biomol Struct* **34**:91-118.
21. **Petroski, M. D., and R. J. Deshaies.** 2005. Function and regulation of cullin-RING ubiquitin ligases. *Nat Rev Mol Cell Biol* **6**:9-20.
22. **Petroski, M. D., and R. J. Deshaies.** 2005. Mechanism of lysine 48-linked ubiquitin-chain synthesis by the cullin-RING ubiquitin-ligase complex SCF-Cdc34. *Cell* **123**:1107-20.
23. **Pickart, C. M., and M. J. Eddins.** 2004. Ubiquitin: structures, functions, mechanisms. *Biochim Biophys Acta* **1695**:55-72.
24. **Pierce, N. W., J. E. Lee, X. Liu, M. J. Sweredoski, R. L. Graham, E. A. Larimore, M. Rome, N. Zheng, B. E. Clurman, S. Hess, S. O. Shan, and R. J. Deshaies.** 2013. Cnd1 Promotes Assembly of New SCF Complexes through Dynamic Exchange of F Box Proteins. *Cell*.
25. **Rabut, G., and M. Peter.** 2008. Function and regulation of protein neddylation. 'Protein modifications: beyond the usual suspects' review series. *EMBO Rep* **9**:969-76.
26. **Scott, D. C., J. K. Monda, E. J. Bennett, J. W. Harper, and B. A. Schulman.** 2011. N-terminal acetylation acts as an avidity enhancer within an interconnected multiprotein complex. *Science* **334**:674-8.
27. **Scott, D. C., J. K. Monda, C. R. Grace, D. M. Duda, R. W. Kriwacki, T. Kurz, and B. A. Schulman.** 2010. A dual E3 mechanism for Rub1 ligation to Cdc53. *Mol Cell* **39**:784-96.
28. **Soucy, T. A., P. G. Smith, M. A. Milhollen, A. J. Berger, J. M. Gavin, S. Adhikari, J. E. Brownell, K. E. Burke, D. P. Cardin, S. Critchley, C. A.**

- Cullis, A. Doucette, J. J. Garnsey, J. L. Gaulin, R. E. Gershman, A. R. Lublinsky, A. McDonald, H. Mizutani, U. Narayanan, E. J. Olhava, S. Peluso, M. Rezaei, M. D. Sintchak, T. Talreja, M. P. Thomas, T. Traore, S. Vyskocil, G. S. Weatherhead, J. Yu, J. Zhang, L. R. Dick, C. F. Claiborne, M. Rolfe, J. B. Bolen, and S. P. Langston.** 2009. An inhibitor of NEDD8-activating enzyme as a new approach to treat cancer. *Nature* **458**:732-6.
29. **Tolbert, T. J., and C. H. Wong.** 2004. Conjugation of glycopeptide thioesters to expressed protein fragments: semisynthesis of glycosylated interleukin-2. *Methods Mol Biol* **283**:255-66.

CHAPTER 4

Conformational dependence of Vif on the complement of bound ligands

David J. Stanley^{1,2}, and John D. Gross^{2,3}

¹Graduate Program in Biophysics, UCSF, 600 16th Street,
San Francisco, CA 94158, USA

²Dept. of Pharmaceutical Chemistry, UCSF, 600 16th Street,
San Francisco, CA 94158, USA

³California Institute for Quantitative Biosciences, QB3, UCSF, 600 16th Street,
San Francisco, CA 94158, USA

ABSTRACT

The HIV Viral infectivity factor (Vif) Vif protein bypasses host defenses by promoting the degradation of the anti-viral APOBEC3 (A3) proteins through interaction with the Ubiquitin E3 ligase CUL5. In addition to the protein-protein interactions that are necessary for A3 ubiquitylation, a number of other physical interactions have been reported between Vif and cellular factors, although the functional and phenotypic significance of these putative complexes is typically not well characterized. Vif is a relatively small protein, and it remains unclear how the repertoire of distinct interactions attributed to Vif are accommodated. We show that Vif can simultaneously bind to nucleic acids and E3 ligase components. Furthermore, gel filtration and SAXS analysis indicate that a conformational change takes place in Vif-CBF β -EloB-Eloc (VCBC) upon binding to oligonucleotide. Our results suggest that an unusually broad conformational landscape may be an adaptation by which Vif fulfills a variety of roles given limited genomic capacity, and that a full consideration of conformational plasticity will be necessary for a comprehensive structural understanding of Vif.

INTRODUCTION

Circumvention of the host immune system is a ubiquitous pathogenic strategy. Human T-lymphocytes express a subset of the APOBEC3 (A3) family of cytidine deaminase enzymes that are able to reduce the infectivity of viral progeny through hypermutation of the viral genome, an effect that is overcome by the Viral infectivity protein (Vif) of HIV (7, 14, 22, 33). Vif confers A3-resistance to HIV by assembling an E3 ubiquitin ligase complex that catalyzes the formation of K48-linked polyubiquitin chains on A3 proteins, thereby targeting them for proteasomal degradation (11, 31). This is the most well characterized function of Vif, but numerous other roles and properties have been proposed, including but not limited to: non-degradative counteraction of A3 enzymes through both additional direct and indirect mechanisms (6, 17, 18, 24), proteasomal degradation of Vpr (28), oligomerization (27), cell cycle arrest (9), and RNA chaperone activity (1). Proteomic studies in human cells indicate an unusually large array of potential Vif interactors, indicating that the full repertoire of Vif functions is possibly even more expansive than currently thought (3, 10).

Vif is a small, highly basic protein that in the apo-state displays significant amounts of conformational disorder, a characteristic of RNA chaperones (1, 4, 19). Standard biochemical and biophysical techniques are generally not well suited to the study of natively disordered proteins, as disordered proteins are typically aggregation-prone and challenging to obtain at the concentrations

needed. Introducing binding partners to disordered proteins can overcome this barrier, by stabilizing a specific conformation or assisting in folding (8). Our lab has recently found that by co-expressing Vif with the transcription factor CBF β as well as the E3 ligase components ElonginB and ElonginC (EloB/C) large amounts of a four protein Vif-CBF β -EloB-EloC (VCBC) complex can be obtained that is folded, active, and aggregation-resistant (11, 12). Previous attempts to stabilize Vif by co-expression with EloB/C alone failed to stabilize the full-length protein, but did result in biochemically tractable complexes of EloB/C with short peptides corresponding to the SOCS-box sequence found in the C-terminal region of Vif (23). In agreement with these results, hydrogen-deuterium exchange experiments suggest that binding of EloB/C to Vif induces local folding in the same region (15). Interestingly, whereas EloB/C interacts with the C-terminal region of Vif, CBF β is able to immunoprecipitate shorter fragments of Vif corresponding to N-terminal sequences not previously accessible to *in vitro* biochemistry (12). Furthermore, binding to monomeric Vif of an oligonucleotide corresponding to the HIV TAR element induced both a degree of folding and the formation of high molecular weight complexes (2). These studies illustrate the generality of a description of Vif conformation as highly dependant on the presence of binding partners, consistent with an emerging understanding of a strategy identified in an increasing number of viral proteins whereby conformationally plastic proteins are utilized to maximize the phenotypic potential of tightly constrained genetic coding capacity (5, 26, 30).

While the local conformation of Vif clearly depends on whether a specific region is bound to ligand, it is not known whether the disorder-to-order transitions observed thus far are exclusive, or if cooperativity between multiple ligands may play a role in determining the overall fold of Vif. Understanding the relationship between the global fold of Vif and its ligand binding properties will allow the classification of the myriad Vif functions by conformation, and will be important for a complete description of the protein. The stable heterotetrameric VCBC complex is a useful tool to begin to study the exclusivity of Vif complexes. VCBC displays a high degree of foldedness as measured by circular dichroism (12), and unlike other known Vif complexes this foldedness is necessarily present in both N- and C-terminal domains (2, 16).

If the conformation of Vif in VCBC is specific to its function as a substrate receptor for an E3 ligase, other Vif ligands such as RNA/DNA will fail to bind VCBC or compete with CBF β or EloB/C for Vif binding. We tested this hypothesis by characterizing the interaction of VCBC with nucleic acids. Gel shift and fluorescence anisotropy measurements demonstrate that VCBC is competent to bind nucleic acids, albeit with an altered base preference relative to that reported for monomeric Vif (32). Complexes of VCBC with a minimal oligonucleotide were examined by gel filtration and small angle X-ray scattering (SAXS), and found to have a compacted shape relative to VCBC lacking bound oligonucleotide. Thus, Vif is capable of simultaneously interacting with a surprising number of ligands. Moreover, there is no conformational exclusivity

between substrate-receptor forming and nucleic acid-binding activities. However, it is important to note that the properties of nucleotide-bound Vif appear to differ; whereas nucleotide stimulated Vif oligomerization in other studies, DNA-VCBC is conversely more resistant to aggregation than VCBC alone (2, 12). While binding of nucleotide is not exclusive to formation of the VCBC complex the overall properties of the Vif complex are drastically different, suggesting that the influence of each binding partner may be integrated by Vif into a functional state that can be influenced strongly by the association of a single ligand. Further work to extend the initial observations reported here, and to examine co-occupancy of Vif among a broader panel of proposed interactors is warranted to extend our understanding of the relationship between ligand binding, conformation and function in Vif.

RESULTS & DISCUSSION

EMSA analysis of interactions between VCBC and homopolymeric RNA

Although Vif has been shown to bind a variety of nucleic acids, it is not known how the nucleic acid-binding activity of Vif is influenced by the formation of the VCBC complex (1, 2). Relative to monomeric Vif, VCBC has increased stability and foldedness (11, 12). The electrophoretic mobility shift assay (EMSA) is a useful technique for the direct observation of stable protein-nucleic acid complexes in solution (5). Therefore, we tested the ability of VCBC to bind 40-mer homopolymeric oligonucleotides of each RNA base type that had been end-labeled with ^{32}P by native electrophoretic mobility shift assay (EMSA).

Not all base types were accessible by this method; poly(G)₄₀ and poly(A)₄₀ oligonucleotides were retained in the well, presumably due stable intermolecular interactions of these homopolymer types (21). Titration of poly(U)₄₀ with increasing amounts of VCBC caused an apparent shift in the electrophoretic mobility of the labeled oligonucleotide that could be fit to a standard ligand binding equation, yielding a K_d of ~75 nM (**Fig. 1A**). Interestingly, although poly(C)₄₀ alone had a mobility indistinguishable from that of poly(U)₄₀ indicating a lack of self-association, it failed to interact with VCBC at similar concentrations to poly(U)₄₀ (**Fig. S1**). Our finding that VCBC binds tightly to poly(U)₄₀ contrasts with previously published work on monomeric Vif, in which it was reported that Vif bound preferentially to poly(G) and poly(A), but not poly(U) or poly(C) (32).

This apparent conflict suggests that the overall nucleic acid-binding properties of VCBC may differ from those of monomeric Vif.

EMSA analysis of interactions between larger Vif complexes and poly(U)₄₀

Based on our result that VCBC may have altered nucleic acid-binding capabilities relative to Vif alone, we asked whether the addition of CUL5-RBX2 (C5R2) to form the six-protein C5R2-VCBC complex might further alter the properties of Vif. Titration of poly(U)₄₀ with pre-formed C5R2-VCBC yielded a K_d similar to that measured for VCBC. However, the electrophoretic mobility of the larger complex appeared to be similar to that of VCBC alone (**Fig. 2A**). We next directly compared the apparent gel shift of VCBC (V) to pre-formed or mixed C5R2-VCBC (V-C or V+C), and included C5R2 alone as a control (**Fig. 1B**). Surprisingly, all tested protein solutions produced gel shifts indistinguishable from that of VCBC; C5R2 failed to supershift the VCBC complex. It was apparent from this experiment that C5R2 alone could bind poly(U), and we characterized this activity by performing an EMSA titration of poly(U)₄₀ with C5R2 (**Fig. 2B**). C5R2 bound more weakly poly(U)₄₀, and unlike that of the Vif complexes, C5R2 data did not fit to a standard ligand binding curve; the use of a Hill coefficient of $n=1.77$ was necessary to fit the data. We hypothesize that the “basic channel” in the CTD of CUL5 may nonspecifically bind the negatively charged RNA backbone (13). In order to determine whether a non-Vif substrate receptor could supershift C5R2, we performed an EMSA with SOCS2-EloB-EloC-C5R2 and found that unlike the VCBC-C5R2 complex a slower

electrophoretic mobility was observed than for either VCBC or C5R2 alone. These results are puzzling, as they suggest that either the full 6-protein complex has the same mobility as the 4-protein complex, compared to which it has more than twice the mass and a significantly larger volume (12), or the 6-protein complex dissociates upon treatment with poly(U)₄₀. One explanation is that the cooperativity observed in C5R2 binding is indicative of self-association, and that poly(U)₄₀ may induce aggregation of the protein that somehow liberates VCBC. A shortcoming of this explanation is that VCBC-like shifts are seen even for very low concentrations of VCBC-C5R2, at which no binding is observed for C5R2 alone. Alternatively, binding of RNA to VCBC could potentially disfavor engagement of VCBC with C5R2, although it is difficult to imagine how this could work, as the VCBC-C5R2 affinity is very tight (12). Ongoing experiments in the lab aim to address this issue directly.

VCBC protects a 12-nt fragment of poly(U)

In order to define the minimal oligonucleotide ligand for VCBC, we synthesized long poly(U) body-labeled with ³²P, and tested the ability of VCBC to protect fragments from degradation by RNase A. By comparison to fragments protected by yeast Upf1 which is known to protect an 11-nt fragment, VCBC protects a fragment 1 nt longer than Upf1, or 12 nt (**Fig 3**). This result was confirmed by fluorescence polarization measurements of 20-, 15-, and 10-mer poly(U) oligonucleotides (Data not shown). The 20- and 15-mers bound equally

well with high affinity, whereas binding of the 10-mer was impaired, in agreement with a minimal ligand size between 10 and 15 nt.

VCBC has varying affinity for homopolymeric oligonucleotides

Having defined a length requirement for VCBC-oligonucleotide binding, we then asked whether the base-type preference could be further defined than in the initial EMSA experiments by employing a fluorescence anisotropy assay using shorter, fluorescently labeled oligonucleotides. 15-mers of each of the 8 RNA or DNA base types were synthesized and used in competition binding experiments with either poly(U)₁₅ or poly(dA)₁₅ (**Fig. 4**). K_d values varied over 100-fold, with poly(dT) binding most tightly ($K_d = 4.9$ nM) and poly(C) binding most weakly (743 nM). It is worth noting that poly(dT) is thought to lack any defined structure in solution whereas poly(C) can readily self-associate at neutral pH; however poly(G) does not fit this trend, binding only ~3-fold weaker than poly(dT) and having significant structure (21). We selected poly(dT)₁₅, being the tightest binder, for use in further experiments described herein.

Binding oligonucleotide causes a compaction of VCBC

Complexes between VCBC and oligonucleotides were readily formed, and gel filtration chromatography was performed on VCBC alone and bound to poly(dT)₁₅. Absorption at both 260 nm and 280 nm was recorded. Specific differences between the two elution profiles are apparent: the +poly(dT)₁₅ sample has both an increased A_{260}/A_{280} ratio and an later elution volume relative

to -poly(dT)₁₅, indicative of nucleotide association and a decrease in the parameter R_s , or the steric exclusion radius, a term describing the mean span of a polymer in solution that correlates well with the elution volume (**Fig. 5**) (29).

A change in molecular shape overt enough to be directly observable by gel filtration chromatography typically must correspond to a change in secondary or tertiary structure. To begin to address the nature of this conformational change associated with oligonucleotide binding, we performed small angle X-ray scattering analysis (SAXS) on VCBC in complex with poly(dT)₁₅ and not. A significant decrease in the maximum scattering distance (D_{max}) was observed in plots of the real space pair distance function, $P(r)$ (**Personal communication, D.Y. Kim**). For each case, a molecular envelope was modeled using GASBOR (25). A distinct compaction of the rod-like envelope of VCBC was observed when bound to poly(dT)₁₅ (**Personal communication, D.Y. Kim**).

Taken together, the gel filtration and SAXS-based observations support a model in which binding of oligonucleotide to the VCBC complex induces a conformational change (**Fig. 6**). The nature of the conformational change remains at this point unclear. It has been reported that binding of the TAR element sequence can promote a disorder-to-order conformational transition in the N-terminal domain of monomeric Vif, so it is tempting to speculate that a similar transition may be described by the observations we report here (2). However, the physical properties of the VCBC-DNA complex are quite different

than those reported for Vif-TAR (2). Rather than induce oligomerization, we found that binding of DNA to VCBC increased stability and disfavored aggregation. We favor a model in which the context of oligonucleotide binding is important in determining the physical properties of the complex, and depends on the presence or absence of other binding partners.

MATERIALS AND METHODS

Protein purification

VCBC was purified as described previously (12). Whereas the HXB2 Vif sequence was used in previous studies from our lab, here we use a consensus Vif sequence we term Vif_{cons}.

Radiolabeling of RNA

Oligonucleotides were end-labeled by polynucleotide kinase with [γ -³²P] ATP, according to the manufacturer's recommendations (New England Biolabs).

Reaction products were purified by buffer exchange over an Illustra G-50 column (GE Healthcare).

Long poly(U) strands synthesized by poly(U) polymerase according to the manufacturer's recommendations (New England Biolabs). The RNA was body-labeled by incorporation of [α -³²P] UTP into product RNA during synthesis. After 30 minutes reactions were applied to a QIAgen RNAeasy Mini column to remove buffer exchange and remove short reaction products, and purified according to the manufacturer's recommendations. Eluate from the column was aliquoted and stored at -20° C.

Gel shift assays

100 pmol probe RNA was mixed with varying amounts of protein in NEB Buffer 2, and incubated at room temperature for 15 minutes. Native gel electrophoresis followed by phosphorimagine was used to visualize the formation of RNA-protein complexes.

RNAse protection assays

1 μL of 2×10^5 cpm / μL body-labeled poly(U) was mixed with varying 2 μM VCBC, Upf1 or no water in 1/2X NEB Buffer 2. RNAse A was added at a final concentration of between 2-10 μg / mL, and reactions were mixed and allowed to proceed for one hour. Protected products were purified by two successive chloroform-phenol extractions followed by ethanol precipitation overnight at -80°C . Inclusion of glycogen at a final concentration of 15 μg / mL during ethanol precipitation was critical for the recovery of small RNAse protection products. Protected fragments were visualized by denaturing gel electrophoresis and visualized by phosphorimaging.

Fluorescence anisotropy

5' fluorescein-labeled poly(U)₁₅ and poly(dT)₁₅ were purchased from IDT. All measurements were made using an Analyst AD system (LJL BioSystems). For direct binding assays, VCBC was serially diluted into a solution containing 25 mM HEPES pH 7.9, 25 mM NaCl, 1.25 mM MgCl₂, 1 mM DTT, and 1 nM fluorescent probe. For competitive binding assays, a competitor oligonucleotide

was diluted into a solution containing containing 25 mM HEPES pH 7.9, 25 mM NaCl, 1.25 mM MgCl₂, 1 mM DTT, 1 nM fluorescent probe, and VCBC at a concentration equal to the K_d value determined for probe-VCBC association. All data was fit in SigmaPlot; direct binding experiments were fit using a single-site saturation binding model, and competitive binding experiments were fit as described (20).

Gel filtration chromatography

Gel filtration of VCBC complexes was performed over an Superdex 200 16/60 column (GE Healthcare) equilibrated in the following buffer: 25 mM HEPES pH 7.5, 1 mM DTT, on an AKTA Explorer FPLC (GE Healthcare). Samples were filtered through a 0.45 μm filter prior to injection into a 2 mL sample loop. UV Absorption was measured at 260 nm and 280 nm throughout the runs.

FIGURE LEGENDS

Figure 1. Gel-shift analysis of interactions between Vif complexes and poly(U)-RNA

A, VCBC binds $^{32}\text{P-r(U)}_{40}$ with an apparent K_d of ~ 75 nM. Species are indicated by cartoons adjacent to the associated band. End-labeled $^{32}\text{P-r(U)}_{40}$ is depicted by a red circle attached to a black line, and the VCBC complex is labeled. **B**, VCBC, C5R2-VCBC, and C5R2 complexes with $^{32}\text{P-r(U)}_{40}$ co-migrate by native gel electrophoresis. C5R2-S2BC bound to $^{32}\text{P-r(U)}_{40}$ runs more slowly than C5R2, as expected. Species are indicated by cartoons adjacent to the associated band. End-labeled $^{32}\text{P-r(U)}_{40}$ is depicted by a red circle attached to a black line, and protein complexes are labeled.

Figure 2. Modes of C5R2-VCBC and C5R2 interaction with poly(U)-RNA are distinct

A, C5R2-VCBC binds $^{32}\text{P-r(U)}_{40}$ with an apparent K_d of ~ 100 nM. Species are indicated by cartoons adjacent to the associated band. End-labeled $^{32}\text{P-r(U)}_{40}$ is depicted by a red circle attached to a black line, and the C5R2-VCBC complex is labeled. **B**, C5R2 binds $^{32}\text{P-r(U)}_{40}$ with an apparent K_d of ~ 250 nM. Species are indicated by cartoons adjacent to the associated band. End-labeled $^{32}\text{P-r(U)}_{40}$ is depicted by a red circle attached to a black line, and the C5R2 complex is labeled. **C**, Integrated intensities from bands in **A** and **B** are plotted and used

to determine K_d values for C5R2-VCBC and C5R2 complexes with $^{32}\text{P-r(U)}_{40}$. C5R2 alone displays cooperative binding.

Figure 3. VCBC protects a ~12-base fragment of poly-r(U) from RNase degradation

A, RNase A protection patterns are shown for either no RNase control (lane 1), no VCBC control (lane 2), VCBC (lane 3 and adjacent as indicated above, and lane 5), or yeast Upf1 (lane 4 and adjacent as indicated above). **B**, Intensity profiles of lanes from the gels shown in panel **A**, as labeled. A dotted red line indicates the peak corresponding to fragments 12 bases in length.

Figure 4. Base-type preference of VCBC

A, K_d values are plotted for oligonucleotide-VCBC pairs as determined by fluorescence anisotropy under direct or competitive binding conditions. Base type is indicated below. Error bars indicate the standard deviation in K_d from multiple independent experiments. **B**, Representative curves are shown for fits used to determine values plotted in **A**, where data are colored as follows: dT_{15} is shown in black with circles, rU_{15} is shown in red with triangles, and rC_{15} is shown in blue with squares. Error bars indicate the standard deviation in $\langle r \rangle$ from multiple independent experiments.

Figure 5. VCBC- dT_{15} has a decreased R_s relative to VCBC alone

A, Absorption curves at both 260 nm and 280 nm for gel filtration of VCBC in complex with dT₁₅ or not. Coloring is as indicated. Difference in elution volume and A_{260}/A_{280} ratio is apparent in inset, indicating a decrease in R_s .

Figure 6. Vif conformation depends on ligand binding state

A model illustrating the hypothesized trend toward increased folding and compaction in Vif concomitant with the recruitment of additional binding partners. Monomeric Vif is mostly disordered. Simultaneous association with CBF β and EloB/C promotes a stable fold of Vif in which both the N- and C-terminal domains are significantly structured. Additional ligands such as oligonucleotides can promote further compaction of the VCBC particle, indicating either a change or increase in the folding state of Vif.

SUPPLEMENTARY FIGURE LEGENDS

Supplementary Figure 1. VCBC binds weakly to poly(C)

A, Native gel shift analysis of VCBC binding to poly(C). VCBC binds $^{32}\text{P-r(C)}_{40}$ with an apparent K_d of >250 nM. Molecular species are indicated by cartoons adjacent to the associated band. End-labeled $^{32}\text{P-r(U)}_{40}$ is depicted by a red circle attached to a black line, and the well-shifted bound complex is indicated with an asterix.

Figure 1

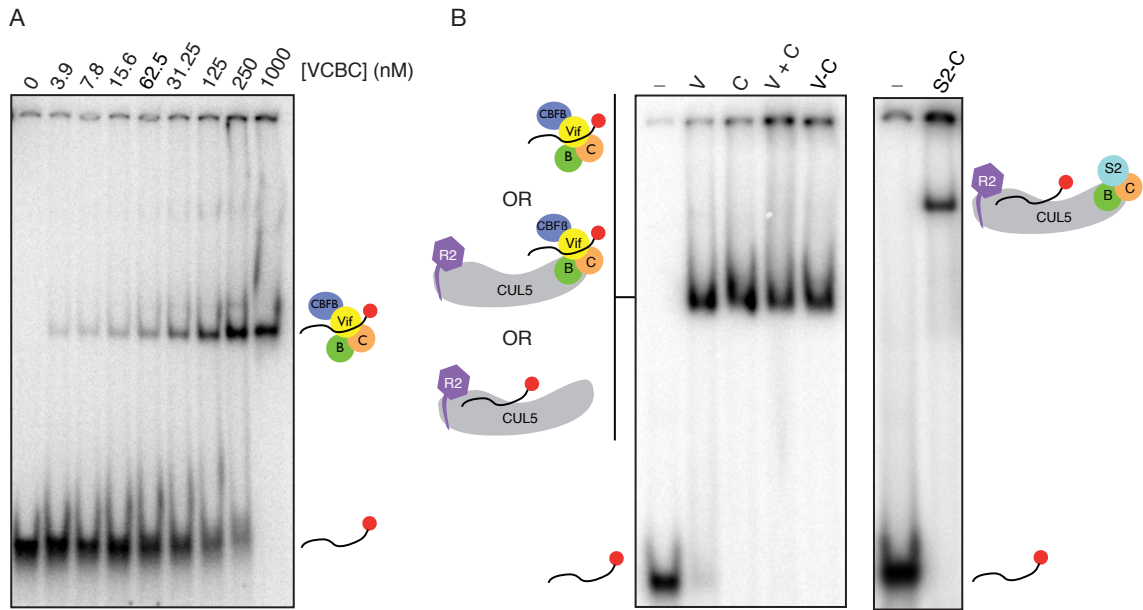


Figure 2

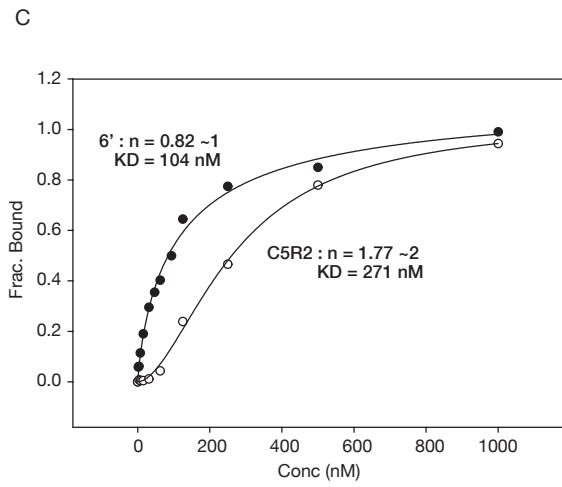
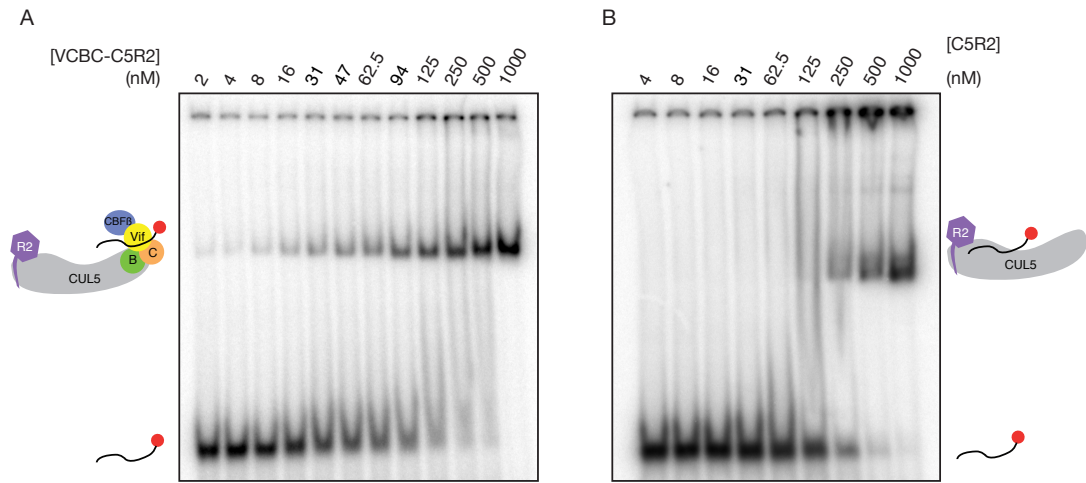


Figure 3

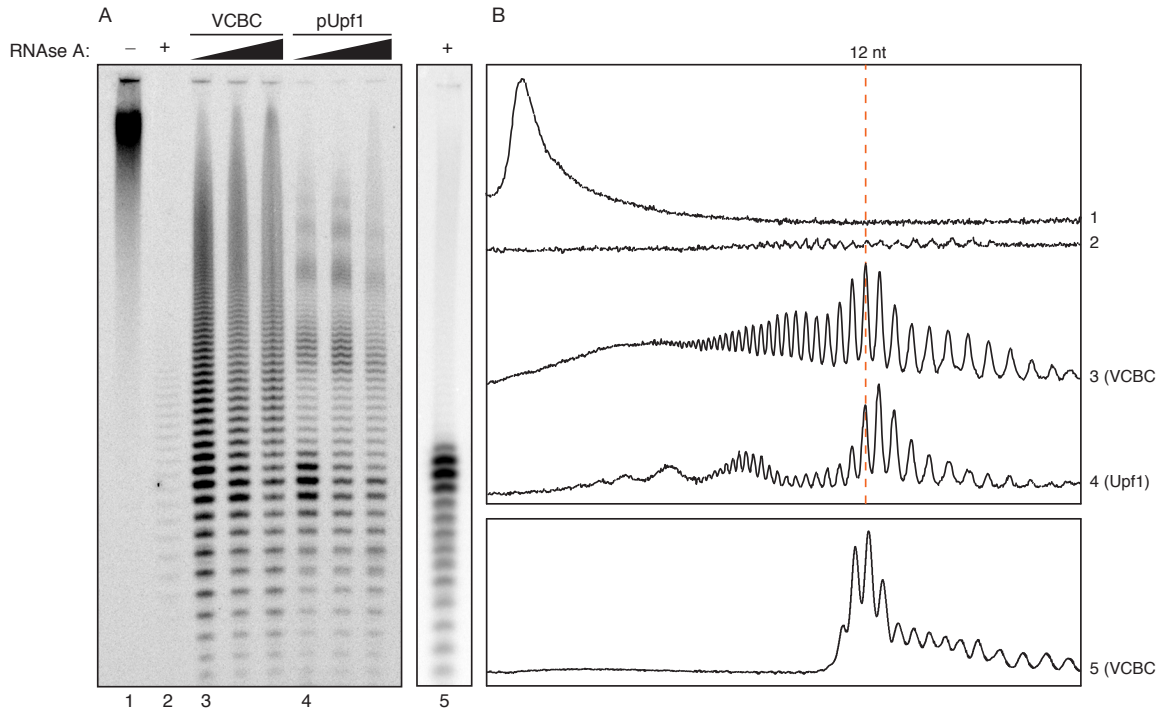
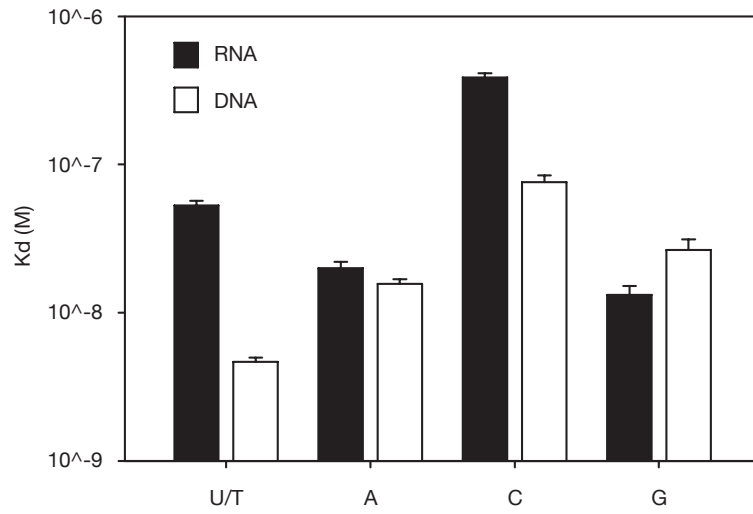


Figure 4

A



B

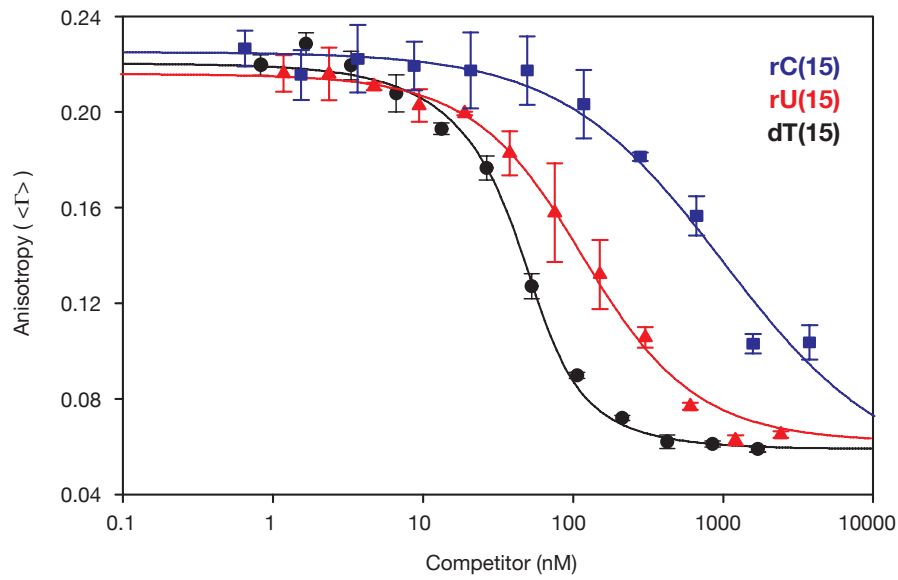


Figure 5

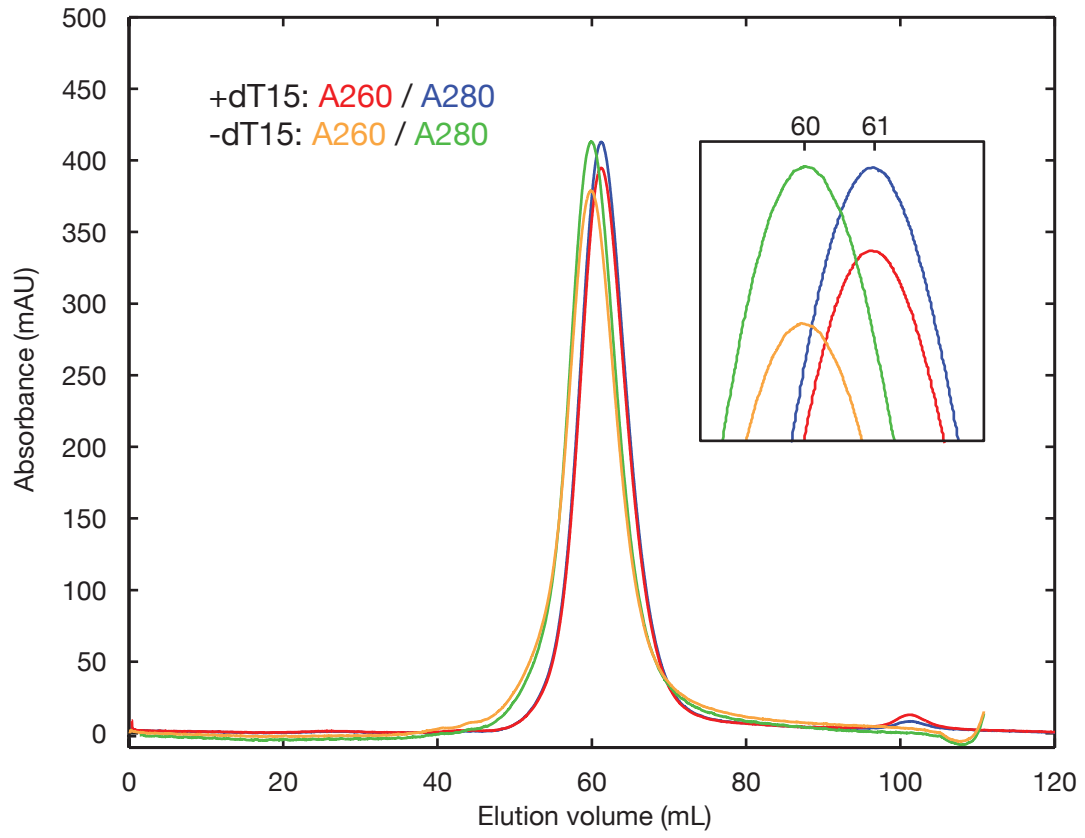
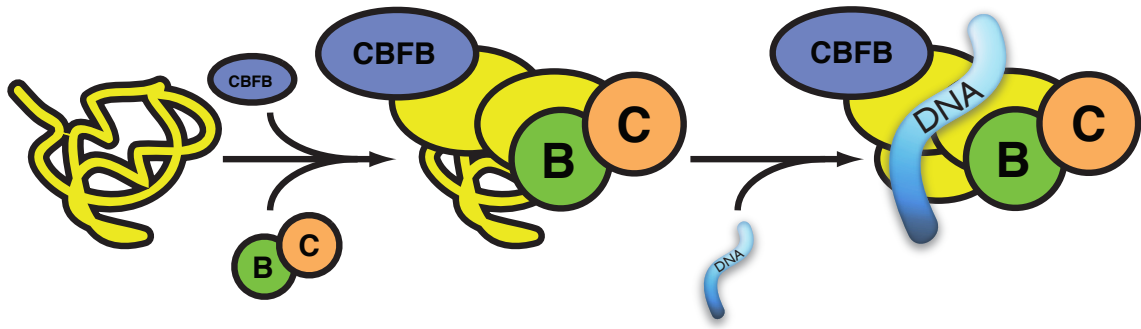
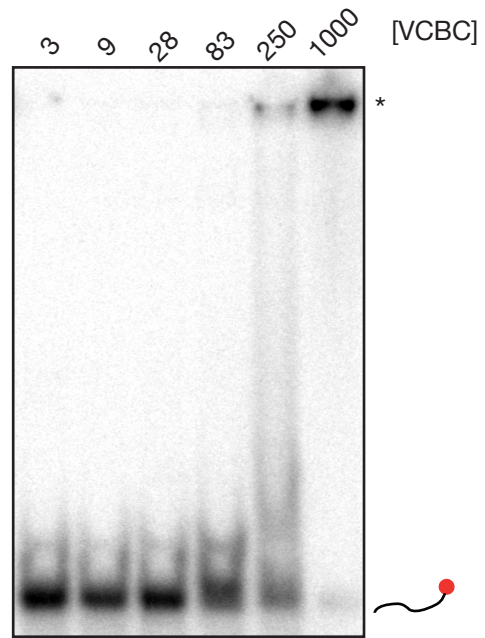


Figure 6



Supplemental Figure 1



1. **Batisse, J., S. Guerrero, S. Bernacchi, D. Sleiman, C. Gabus, J. L. Darlix, R. Marquet, C. Tisne, and J. C. Paillart.** 2012. The role of Vif oligomerization and RNA chaperone activity in HIV-1 replication. *Virus Res* **169**:361-76.
2. **Bernacchi, S., G. Mercenne, C. Tournaire, R. Marquet, and J. C. Paillart.** 2011. Importance of the proline-rich multimerization domain on the oligomerization and nucleic acid binding properties of HIV-1 Vif. *Nucleic Acids Res* **39**:2404-15.
3. **Bushman, F. D., N. Malani, J. Fernandes, I. D'Orso, G. Cagney, T. L. Diamond, H. Zhou, D. J. Hazuda, A. S. Espeseth, R. Konig, S. Bandyopadhyay, T. Ideker, S. P. Goff, N. J. Krogan, A. D. Frankel, J. A. Young, and S. K. Chanda.** 2009. Host cell factors in HIV replication: meta-analysis of genome-wide studies. *PLoS Pathog* **5**:e1000437.
4. **Cristofari, G., and J. L. Darlix.** 2002. The ubiquitous nature of RNA chaperone proteins. *Prog Nucleic Acid Res Mol Biol* **72**:223-68.
5. **Daugherty, M. D., I. D'Orso, and A. D. Frankel.** 2008. A solution to limited genomic capacity: using adaptable binding surfaces to assemble the functional HIV Rev oligomer on RNA. *Mol Cell* **31**:824-34.
6. **Feng, Y., R. P. Love, and L. Chelico.** 2013. HIV-1 Viral Infectivity Factor (Vif) Alters Processive Single-stranded DNA Scanning of the Retroviral Restriction Factor APOBEC3G. *J Biol Chem* **288**:6083-94.
7. **Harris, R. S., K. N. Bishop, A. M. Sheehy, H. M. Craig, S. K. Petersen-Mahrt, I. N. Watt, M. S. Neuberger, and M. H. Malim.** 2003. DNA deamination mediates innate immunity to retroviral infection. *Cell* **113**:803-9.
8. **He, B., K. Wang, Y. Liu, B. Xue, V. N. Uversky, and A. K. Dunker.** 2009. Predicting intrinsic disorder in proteins: an overview. *Cell Res* **19**:929-49.
9. **Izumi, T., K. Io, M. Matsui, K. Shirakawa, M. Shinohara, Y. Nagai, M. Kawahara, M. Kobayashi, H. Kondoh, N. Misawa, Y. Koyanagi, T. Uchiyama, and A. Takaori-Kondo.** 2010. HIV-1 viral infectivity factor interacts with TP53 to induce G2 cell cycle arrest and positively regulate viral replication. *Proc Natl Acad Sci U S A* **107**:20798-803.
10. **Jager, S., P. Cimermanic, N. Gulbahce, J. R. Johnson, K. E. McGovern, S. C. Clarke, M. Shales, G. Mercenne, L. Pache, K. Li, H. Hernandez, G. M. Jang, S. L. Roth, E. Akiva, J. Marlett, M. Stephens, I. D'Orso, J. Fernandes, M. Fahey, C. Mahon, A. J. O'Donoghue, A. Todorovic, J. H. Morris, D. A. Maltby, T. Alber, G. Cagney, F. D. Bushman, J. A. Young, S. K. Chanda, W. I. Sundquist, T. Kortemme, R. D. Hernandez, C. S. Craik, A. Burlingame, A. Sali, A. D. Frankel, and N. J. Krogan.** 2012. Global landscape of HIV-human protein complexes. *Nature* **481**:365-70.
11. **Jäger, S., D. Y. Kim, J. F. Hultquist, K. Shindo, R. S. LaRue, E. Kwon, M. Li, B. D. Anderson, L. Yen, D. Stanley, C. Mahon, J. Kane, K. Franks-Skiba, P. Cimermanic, A. Burlingame, A. Sali, C. S. Craik, R. S. Harris, J. D. Gross, and N. J. Krogan.** 2012. Vif hijacks CBF-beta to degrade APOBEC3G and promote HIV-1 infection. *Nature* **481**:371-5.

12. **Kim, D. Y., E. Kwon, P. D. Hartley, D. C. Crosby, S. Mann, N. J. Krogan, and J. D. Gross.** 2013. CBFbeta Stabilizes HIV Vif to Counteract APOBEC3 at the Expense of RUNX1 Target Gene Expression. *Mol Cell* **49**:632-44.
13. **Kleiger, G., A. Saha, S. Lewis, B. Kuhlman, and R. J. Deshaies.** 2009. Rapid E2-E3 assembly and disassembly enable processive ubiquitylation of cullin-RING ubiquitin ligase substrates. *Cell* **139**:957-68.
14. **Mangeat, B., P. Turelli, G. Caron, M. Friedli, L. Perrin, and D. Trono.** 2003. Broad antiretroviral defence by human APOBEC3G through lethal editing of nascent reverse transcripts. *Nature* **424**:99-103.
15. **Marcisin, S. R., and J. R. Engen.** 2010. Molecular insight into the conformational dynamics of the Elongin BC complex and its interaction with HIV-1 Vif. *J Mol Biol* **402**:892-904.
16. **Marcisin, S. R., P. S. Narute, L. A. Emert-Sedlak, M. Kloczewiak, T. E. Smithgall, and J. R. Engen.** 2011. On the solution conformation and dynamics of the HIV-1 viral infectivity factor. *J Mol Biol* **410**:1008-22.
17. **Mariani, R., D. Chen, B. Schrofelbauer, F. Navarro, R. Konig, B. Bollman, C. Munk, H. Nymark-McMahon, and N. R. Landau.** 2003. Species-specific exclusion of APOBEC3G from HIV-1 virions by Vif. *Cell* **114**:21-31.
18. **Mercenne, G., S. Bernacchi, D. Richer, G. Bec, S. Henriët, J. C. Paillart, and R. Marquet.** 2010. HIV-1 Vif binds to APOBEC3G mRNA and inhibits its translation. *Nucleic Acids Res* **38**:633-46.
19. **Reingewertz, T. H., H. Benyamini, M. Lebendiker, D. E. Shalev, and A. Friedler.** 2009. The C-terminal domain of the HIV-1 Vif protein is natively unfolded in its unbound state. *Protein Eng Des Sel* **22**:281-7.
20. **Roehrl, M. H., J. Y. Wang, and G. Wagner.** 2004. A general framework for development and data analysis of competitive high-throughput screens for small-molecule inhibitors of protein-protein interactions by fluorescence polarization. *Biochemistry* **43**:16056-66.
21. **Saenger, W.** 1984. Principles of nucleic acid structure. Springer-Verlag, New York.
22. **Sheehy, A. M., N. C. Gaddis, J. D. Choi, and M. H. Malim.** 2002. Isolation of a human gene that inhibits HIV-1 infection and is suppressed by the viral Vif protein. *Nature* **418**:646-50.
23. **Stanley, B. J., E. S. Ehrlich, L. Short, Y. Yu, Z. Xiao, X. F. Yu, and Y. Xiong.** 2008. Structural insight into the human immunodeficiency virus Vif SOCS box and its role in human E3 ubiquitin ligase assembly. *J Virol* **82**:8656-63.
24. **Stopak, K., C. de Noronha, W. Yonemoto, and W. C. Greene.** 2003. HIV-1 Vif blocks the antiviral activity of APOBEC3G by impairing both its translation and intracellular stability. *Mol Cell* **12**:591-601.
25. **Svergun, D. I., M. V. Petoukhov, and M. H. Koch.** 2001. Determination of domain structure of proteins from X-ray solution scattering. *Biophys J* **80**:2946-53.
26. **Tahirov, T. H., N. D. Babayeva, K. Varzavand, J. J. Cooper, S. C. Sedore, and D. H. Price.** 2010. Crystal structure of HIV-1 Tat complexed with human P-TEFb. *Nature* **465**:747-51.

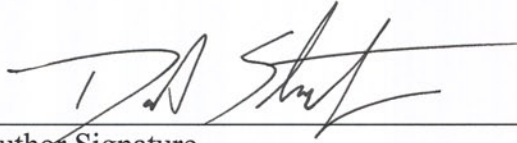
27. **Techtman, S. M., R. Ghirlando, S. Kao, K. Strebel, and E. L. Maynard.** 2012. Hydrodynamic and functional analysis of HIV-1 Vif oligomerization. *Biochemistry* **51**:2078-86.
28. **Wang, J., J. M. Shackelford, N. Selliah, D. K. Shivers, E. O'Neill, J. V. Garcia, K. Muthumani, D. Weiner, X. F. Yu, D. Gabuzda, and T. H. Finkel.** 2008. The HIV-1 Vif protein mediates degradation of Vpr and reduces Vpr-induced cell cycle arrest. *DNA Cell Biol* **27**:267-77.
29. **Wang, Y., I. Teraoka, F. Y. Hansen, G. H. Peters, and O. Hassager.** 2010. A Theoretical Study of the Separation Principle in Size Exclusion Chromatography. *Macromolecules* **43**:1651-1659.
30. **Xue, B., M. J. Mizianty, L. Kurgan, and V. N. Uversky.** 2012. Protein intrinsic disorder as a flexible armor and a weapon of HIV-1. *Cell Mol Life Sci* **69**:1211-59.
31. **Yu, X., Y. Yu, B. Liu, K. Luo, W. Kong, P. Mao, and X. F. Yu.** 2003. Induction of APOBEC3G ubiquitination and degradation by an HIV-1 Vif-Cul5-SCF complex. *Science* **302**:1056-60.
32. **Zhang, H., R. J. Pomerantz, G. Dornadula, and Y. Sun.** 2000. Human immunodeficiency virus type 1 Vif protein is an integral component of an mRNP complex of viral RNA and could be involved in the viral RNA folding and packaging process. *J Virol* **74**:8252-61.
33. **Zhang, H., B. Yang, R. J. Pomerantz, C. Zhang, S. C. Arunachalam, and L. Gao.** 2003. The cytidine deaminase CEM15 induces hypermutation in newly synthesized HIV-1 DNA. *Nature* **424**:94-8.

Publishing Agreement

It is the policy of the University to encourage the distribution of all theses, dissertations, and manuscripts. Copies of all UCSF theses, dissertations, and manuscripts will be routed to the library via the Graduate Division. The library will make all theses, dissertations, and manuscripts accessible to the public and will preserve these to the best of their abilities, in perpetuity.

Please sign the following statement:

I hereby grant permission to the Graduate Division of the University of California, San Francisco to release copies of my thesis, dissertation, or manuscript to the Campus Library to provide access and preservation, in whole or in part, in perpetuity.



Author Signature

3.29.2013

Date